DESIGN OF A HYBRID ROCKET / INFLATABLE WING UAV

By

CORY SUDDUTH

Bachelor of Science in Mechanical and Aerospace

Engineering

Oklahoma State University

Stillwater, OK

2012

Submitted to the Faculty of the
Graduate College of the
Oklahoma State University
in partial fulfillment of
the requirements for
the Degree of
MASTER OF SCIENCE
December, 2012

DESIGN OF A HYBRID

ROCKET / INFLATABLE

WING UAV

Thesis Approved:

Dr. Jamey Jacob

Thesis Adviser

Dr. Andy Arena

Dr. Joe Conner

Name: CORY SUDDUTH

Date of Degree: DECEMBER, 2012

Title of Study: DESIGN OF A HYBRID ROCKET / INFLATABLE WING UAV

Major Field: MECHANICAL AND AEROSPACE ENGINEERING

This paper discusses the design challenges and development of a UAV that transitions from a rocket, which allows the aircraft to reach a target altitude rapidly, and then deploys an inflatable wing from an enclosed shell in midflight to allow for loitering and surveillance. The wing deployment and transition is tested in static and dynamic environments, while the performance and stability of both the aircraft mode and rocket mode are examined analytically. An in-depth discussion of key components, including the design, analysis and testing, is also included. Designing an UAV that transitions from a high velocity rocket, to a slow velocity UAV provides many difficult and unique design challenges. For example, the incorporation of deployable wing technology into a full UAV system results in many design constraints. In this particular design inflatable wings are used to generate lift during aircraft mode, and the stabilizing fins for the main wing also acted as the fins for the vehicle during its rocket phase. This required the balancing of the two different vehicle configurations to ensure that the aircraft would be able to fly stably in both modes, and transition between them without catastrophic failure. Significant research, and testing went into the finding the best method of storing the inflatable wing, as well as finding the required inflation rate to minimize unsteady aerodynamic affects. Design work was also invested in the development of an inflation system, as it had to be highly reliable, and yet very light weight for use in this small UAV.

This paper discusses how these design challenges were overcome, the development and testing of individual sub-components and how they are incorporated into the overall vehicle. The analysis that went into this UAV, as well as methods used to optimize the design in order to minimize weight and maximize the aircraft performance and loitering time is also discussed.

TABLE OF CONTENTS

CHAPTER PAGE

CHAPTER PAGE

LIST OF TABLES

TABLE PAGE

LIST OF FIGURES

FIGURE PAGE

FIGURE PAGE

FIGURE PAGE

CHAPTER I

INTRODUCTION

1.1 Motivation and Scope

The application of UAVs in aerial surveillance and munitions strikes has been on the rise in our military, and ability to have a compact UAV reach its target location quickly and perform reconnaissance and support ground units is an area of interest for our military. Furthermore, small man-portable UAVs allow for a wider range of utilization and missions in addition to making the aircraft more accessible to the ground forces that need support. Inflatable wing UAVs have shown to have several key advantages over conventional rigid wing and folding wing aircraft. Inflatable wing UAVs have a high packing efficiency (low packed volume), and high G deployment capabilities. Inflatable wings also are very durable and reliable, due to the lack of moving parts; they are easily recovered and repaired [1] [2]. Unlike rigid wing aircraft, inflatable wing UAVs also have the ability to recover their shape without any damage if their wings happen to buckle during flight (high gusts, or high G-load banking) as shown in Figure 1.1.1. In addition, the ability to have the aircraft fully assembled with the wings stowed in the deflated position, allows for ease of transport and rapid deployment.

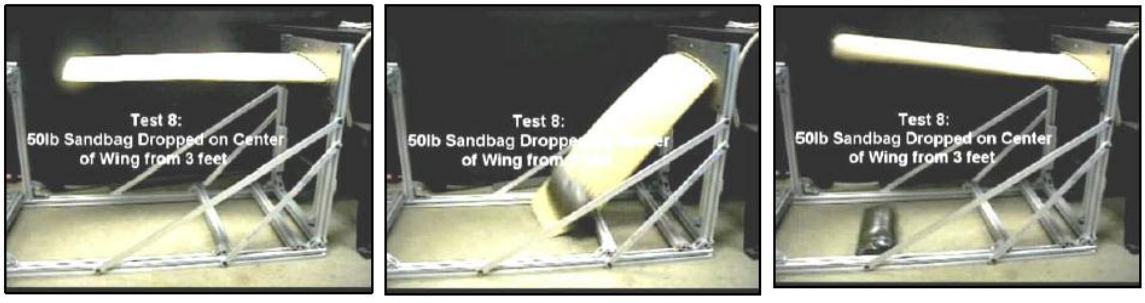

Figure 1.1.1 Inflatable wing recovery from adverse loads [3]

The small compact volume, reliability and robustness, combined with the ability to rapidly deploy the wings on the ground or inflight while maintaining a small system mass makes inflatable wings an ideal candidate for a man-portable, rapid-deployment UAV.

1.2 Goals and Objectives

The goal behind this thesis is to develop a man-portable, rapid-deployment UAV that takes advantage of the capabilities that an inflatable wing provides. Some of the key abilities of an inflatable wing, that is lost amongst fixed wings, is its minimal compact volume and ability to be deployed in mid-flight. Thus, a UAV is developed that is capable of transitioning from a high velocity cruise with the inflatable wing stowed internally to a low velocity loitering mode when the wings are deployed in mid-flight. Calling upon previous experience, it was decided that the propulsion for the initial boost/cruise phase of the aircraft's flight would be a solid rocket motor, often used in high-powered rocketry.

Goal: Design and develop an aircraft that incorporates a solid rocket booster for rapid cruise phase and an inflatable wing that is deployed in midflight for loitering.

Objectives:

- Evaluate the aircraft's stability throughout all portions of its mission
  - Analyze the stability of the UAV during flight mode, and rocket-booster phase
    - Balance the aircraft's design between stability in aircraft mode and rocket mode
    - Optimize aircraft for minimal weight
  - Conduct testing on the aircraft during transition phase
    - Explore packing methods of inflatable wing
    - Conduct static and dynamic deployment tests.
    - Evaluate stability and determine optimal inflation rate

- Develop inflation system for deploying inflatable wing
  - Evaluate options and select method for producing inflation pressure
  - Design, construct and test inflation system
    - Construct initial inflation system for proof of concept
    - Re-design and optimize for minimal weight. Develop new version.
    - Conduct extensive testing of inflation system and inflatable wing
- Conduct flight tests of UAV
  - Perform rocket launch of vehicle to verify boost-phase capability
  - Perform launch and test mid-air deployment and flight capability

Throughout this paper, the design, analysis, and construction of the aircraft is discussed. After some preliminary design considerations, sizing and analysis the Concept of Operations (Figure 1.2.1) was developed for an aircraft that could meet these goals and objectives. Eventually, the final aircraft configuration and design was developed through significant analysis, testing, and construction of subcomponents. The final aircraft design and configuration is described in Figures 1.2.2 and 1.2.3.

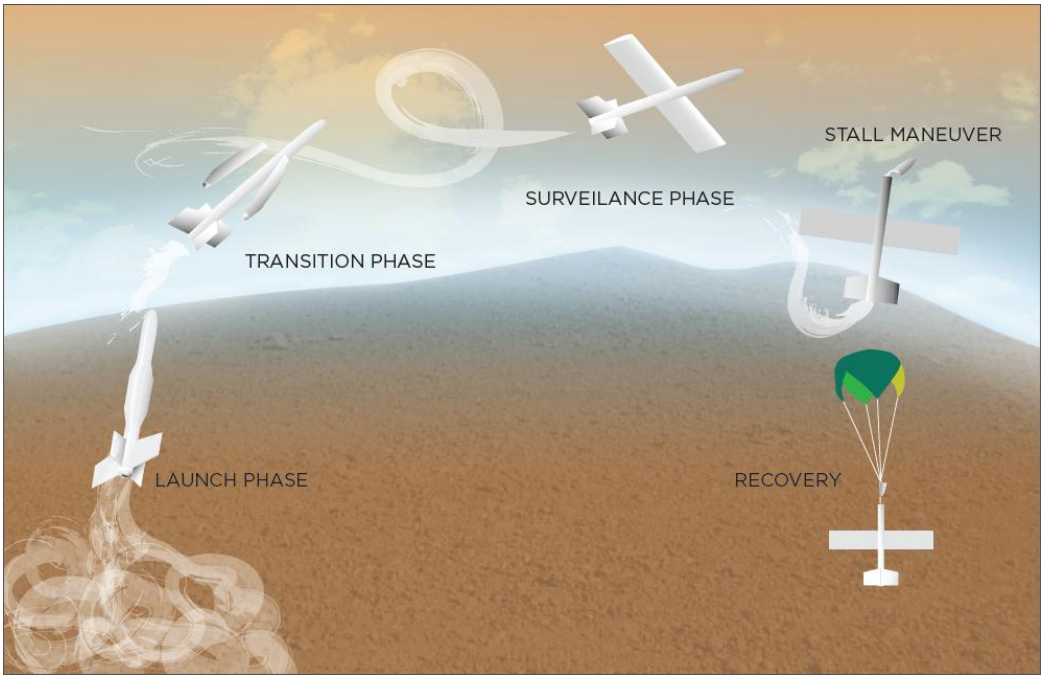

Figure 1.2.1: Concept of Operations

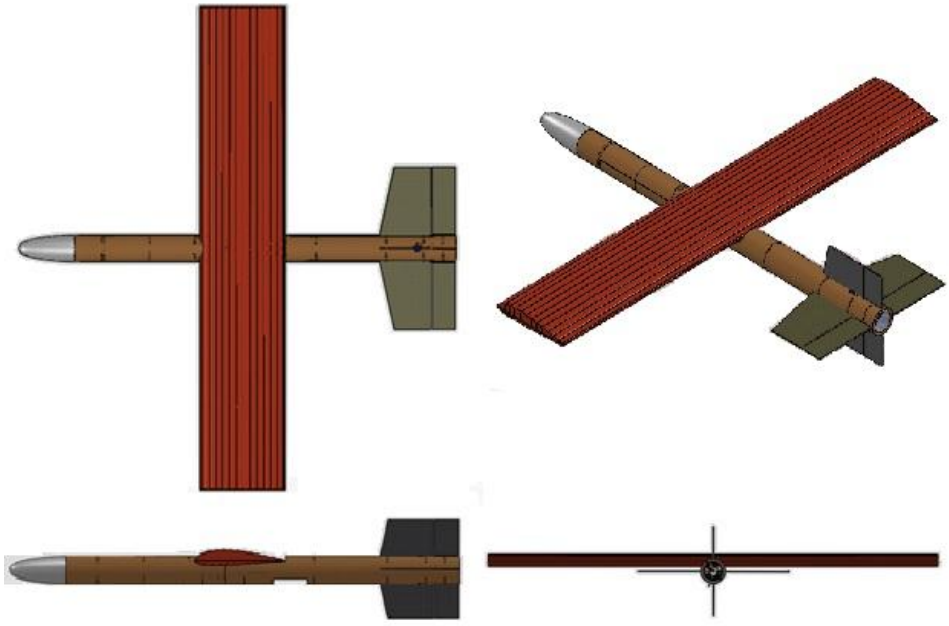

Figure 1.2.2: Final Aircraft Configuration

Wing Area, S	900	in^2
Span, b	72	in
Aspect Ratio	5.76	
Dihedral (level flight)	1.6^o	
Sweep, Taper	0	
Horizontal tail area	200	in^2
Vertical tail area	100	in^2
In-flight weight	12.02	lb
Wing Loading	1.9232	lb/ft^2
Propulsion System	EDF - Lander LEDF68-1A21	
EDF Max Thrust	3.5	lb
Launch Weight	15.17	lb
Rocket Booster	Aerotech J350	
Booster Total Impulse	700	N*s

Figure 1.2.3: Final Aircraft Design Specifications

CHAPTER II

REVIEW OF LITERATURE

2.1 DEPLOYABLE RIGID WING AIRCRAFT

Often times when the idea of an aircraft flying in dissimilar flight regimes researchers and aerodynamicists often look to the idea of a "morphing-wing" aircraft to fill this niche. A morphing wing aircraft often implies that a fixed-wing aircraft has the ability to change its aerodynamic performance by altering the wing's shape, span, sweep, or chord length. However, for this project there is one aircraft that stands-out and has a lot of design traits that were found useful; the Tomahawk Cruise Missile (Figure 2.1.1). It is debatable whether or not the Tomahawk is considered a true morphing UAV, though it does have deployable wings, as well as deployable stabilizers and engine inlet.

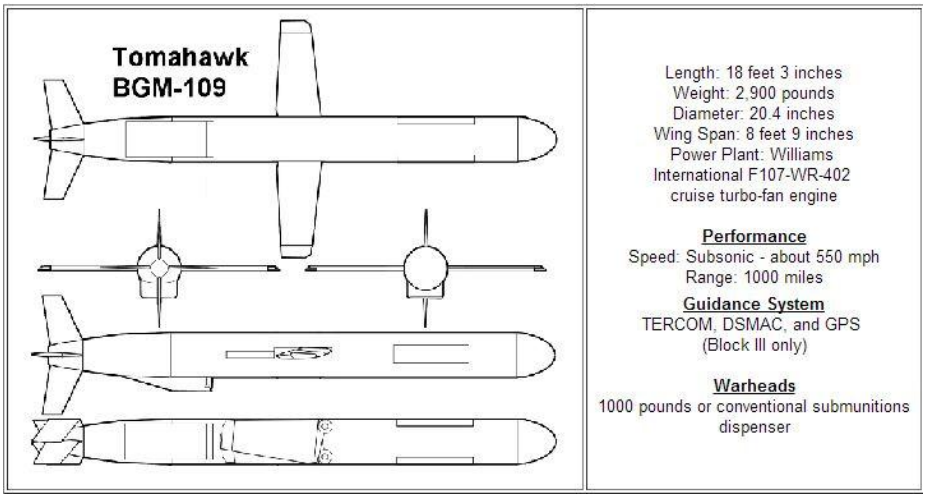

Figure 2.1.1: Tomahawk Cruise Missile Specifications [4]

The Tomahawk cruise missile was originally designed by General Dynamics in the 1970's, and is currently produced by Raytheon. It has a solid rocket booster section that propels the vehicle from its launcher. The solid rocket booster contains 322 pounds of Arcadene 360B HTPB propellant that burns for approximately 14 seconds during its launch [5]. As the thrust of the rocket booster begins to decay, the booster is jettisoned and the deployable wings and stabilizers unfold and engine inlet opens The Tomahawk cruise missile contains an F107-402 turbofan engine that allows the aircraft to cruise at a speed of 550 mph (subsonic) before it reaches its target 1350 nmi away(depending on variant). The general layout of the subcomponents that make up the Tomahawk Cruise Missile are shown below, in Figure 2.1.2.

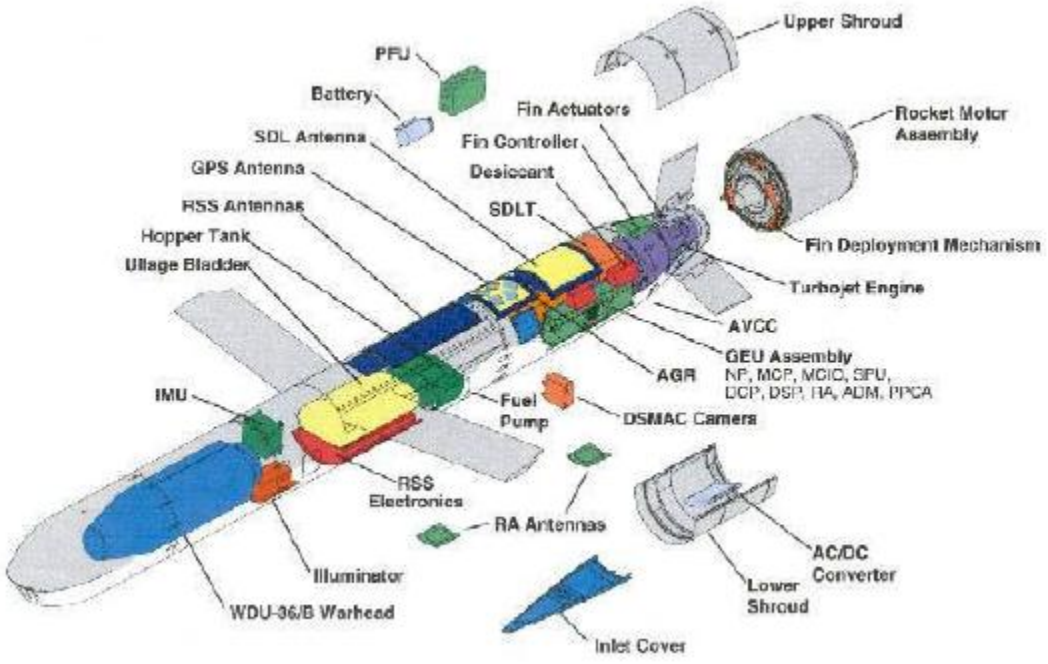

Figure 2.1.2: Tomahawk Cruise Missile General Arrangement [5]

The Tomahawk cruise missile was of particular interest during the design phase of the Hybrid UAV-Rocket as it contains similar abilities and design constraints. Both vehicles were designed to have a solid rocket-booster phase as it begins its mission. Both vehicles contained a main wing that is deployed in mid-flight; neither of which has aerilons. The Tomahawk cruise missile also had the capabilities to have an optional parachute recovery system (Figure 2.1.3) that would allow the vehicle to be recovered at sea, as well as on land. The Hybrid Rocket-UAV also utilizes a parachute system for recovery, as discussed in Chapter 3. Both vehicles fly at subsonic speeds, and both aircraft contain an internal ducted fan for propulsion during the aircraft's flight-phase. The design of the Hybrid Rocket-UAV and how attributes from the Tomahawk were investigated and incorporated as needed is discussed further in Chapter 3.

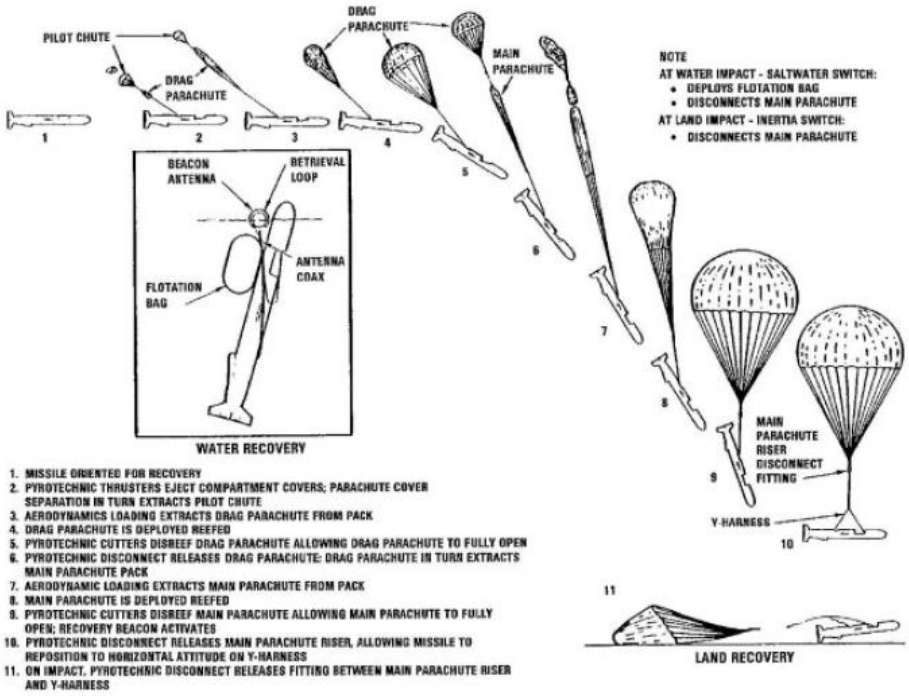

Figure 2.1.3: Tomahawk Parachute Recovery [5]

The Naval Research Laboratory also created an aircraft with similarities to the aircraft discussed in this report. The Flying Radar Target (FLYRT) was developed as a ship-launched electronic warfare payload carrying aircraft, designed to be an expendable active electronic RF decoy. The aircraft features a solid rocket booster/separator that boosts the rocket from its launcher. Once the aircraft exits the launch tube, its spring-loaded cruciform tail deploy, and its built in autopilot guide the aircraft as it reaches apogee. Once the solid rocket booster reaches burnout, the aircraft jettisons the booster, and the folding rigid wings deploy. At this point, the electronic payload antennas deploy and the built in electric motor starts up allowing the aircraft to fly and perform its mission. The deployment sequence for the FLYRT aircraft can be seen in Figure 2.1.4. The aircraft weighed 58 pounds, and had a wing span of over eight feet. The overall aircraft length was 5.3 feet, and the aft section of the aircraft, including the folding tails and rocket motor fit inside of a 5.125 inch diameter launcher barrel [6].

Figure 2.1.4: FLYRT Aircraft Deployment Sequence

The Navy conducted a multitude of simulations, wind tunnel tests, and drop tests on the aircraft during the early development of this project which significantly reduced the risk of the

program. During this time, the Navy also conducted several flight tests, all of which utilized the booster motor. Many of the early flight test included RC control with a skilled pilot operating the vehicle. From these tests, several flights worth of deployment data was acquired and evaluated allowing the researchers to fine-tune their autopilot program. After a multitude of successful flight testing, The Navy conducted a final demonstration of the aircraft in September of 1993.

2.2 INFLATABLE-WINGED AIRCRAFT

In addition to morphing-wing aircraft and deployable-wing aircraft, inflatable-wing aircraft were also investigated. While inflatable-wing aircraft may seem to be a lesser-known technology than others, it has been in development for decade. Inflatable wing aircraft have been successfully demonstrated as early as the 1950's with the Goodyear Inflatoplane Model GA-468 (Figure 2.2.1) [6]. The inflatoplane was designed and built in 12 weeks, with the goal of being a rescue plane that would be air-dropped behind enemy lines. The inflatable wing took about five minutes to inflate. The pilot would then hand-start the engine, and take off from a turf runway, requiring only 250 feet before the plane was off the ground. Several models were made, ranging from a single capacity, to two-person capacity aircraft, each with a 28 foot inflatable wing.

Figure 2.2.1 Goodyear Model GA-468 Inflatoplane

2.2.1 NASA I2000

In recent years there have been a handful of inflatable UAV systems that have incorporated rapid deployment and inflation. In 2002, NASA Dryden Flight Research Center produced an inflatable wing UAV, called I2000, and conducted a mid-air deployment. The aircraft was dropped from a larger carrier-aircraft in mid-flight. Upon release, the wings were immediately deployed. The aircraft's inflation system utilized a COTS (Commercial Off the Shelf) high pressure, refillable cylinder to supply the inflation gas. Once the wings were released, the inflation system would inflate the wings in less than a third of a second, as shown in Figure 2.2.1.1. The entire process from aircraft being dropped, wing deployment to fully inflated wings took about one second. The rate of inflation was determined from NASA's simulations of pullout maneuvers from a predicted ballistic trajectory [7]. As the aircraft transitioned from falling to flight, using its inflated wings, there were no indications of instability or divergence during deployment. Once the wings were inflated, the unpowered I200 aircraft glided to a smooth landing [2].

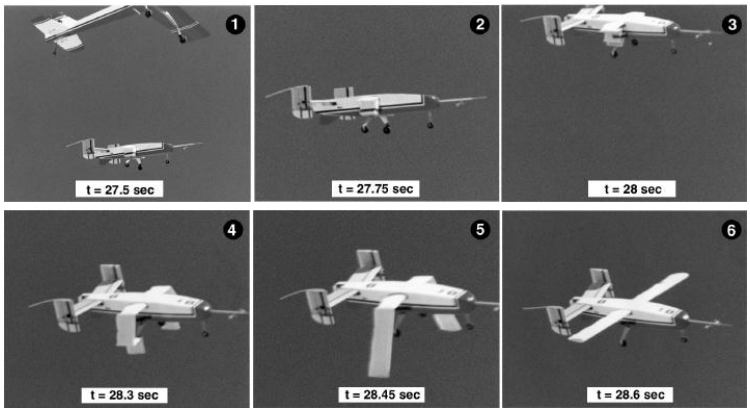

Figure 2.2.1.1: NASA Dryden I2000 in-flight deployment sequence [7].

The inflatable wings used in the NASA I2000 was developed and fabricated by Vertigo Inc. It included five inflatable cylindrical spars that ran span-wise from tip to tip with open-cell foam between the spars, making the airfoil shape. The wing is shown below, in Figure 2.2.1.2. Each spar was made from braided Vectran (similar to Kevlar). The wing's airfoil was a relatively thick, and symmetrical section NACA-0021. The wing did not contain control surfaces, while the tail stabilizers provided all of the control for the aircraft [7] [6]. The inflatable wing was packed into a z-fold method for storage prior to deployment. NASA conducted several load tests on the inflatable wing with inflation pressures ranging from 150 psig to 300 psig. At these pressures the inflatable wing was able to withstand wing tip loads from approximately 11lbs to 22 lbs (max vehicles load of 22lbs to 44 lbs). The aircraft had a maximum weight of 15.7 lb throughout the flight program and a reported allowable load factor capability from 3 to 5 depending on the main wing inflation pressure ranging between 150 to 300 psig with a 15 lb aircraft [7].

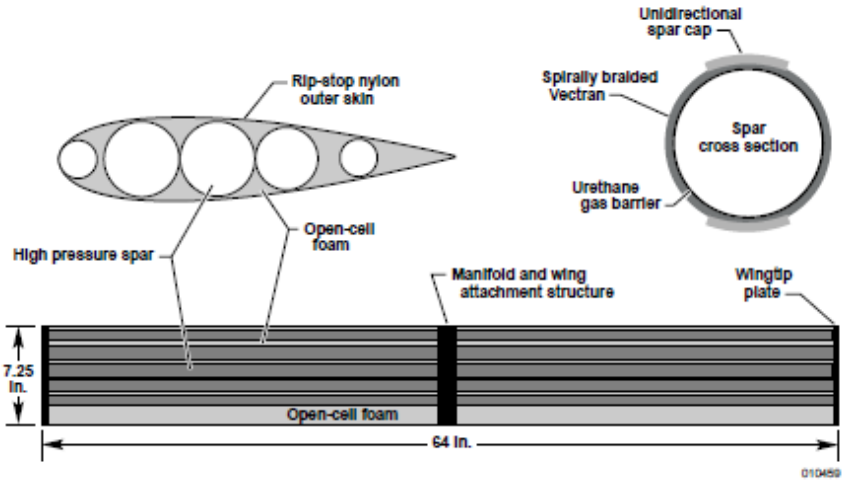

Figure 2.2.1.2: NASA I2000 Inflatable Wing Structure [7]

The inflation system used for the NASA I2000 aircraft included a small, refillable pressure vessel with approximately 35 cubic inches of volume and maximum pressure rating of 1800 psig. The inflation system used for this program is shown in Figure 2.2.1.3. The inflation gas used in this experiment was dry nitrogen gas that was regulated to a pressure between 240 and 180 psig. The inflation system also included a relief valve that would allow access nitrogen gas to vent. When the aircraft was assembled in the in-flight inflation configuration the adjustable regulator was used as an adjustable orifice (it could not regulate properly) and the wing inflation system had an unregulated system inflation rate. "The final wing pressure was controlled exclusively by the initial pressure of the high-pressure source tank; an initial tank pressure of approximately 1800 psig would yield the desired final wing (and tank) pressure of approximately 180 psig [7]."

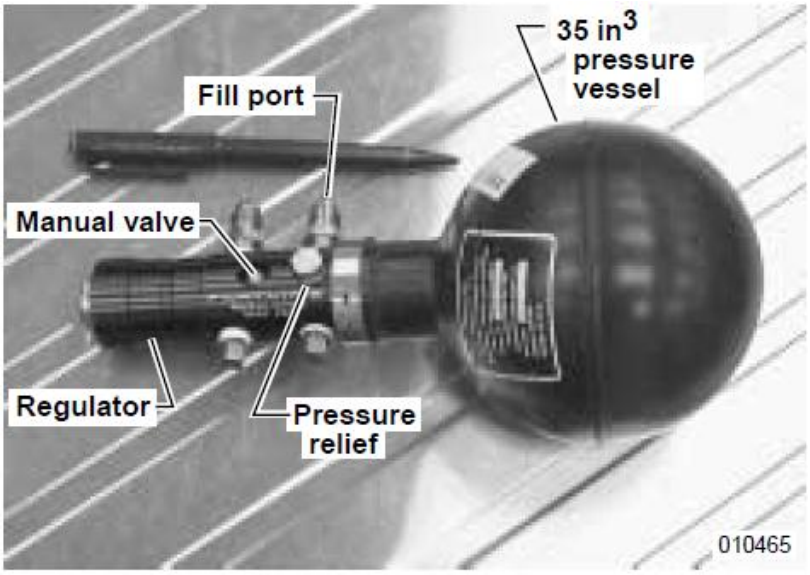

Figure 2.2.1.3: NASA I2000 Inflation System **[7]**

The inflation system, or rather the mechanisms and means used to initiate the inflation process was a very complex series of plumbing, piston cylinders, spool valves, and servos. A spool valve is a type of valve that contains an internal rod-like object (called the spool) that can be used to change the path of the air flow, by means of an external input. This input is often times pneumatic, as in the pressure on one end of the spool is increased or decreased in order to cause the spool to move from one side or the other. In the case of the I2000 inflation system, it is shown in schematic (Figure 2.2.1.5) that a servo was used to actuate the spool within the spool valve. The spool valve shown below, in Figure 2.2.1.4 is not a representation of the one used in the I2000, rather it is simply an example of a spool valve.

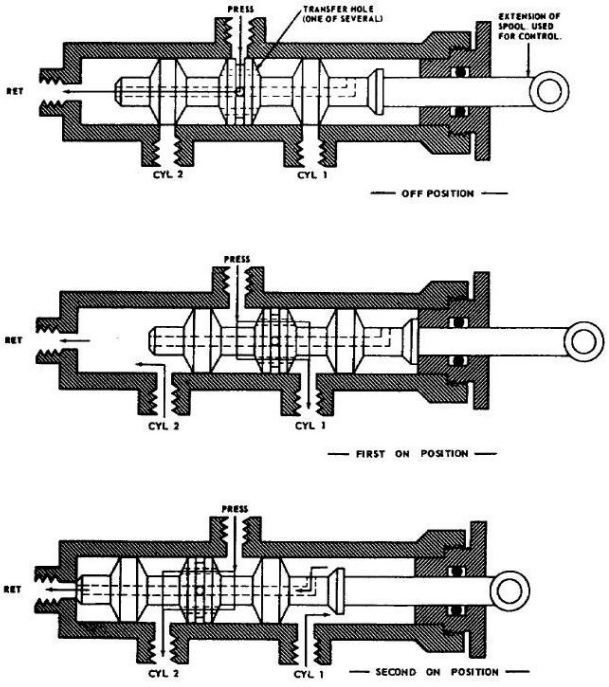

Figure 2.2.1.4 Spool Valve Schematic example [8].

Prior to the wings being inflated, the I2000 inflatable wings were held in place by a mechanical-pneumatic retention system- A pneumatic cylinder, or pin, was used to hold the wings in place, until a spool valve was actuated by a servo allowing the gas to flow through the system. In addition, the actuation for the main wing inflation system was a mechanical mechanism as well [7]. It is my understanding that a pneumatic cylinder was used to hit the manual valve (shown in Figure 2.2.13) on the inflation system, allowing air to flow from the high pressure cylinder to the inflatable wing. The pneumatic cylinder in this situation was connected to another spool valve, which again was controlled by a servo [7]. A schematic of the piston systems, and inflation systems used in the I2000 is shown below in Figure 2.2.1.5.

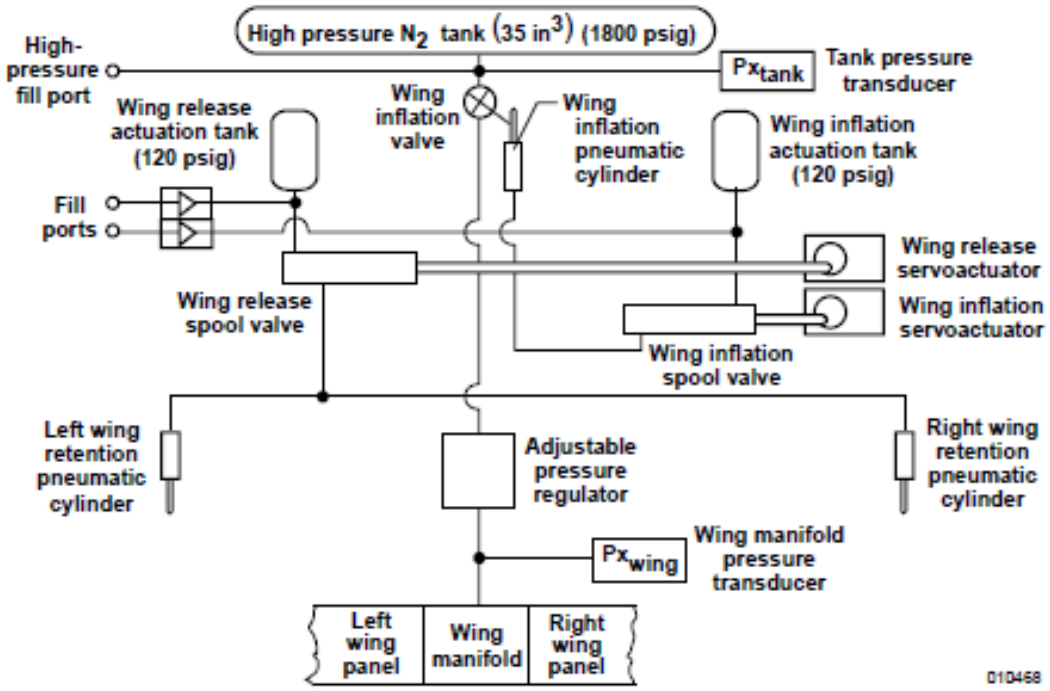

Figure 2.2.1.5: I2000 Inflation System Schematic [7].

2.2.2 ILC DOVER FASM/QUICKLOOK

ILC Dover (one of the earliest aerospace companies to develop inflatable wings in the 1970's) has also conducted rapid inflation of an inflatable wing in midflight for the purpose of a UAV developed as a joint-funded program by the US Navy and US Army. The program, called FASM/Quicklook featured a UAV that would be fired from a 155-mm howitzer and shortly thereafter, deploy a ballute for deceleration and stabilization At apogee, the inflatable wings were deployed and the ballute module was jettisoned as the vehicle moved into the flight phase of the mission [9]. In the figure below, Figure 2.2.2.1, one can see that the inflatable wings used in FASM and, presumably also in Quicklook were packed in a Z-fold configuration internally.

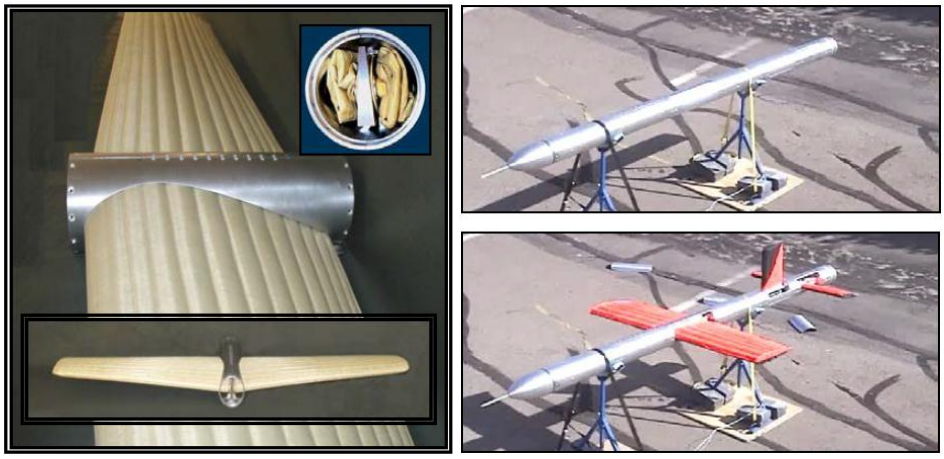

Figure2.2.2.1: ILC Dover Inflatable Wing (left) **[3]**, FASM / Quicklook UAV Testing (right) **[9]**

In the case of FASM/Quicklook, a chemical gas generator was utilized in order to provide a large amount of inflation gas (Figure 2.2.2.2). This chemical generator provided the necessary gas to initially deploy the deceleration ballute, as well as inflate the inflatable wings and inflatable stabilizers [9]. The chemical gas generator provided a large amount of gas in a fraction of a second, creating a pressure surge that ejected the packed ballute out of the canister.

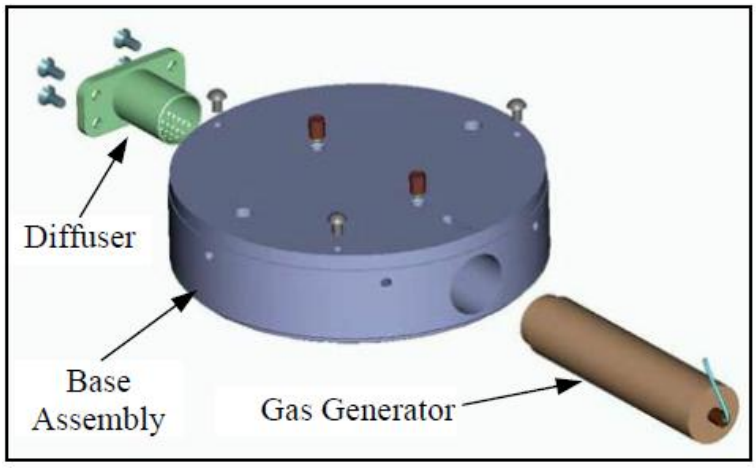

Figure 2.2.2.2: FASM/Quicklook Inflation System **[9]**

A reoccurring problem persisted throughout the program with the gas generator. The inflation gas exiting from the generator was at a very high temperature that could easily burn through the inflatable ballute, as shown in Figure 2.2.2.3. Measures were taken to deflect the gases and protect the ballute, but ultimately during the test flight, the gas generator again burned through the ballute.

Figure 2.2.2.3: Gas Generator Destroyed Ballute [9]

2.3 PREVIOUS OSU RESEARCH

Research has also been conducted at Oklahoma State University on the effects of Inflatable wing deployment during slow inflation. In their research an inflatable wing was integrated into a rigid wing, allowing for the expansion of the aircraft's wing span. A method was developed that utilized Velcro straps integrated into an inflatable wing that was stored using the Roll Method. This would allow for the gradual increase in volume of the inflatable wing, while

maintaining approximately constant operational pressure. The research was primarily focused on the deployment characteristics of an inflatable wing during cruise while utilizing a slow inflation rate (inflation time varying from 10 seconds to 150 seconds) [2]. The results from one of these tests are shown below in Figure 2.3.1.

(a) t =0 s. (b) t = 0.5 s. (c) t = 6 s. (d) t = 11 s (e) t = 33.3 s

Figure 2.3.1: Deployment Test with Slow Inflation

In this thesis, a high mass flow rate inflation system as an ideal case for deploying inflatable wings in midflight. The report explored a couple of different methods of achieving this high flow rate, both of which utilized a COTS Co2 bottle that is typically used for paintball guns, as shown in Figure 2.3.2. In the report, two different mechanisms to trigger the inflation system were developed, one being a mechanical ball valve, and the other an electric solenoid valve from a paintball gun [2].

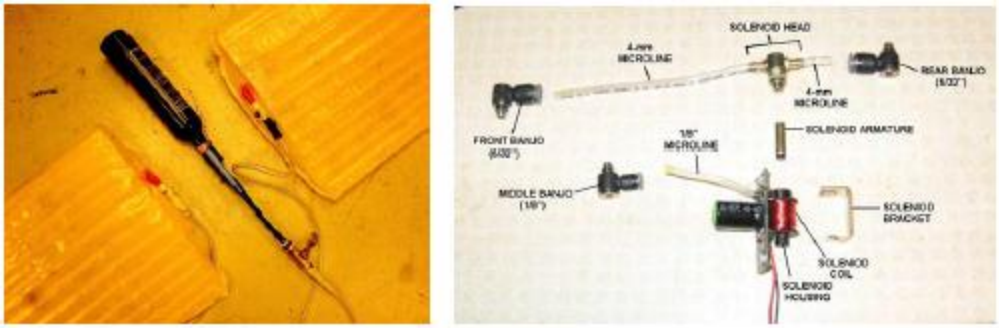

(a) CO2 canister with ball valve (b) Solenoid valve

Figure 2.3.2: Previous OSU High mass flow rate inflation systems [2].

During this research problems were found when trying to integrate either system into an aircraft. One of the biggest problems being that the Co2 canister that was being used was much heavier than any of the other inflation systems that were tested, including small, low mass flow rate pumps. Flight tests with these inflation mechanisms were not completed at the time the report was written [2].

2.4 PRYO-VALVES

Pyro-valves, also known as explosive valves or squib valves, have been used by NASA for decades in space applications. In 1973 NASA published a report on the various valves used on the Saturn V rocket during the Apollo mission and discussed explosive valves, their uses and capabilities, potential problems as well as the advantages and disadvantages. One such explosive valve is depicted in Figure 2.4.1. The description given in the NASA report for these types of explosive valves is quoted below.

“Their generally nonreusable nature makes these valves undesirable for commercial applications, whereas their zero leakage, small size, light weight, rapid response, and self-contained actuation

requiring only a small pulse of electrical energy make them most useful for one-shot space requirements [10].”

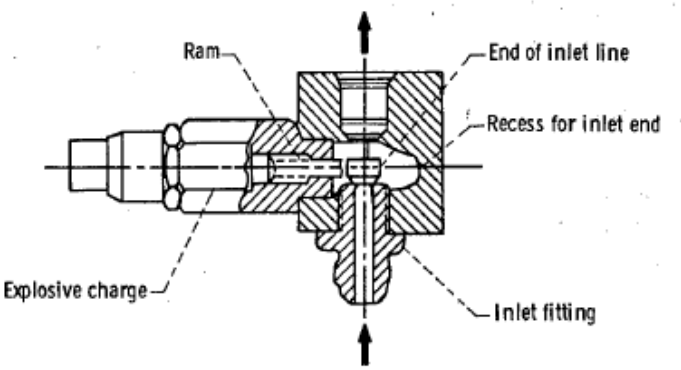

Figure 2.4.1: Explosive Valve Schematic [11].

Throughout the Saturn V and Apollo program NASA used explosive valves in applications where extreme reliability, low voltage requirements, and light weight actuators were needed. These valves ranged from simple normally closed valves, like the one above, to more complicated spool-valves that were actuated (able to be opened and closed) by means of multiple pyrotechnic charges.

Today, there is a hobby rocketry association, known as the National Association of Rocketry (NAR), which was founded by hobbyist that were inspired by the Apollo missions and sought out means to create their own rockets. These hobbyists created the sport of High Powered Rocketry (HPR), where amateurs can learn about rocketry and design and build their own model rockets [12]. While many of these rockets range in size of a few feet long and travel to an altitude of a few thousand feet, there are some cases where a HPR hobbyist have built rockets that could reach space (altitude of 121,000 feet), with a 26 feet long rocket [13].

In most high powered rockets, a small black powder charge, ignited by an electric match (e-match), is used to deploy the parachute. The volume that contains the parachute is pressurized by the large amount of gases produced by the black powder. This causes the aircraft sections to separate, and in turn allows the parachute to be deployed. Often times, multiple parachutes and multiple ejection charges are used to more accurately control the rockets descent rate and prevent the rocket from traveling too far down range; this is known as Dual Deployment. An example of a high powered rocket with a Dual-Deployment configuration is shown below in Figure 2.4.2.

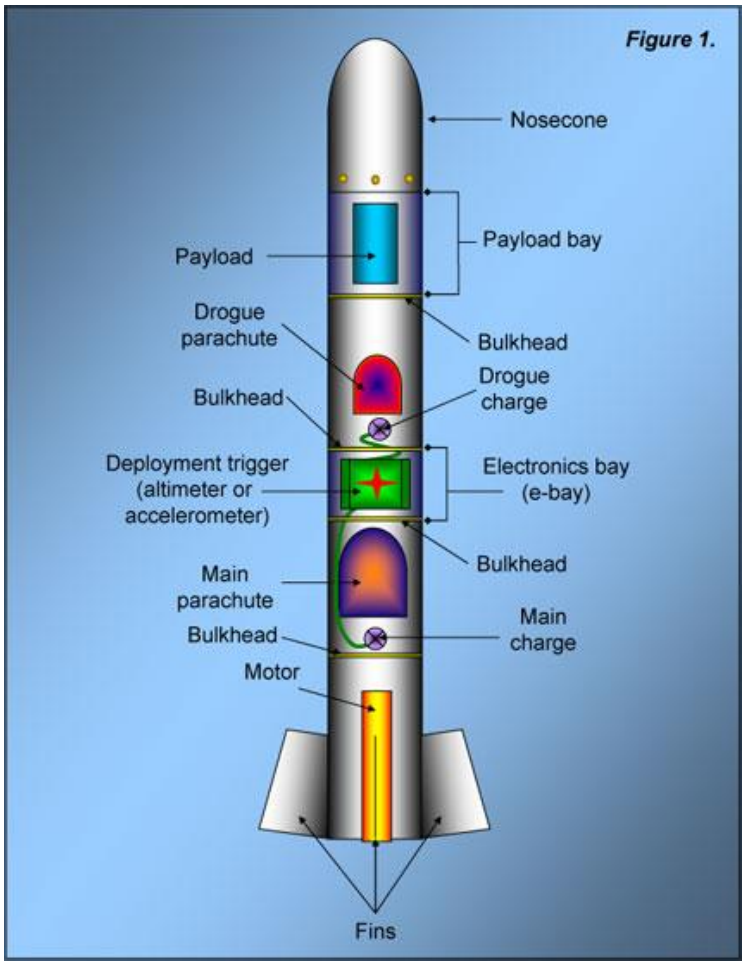

Figure 2.4.2: Typical Dual-Deployment Rocket Schematic [14].

For high altitude rocket launches (above 20,000 feet) there are problems with using typical black powder charges. At these high altitudes, the burn rate of the black powder is significantly reduced, due to the lower density of air. When the ejection charge burns slowly, or does not burn completely it is likely that sufficient gas will not be produced, and the parachute fails to be deployed. This of course causes the rocket to return to Earth at terminal velocity, and destroys the aircraft.

A company, named Rouse-Tech has developed a pyrovalve that resolves this problem by utilizing the gas from a standard Co2 cartridge to deploy the parachute [15]. A diagram describing how the device works is shown below in Figure 2.4.3. In the Rouse-Tech CD3 system, a Co2 cylinder is screwed into the left side of the pyrovalve, while a piercer sits on to in front of the e-match/black powder holder. When a current is passed through the e-match, the e-match ignites, which in turn ignites the black powder. The gas from the black powder propels the piercer into the Co2 cartridge, piercing the cap of the Co2 cartridge. The air from the cartridge then flows through the neck and pushed the piercer back to its original position, while the gas vents out of the holes in the surrounding shell. The gas from the Co2 cartridge then pressurizes the parachute bay, ejecting and deploying the parachute [16].

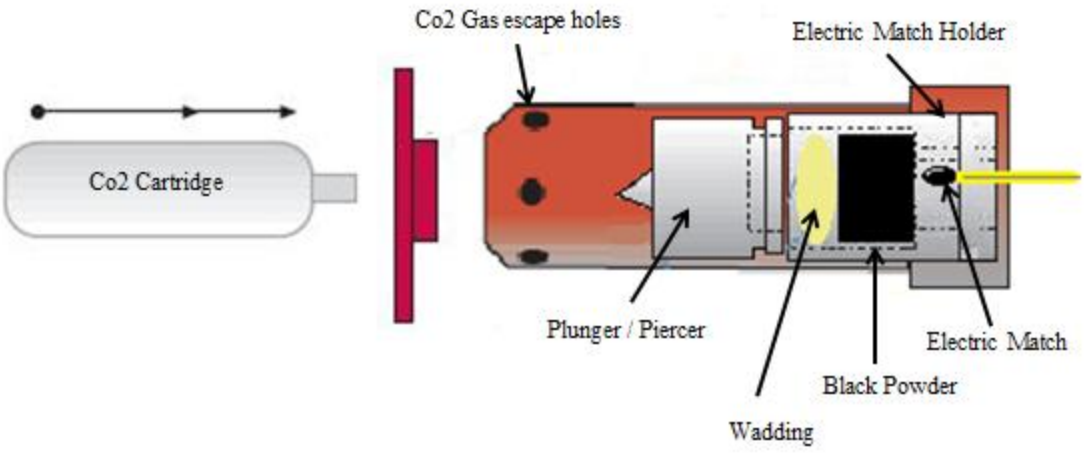

Figure 2.4.3: Rouse Tech CD3 Schematic

The Rouse-Tech CD3 is a very light system, weighing only 77 grams without the Co2 cartridge. In addition, the black powder used in the system is readily available at gun stores, while the e-matches are easy to make or can be purchased from high powered rocketry suppliers. In terms of using the CD3 system as an inflation system, there are a few drawbacks. The system requires cleaning and prepping between uses, and it does not allow for controlling the flow of the Co2 gases, since it was originally designed to allow the gases to easily escape and pressurize a parachute bay. The Rouse Tech CD3 system, in addition to the necessary assembly equipment is shown below in Figure 2.4.4.

Figure 2.4.4: Rouse Tech CD3

An earlier student at OSU first bought this system for his research in inflatable wings. He attempted to make an enclosure for the CD3 system that would capture the Co2 cartridge gas and direct those gases through plumbing, and into an inflatable wing. The enclosure he devised was made of PVC plumbing, which is rated for an operational pressure of about 150 psi, while the Co2 gas that exits the cartridge is at approximately 450 psi. In short, this enclosure proved to be dangerous at best and thus the idea was abandoned. More information about the project and the enclosure can be found in Appendix A on Undergraduate Spacecraft Design Projects.

CHAPTER III

INFLATABLE WING STUDIES

3.1 BACKGROUND INFORMATION

Oklahoma State University and Dr. Jamey Jacob have years of experience when it comes to inflatable structures and inflatable wings. While analyzing an inflatable airbeam, a non-rigid body, may seem like a daunting task, the equations involved at their basic level are fairly straight forward. Using simple pressure vessel equations, the necessary equation for structural analysis is derived. The equation below, Equation 3.1.1, comes from pressure vessel theory. When an inflatable beam experiences a large enough moment, the beam buckles causing the hoop stress at that point to go to zero. Therefore, by setting the left side of Equation 3.1.1 to zero, and solving for the moment, a useful equation for inflatable beams is derived.

$$\sigma = \frac{\pi}{4}\frac{Pd^2}{\pi d} \pm \frac{Md}{2I} \qquad \text{Equation 3.1.1}$$

For an inflatable cylindrical beam, the primary function that is derived, is shown below in Equation 3.1.2, where "P" is the required pressure, "d" is the diameter of the beam, and "M" is the moment applied [17]. While analyzing the necessary pressure and sizing of an inflatable beam may be fairly simple, the true difficulty when designing inflatable structures lies with the material selection and construction process.

$$P = 16\,M/(\pi d^3) \qquad \text{Equation 3.1.2}$$

ILC Dover and OSU often work together on inflatable research programs, and have donated an inflatable wing for our research projects. Initial studies were performed on this wing to evaluate its use as the main wing for this aircraft. A table of the wing's specifications is shown below in Table 3.1.1. The inflatable wing said to have an operational pressure of 8 to 10psi, and an estimated burst pressure of 15 psi.

Inflatable Wing Information				
Airfoil based on the NACA 4318				
b	Wing Span		72	in
c	Chord		12.5	in
t	Thickness		2	in
s	Wing area		900	in^2
AR	Aspect Ratio		5.76	

Table 3.1.1: ILC Dover Inflatable Wing Specifications

The inflatable wing utilizes a concept, known as baffles, to increase the inflatable wings strength, while maintaining the general shaped of an airfoil. A baffle, or baffled wall, is a section of inflatable beams where the circular cross-sections overlap each other and share a common wall. This baffle technique utilizing the same principals as a truss system in bridges and other rigid structures, to help distribute the loads experienced by the inflatable wing's internal pressure. By using this baffled design method, the required pressure needed in order to maintain rigidity is significantly reduced. The bumpy nature of the wing's cross-section causes the wing to experience increased drag and reduced lift compared to their ideal, smooth airfoil counterpart, however they do posses advantages at high angles of attacks over smooth wings [6]. A CAD model of this inflatable wing, as well as its cross section is shown below in Figure 3.1.1 and Figure 3.1.2 for clarification.

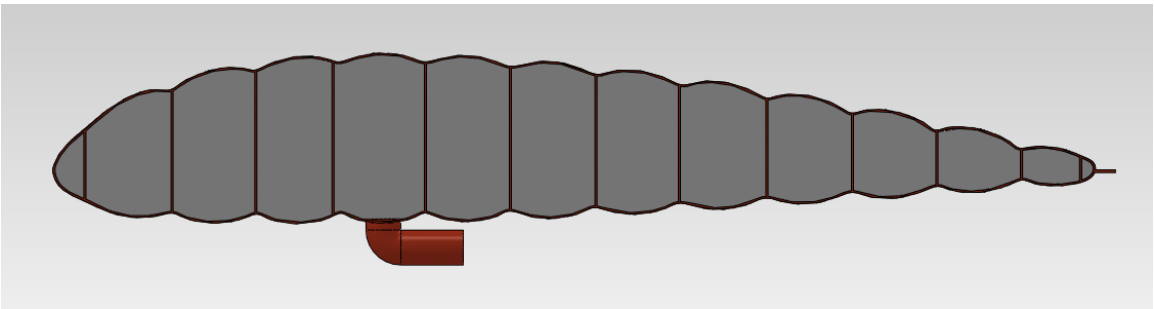

Figure 3.1.1: ILC Dover Inflatable Wing Cross Section

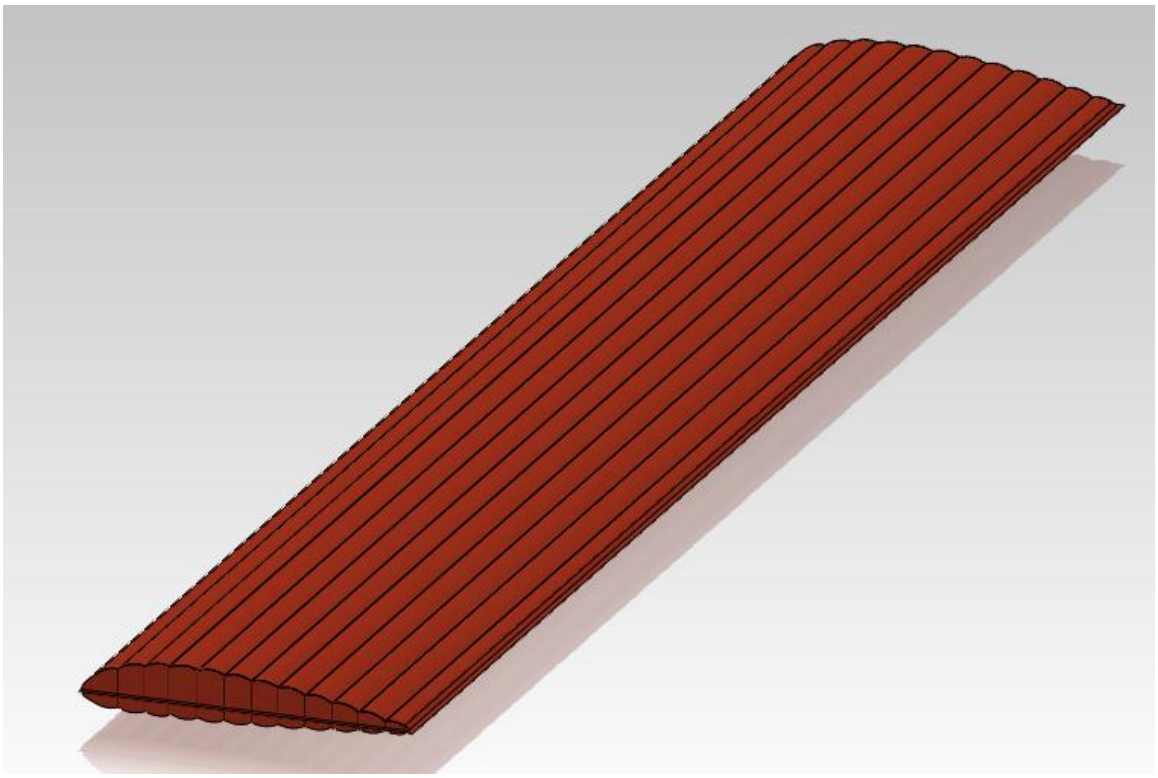

Figure 3.1.2: ILC Dover Inflatable wing CAD model

In order to determine the wings capabilities, some initial information was required. Studies were conducted to determine the wings aerodynamic performance, methods for packing the wing and its stored volume. In addition, wing bending test and leak-rate test were required in order to begin the development of an inflation system.

3.2 THEORETICAL AERODYNAMIC PERFORMANCE

Several reports were utilized in order to evaluate the airfoil of the inflatable wing. Most of the reports utilized CFD in order to evaluate different inflatable airfoils, with different numbers of baffles ranging in size and shape. From these reports, several trends were found when comparing the inflatable version of an airfoil, to their original smooth counter-part. From the figures below, Figure 3.2.1, it can be seen that the coefficient of drag approximately doubles, while the coefficient of lift decreases when the inflatable airfoil is compared to its smooth version. This decrease in lift coefficient is a function of the airfoils angle of attack, and to lesser

extent the coefficient of drag is as well. How much the coefficient of drag and lift is affected, is also very dependent of the Reynolds number that the aircraft is flying at. Inflatable airfoils tend to have an advantage over smoother airfoils at lower Reynolds numbers, as the "bumps" trip the airflow and delay the stall affects so that they occur at higher angles of attack [18] [19] [20].

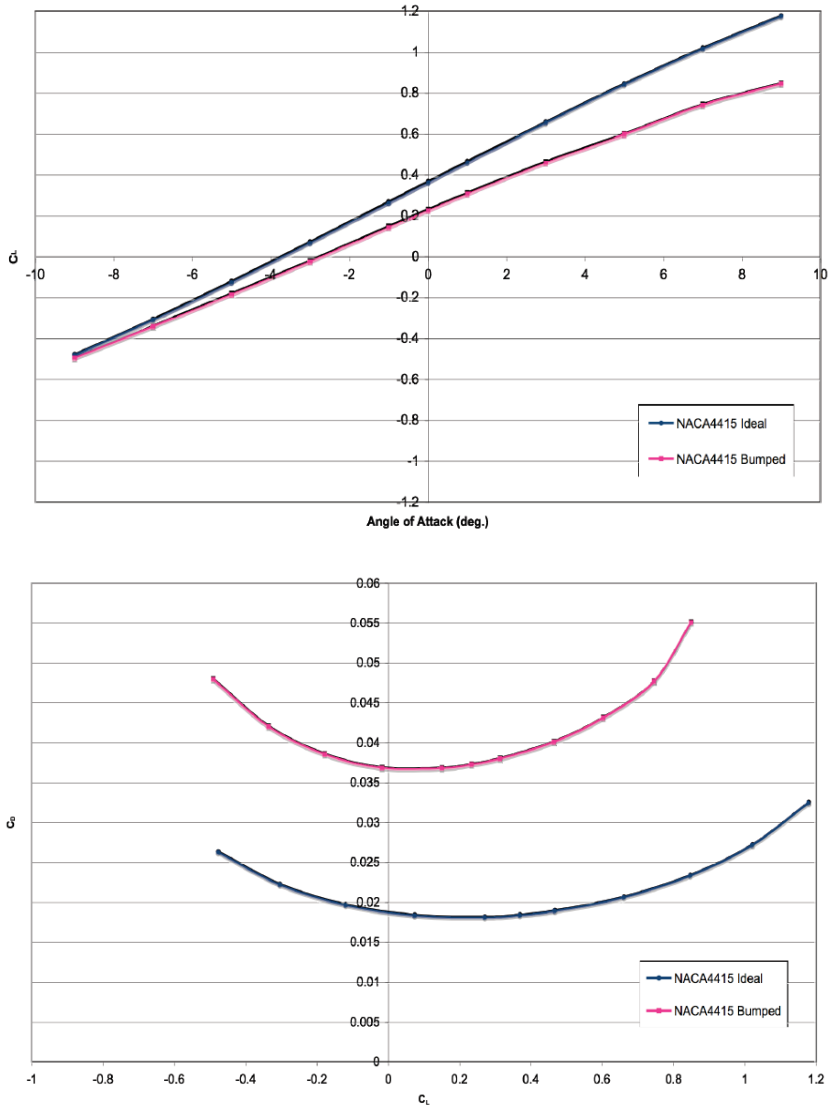

Figure 3.2.1: NACA 4415 CFD Analysis Results **[18]**.

In some cases, graduate students have used these generalizations and simply estimated the Cl and Cd data by modifying the data obtained from programs like XFoil, that utilizes panel

theory to analyze an airfoil and produce Cl and Cd information of a smooth airfoil. In other cases, they have utilized Xfoil, and modified an airfoil to have a trip placed towards the leading edge and/or the trailing edge to simulate an inflatable airfoil [19]. It is important to note, that one cannot simply put a "bumpy" airfoil into Xfoil or Profili and have it analyzed in order to produce this data. This is because both programs utilizes a iterative panel theory analysis technique for each panel, and the iterations are incapable of converging due to the large changes in Cl, Cp, Cd, and Cm data between iterations.

In order to produce this vital information, the student first attempted to simulate the inflatable wing using Profili, by making smoother versions of the same "bumpy" airfoils in hopes that the program would be able to converge. Results were obtained, though the student did not consider them trust worthy, and instead used them more as general guide lines that should prove similar to the actual airfoil data. Instead, the student used the data and results found in *Flight Testing and Simulation of a Mars Aircraft Design Using Inflatable Wings,* as well as the data found in *Computational Fluid Dynamic Study of Flow Over an Inflatable Aerofoil* to develop relations as a function of α, and Re. Both reports utilized CFD analysis to evaluate the performance of inflatable, "bumpy," airfoils and compare them with their ideal, smooth counterparts that they were based on. In addition, Dr. Jacob's students at the University of Kentucky also utilized wind tunnel testing data in order to validate their results. One of the airfoils that was tested during these CFD simulations was the same NACA 4318 airfoil used in the ILC dover inflatable wing. In their testing and analysis, they found that their CFD results closely matched the wind tunnel data [20]. These results and wind tunnel testing data was also utilized by the Richard Innes at Loughborough University to compare and validate the data that he obtained from his CFD simulations. In his report, he discussed program that he developed that allowed him to produce models of a wide range of configurations of inflatable wings and test them using CFD simulations. The student utilized the information from these two reports then,

applied linear interpolation and extrapolation methods in order to produce accurate data, which took into account the changes with angle of attack, and Reynolds number.

As seen in the previous figures, the lift curve slope changes when comparing the bumpy, inflatable airfoil, to the ideal, smooth airfoil. In the report by Daniel Reasor data is supplied for the same ILC Dover airfoil of the inflatable wing, NACA 4318, at two different angles of attacks, and two different Reynolds numbers, as shown in Table 3.2.1. The student utilized this information, and calculated the lift curve slope, and was able to determine the change in lift curve slope, and slope-intercept from the ideal and bumpy airfoils at the two different Reynolds numbers, using Equation 3.2.1. The lift curve slope equation used for these calculations is show below.

Airfoil	Re	α	C_l	C_d	L/D	St
E398 Ideal	$18k$	7^o	1.041	0.012	86.59	1.465
E398 Bumpy	$18k$	7^o	0.467	0.010	47.11	3.418
E398 Ideal	$18k$	10^o	1.232	0.04	29.72	1.465
E398 Bumpy	$18k$	10^o	0.819	0.069	11.877	3.418
E398 Ideal	$36k$	7^o	1.316	0.040	33.19	1.465
E398 Bumpy	$36k$	7^o	0.690	0.028	24.46	3.418
E398 Ideal	$36k$	10^o	1.287	0.099	12.943	1.221
E398 Bumpy	$36k$	10^o	0.873	0.082	10.70	3.418
NACA4318 Ideal	$10k$	0^o	-0.146	0.065	-2.241	1.953
NACA4318 Bumpy	$10k$	0^o	0.111	0.066	1.689	4.638
NACA4318 Ideal	$10k$	10^o	0.727	0.101	7.173	0.732
NACA4318 Bumpy	$10k$	10^o	0.522	0.047	11.08	2.441
NACA4318 Ideal	$200k$	0^o	0.284	0.024	11.597	9.766
NACA4318 Bumpy	$200k$	0^o	0.115	0.042	2.763	3.418
NACA4318 Ideal	$200k$	10^o	1.047	0.129	8.140	1.708
NACA4318 Bumpy	$200k$	10^o	0.676	0.022	31.194	3.418

Table 3.2.1: CFD Results including NACA 4318 Airfoil **[20]**.

$$\frac{dCl}{d\alpha} = \frac{Cl_2 - Cl_1}{\alpha_2 - \alpha_1}$$ Equation 3.2.1

In the report, *Computational Fluid Dynamic Study of Flow Over an Inflatable Aerofoil*, data is given for various airfoils and how their Cl and Cd data change as a function of angle of attack, when compared to their ideal airfoil counterparts, in addition to the raw data obtained from their CFD analysis for the various airfoils. This change in Cl and Cd information was then applied to the data obtained using Xfoil for the ideal smooth airfoil by use of a percent change calculation from the data from the two sets. From this data analysis, the following Cl and Cd information was obtained, shown in Table 3.2.2. The data is graphed and compared against the ideal version of the airfoil in Figures 3.2.2 and 3.2.3. During the early design phase of this aircraft, it was estimated that the cruising speed would result in a Reynolds number of approximately 500,000. The data used for the coefficient of moment was not altered in any way between the ideal and inflatable airfoil, as no information was available in the various reports, on how this coefficient is affected in inflatable airfoils.

naca-4318 - Re = 500000				
Alfa	Cl	Cd	Cl/Cd	Cm
-8	-0.332	0.0152	-21.84	-0.109
-7	-0.24	0.0136	-17.61	-0.105
-6	-0.151	0.0124	-12.21	-0.1
-5	-0.063	0.0117	-5.376	-0.095
-4	0.0238	0.0113	2.1062	-0.09
-3	0.1065	0.0109	9.7706	-0.083
-2	0.1868	0.0106	17.623	-0.076
-1	0.2601	0.0105	24.771	-0.068
0	0.308	0.0095	32.421	-0.055
1	0.3611	0.0093	38.828	-0.042
3	0.6918	0.011	62.891	-0.064
4	0.8548	0.0122	70.066	-0.075
5	1.0004	0.0129	77.55	-0.083
6	1.0385	0.0132	78.674	-0.069
7	1.0919	0.0139	78.554	-0.058
8	1.1654	0.0151	77.179	-0.052
9	1.2284	0.0159	77.258	-0.044
10	1.2937	0.017	76.1	-0.037
12	1.4182	0.0203	69.862	-0.025
13	1.4644	0.0232	63.121	-0.018

Bumpy Airfoil - Re = 500000				
Alfa	Cl	Cd	Cl/Cd	Cm
-8	-0.339	0.026	-12.95	-0.109
-7	-0.266	0.024	-11.15	-0.105
-6	-0.193	0.022	-8.658	-0.1
-5	-0.107	0.022	-4.951	-0.095
-4	-0.123	0.021	-5.746	-0.09
-3	-0.103	0.021	-4.872	-0.083
-2	0.004	0.021	0.1896	-0.076
-1	0.074	0.021	3.5019	-0.068
0	0.125	0.019	6.4927	-0.055
1	0.171	0.019	9.1918	-0.042
3	0.382	0.021	17.906	-0.064
4	0.492	0.023	21.338	-0.075
5	0.595	0.024	25.007	-0.083
6	0.632	0.024	26.639	-0.069
7	0.678	0.024	27.809	-0.058
8	0.735	0.026	28.22	-0.052
9	0.784	0.027	29.108	-0.044
10	0.835	0.028	30.151	-0.037
12	0.932	0.032	29.346	-0.025
13	0.969	0.035	27.868	-0.018

Table 3.2.2: Airfoil Data Comparison, Re=500,000

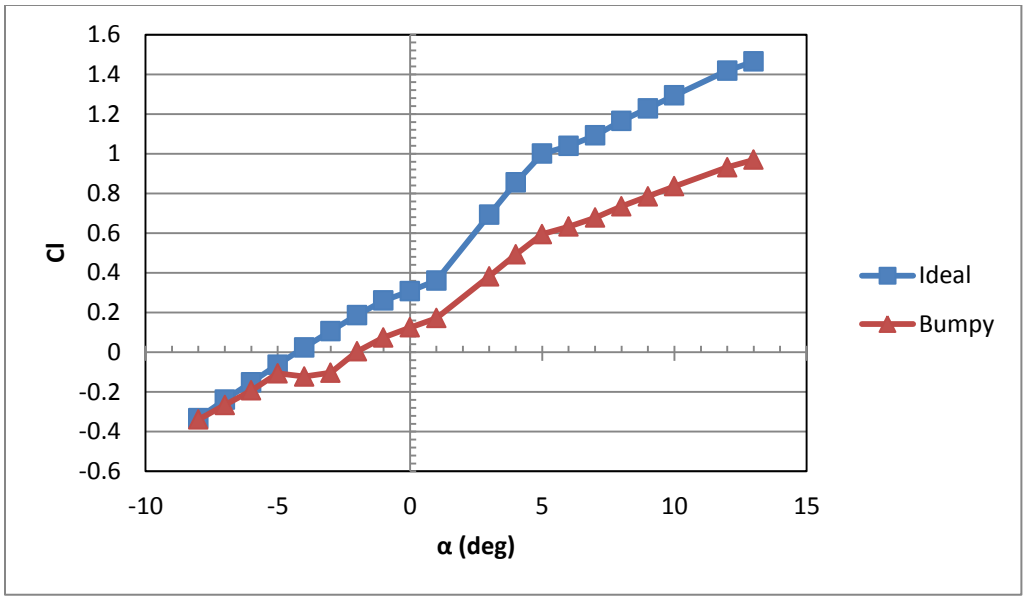

Figure 3.2.2: Cl vs α; NACA 4318, Re=500,000

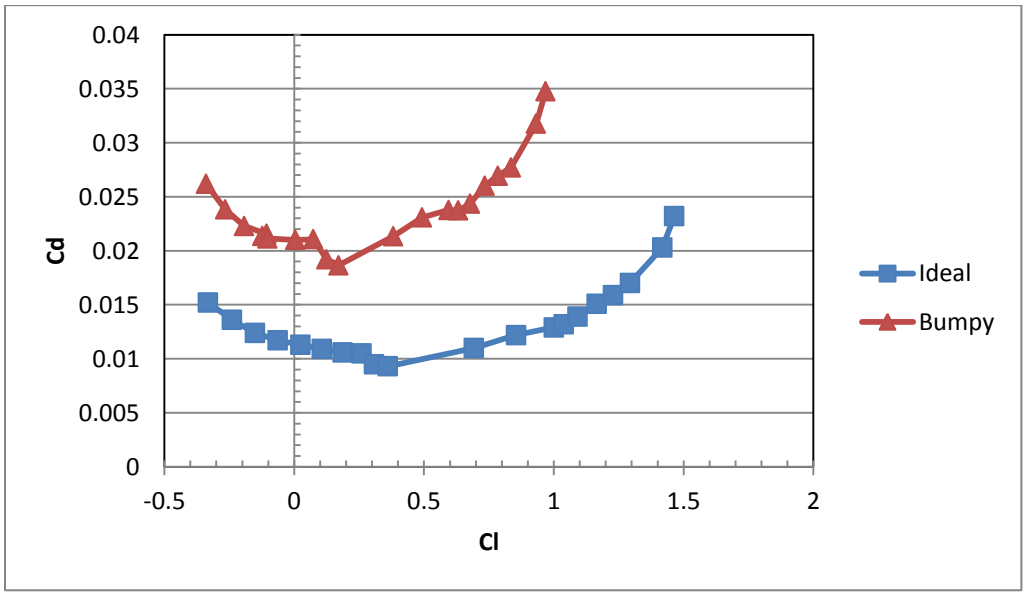

Figure 3.2.3: Cd vs Cl; NACA 4318, Re=500,000

As seen in the data above, the values obtained for Cl and Cd follow closely with the generalizations discussed previously. The coefficient of drag approximately doubles, while the coefficient of lift decreases slightly. The data was also compared to those from the CFD model reports and was proven to be very similar. From these results obtained through these analyses, the

student believes that this method of applying linear interpolation to CFD data on the inflatable wing airfoil is a fairly accurate method. It is also the student's belief that if more accurate data were necessary, that CFD analyses or wind tunnel testing would need to be performed on the airfoil throughout the range of angles of attack. Using the ILC Dover inflatable wing's cross-sectional (two-dimensional) aerodynamic performance obtained from these analyses, the data could then be corrected for aspect ratio, and the three-dimensional wing aerodynamic performance could be obtained. Discussion of the 3D wing aerodynamic performance is discussed further in Chapter 5.

3.3 WING LOADING AND LEAK RATE TESTS

In order to determine the capabilities of the ILC Dover inflatable wing, the load carrying capacity of the inflatable wing, and the leak rate of the wing had to be determined. During my experience as a researcher at OSU we have built many different inflatable beams, structures, and inflatable wings. As a general rule of thumb, the more complicated the object is that is being made, the higher the chance for inconsistencies in the seals that make up that inflatable object, which results in a higher leak rate. As far as inflatable wings go, they have been by far the hardest to make, and most likely to leak excessively.

Initial planning and designing for this inflatable wing aircraft had the estimated flight duration to be between 15 to 20 minutes. When the ILC Dover inflatable wing was being tested for its leak rate, the inflatable wing was inflated to its maximum operational pressure of 10 psig and left to sit. The pressure was initially checked using a digital pressure gauge with tenths of a psi precision, then removed. No pressure gauge or plumbing was connected to the inflatable wing, as experience has taught me that leaks within the plumbing are just as likely (if not more) to occur as in the inflatable object itself. Instead, the inflatable wing's nozzle was capped by use of a one-way valve, and every fifteen minutes over the course of two hours, the wing was checked to see if there was a noticeable change in pressure. Over these two hours no noticeable

change had occurred, and the wing's pressure was checked. The pressure had only decreased by 0.3 psig over the course of the two hours! A change in pressure that small is miraculous when compared to the inflatable wings I have built and tested. In addition, a change that small could have occurred as a result of me checking the pressure, as air escapes each time the pressure gauge is connected and disconnected.

Once it was found that the inflatable wings had a negligible change in pressure over the course of 2 hours – approximately 8 times the estimated flight time, it was determined that if any leaking were going to occur, it would be within the inflation system I designed and built, and not in the inflatable wing. To make these results more conclusive, the inflatable wing was again inflated to its maximum operational pressure (10 psig) and left to sit overnight. The next day, 24 hours later, the inflatable wing's pressure was checked again and found to be 8.7 psig. A pressure change of 1.3 psi over the course of 24 hours! The ILC Dover Inflatable wing has the smallest leak rate I have ever seen.

With this information, the student then performed bending (wing loading) tests on the inflatable wing. The wing loading tests were conducted in order to simulate aircraft G-loads at the upper and lower bounds of the inflatable wings operational pressure range; 8psi and 10 psi respectively. From the initial aircraft conceptual design process, the gross weight of the UAV was predicted to have a total weight of approximately 10 lbs. During early analysis, it was uncertain whether the wing would have an elliptical lift distribution (typical for rectangular shaped wings) or have flat, linear lift distribution (typical for elliptical wings) due to the unconventional nature of the inflatable wing and due to the rounded wing tips on the inflatable wing. Since the resultant force for both elliptical wings and rectangular wings are at approximately at the quarter-span , it was decided to conduct bending tests with supports placed at these locations.

Bending tests were conducted at both 8 and 10 psi, and were performed by having chairs placed at the quarter-span on either side of the inflatable wing for support. Weights were placed at the mid-span to simulate the aircraft weight, or high g-loads, and increased in increments of 2.5 lbs until the wing buckled. The deflection of the inflatable wing's mid-chord was measured at each interval. This data allowed the student to calculate the dihedral angle of the inflatable wing as it undergoes more loading. This dihedral angle plays an important role in the aircraft's flight characteristic and helps to improve stability during flight. The experimental setup used during the experiment is shown below, in Figure 3.3.1.

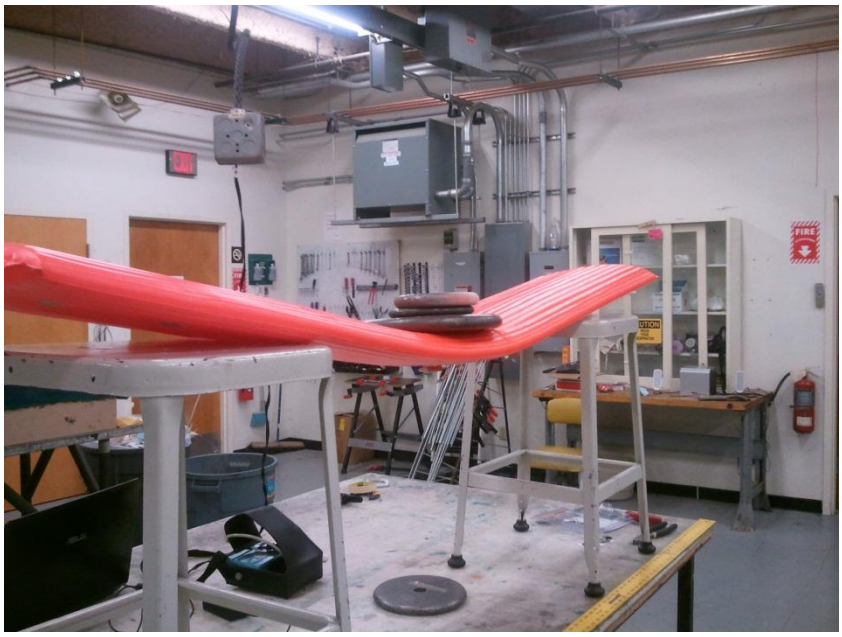

Figure 3.3.1: Inflatable Wing Bending Test Experimental Setup

During the first test with the inflatable wing at 8 psi the wing withstood approximately 37.5 lbs before buckling, meaning that the aircraft could potentially perform a banking maneuver at approximately 4-G's. Meanwhile, at 10 psi the wing was able to withstand 52.5 lbs before buckling, or 5-G's. While it is important to note that these wing loading tests are not representative of actual in-flight conditions, it does provide a reasonable estimation to the wing's

load capabilities. Comparing these G-loads to other commercially off-the-shelf (COTS) RC aircraft, put this inflatable wing in the same class of aircraft as other stunt RC aircraft and some 3D flying aircraft. This means that for this aircraft intended use, the inflatable wing would likely be stronger than necessary for a typical surveillance type mission. On the other hand, it also means that the student could inflate the aircraft to a lower pressure and yet the wings would not buckle during a typical flight. It is also important to note how the dihedral angle changes as a function of wing loading. In terms of stability, an aircraft that utilizes dihedral angle typically has an angle from 1 to 3 degrees, with 5 degrees being considered fairly high. In both cases, the dihedral angle stayed within a reasonable range that would improve the stability of the aircraft. The results from the bending tests are shown below, in Figures 3.3.2 and 3.3.3, while tables of the data are included in Appendix B.

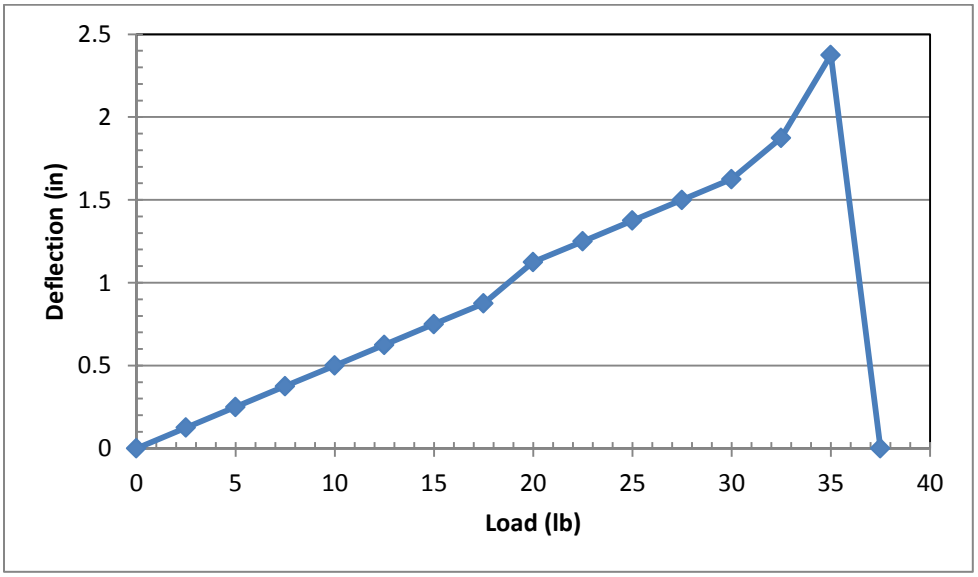

Figure 3.3.2: Wing Loading Test, 8psi

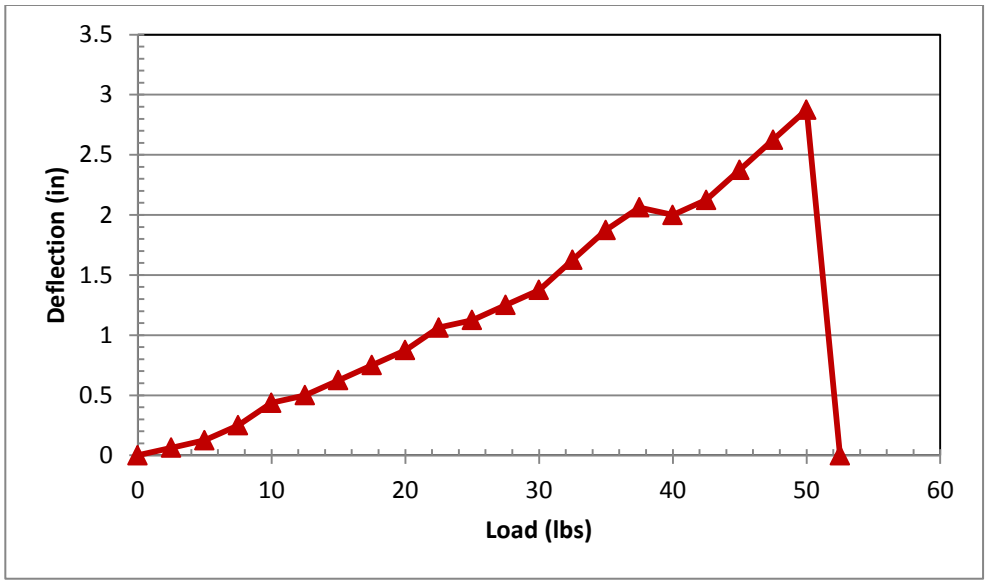

Figure 3.3.3: Wing Loading Test, 10psi

3.4 INITIAL DEPLOYMENT TESTS

How the inflatable wing is stored and deployed from the UAV was a major design consideration during the early design phase. In the NASA Dryden I2000 project, and ILC Dover's Quicklook/FASM UAV, a Z-fold method (Figure 3.4.1) was utilized in order to deploy the inflatable wings [7] [19]. However, in a report released by OSU, a Roll Method was developed and studied, as shown in Figure 3.4.2 [2]. The student chose to study these two methods, as well as another, called Wrap Method, shown in Figure 3.4.3.

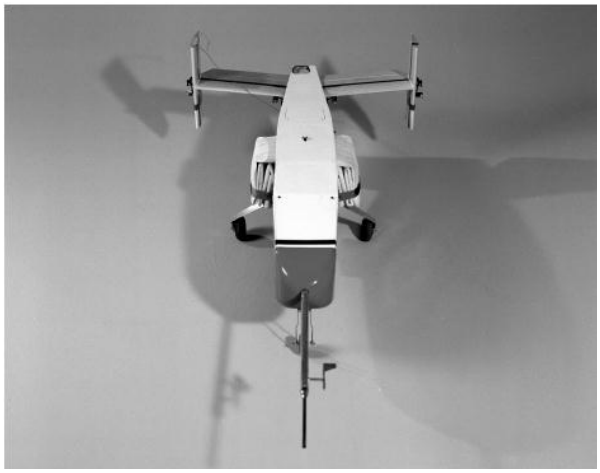

Figure 3.4.1: Z-Fold Method in the NASA I2000 Project **[7]**

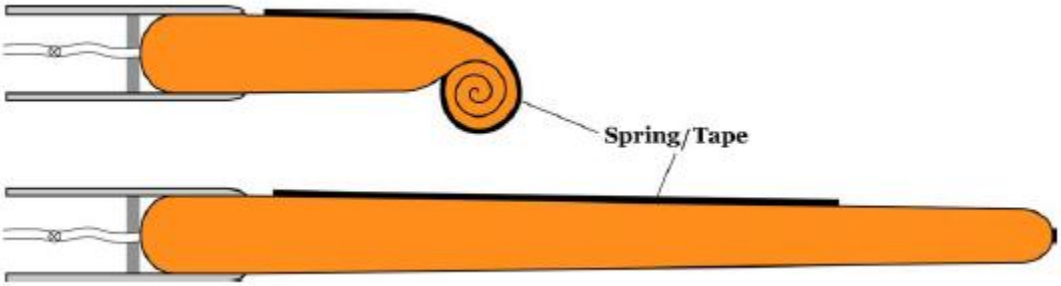

Figure 3.4.2: Roll Method **[2]**

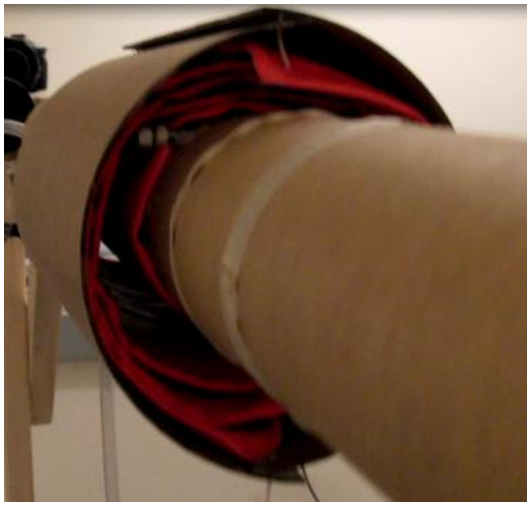

Figure 3.4.3: Wrap Method

Utilizing these three different packing methods, the student studied the compact volume of each, how these different packing methods would affect the aircraft's design, and how these packing methods would affect the aircraft during deployment. The student studied the compact volume for the Roll and Z fold method for internal wing stowage, in addition to studying the three previously stated method of external wing stowage. From the internal wing stowage methods, the student found that storing internally is very difficult for Z-fold methods and would require the aircraft to have a body diameter of at least 5 to 6 inches wide, in order to provide structural connections points as well as a method of attaching the inflation system. Additionally for the Roll method, the aircraft would be required to have a width of approximately 8 to 9 inches in order to accommodate it.

From these tests, it became apparent that storing the wing externally from the aircraft would provide the best results, as there would be little to gain from an increased body diameter. The student found that by storing the wing externally, there would be sufficient space towards the core to provide structural attachment points for the wings, as well as provide space for the inflation system. The wing would be packed in any one of the three methods around the aircraft body with a shell-like structure inclosing the wing until its deployment. A mockup of this shell structure was produced and early inflation rate testing was allowed to proceed. The shell mockup is shown below in Figure 3.4.4.

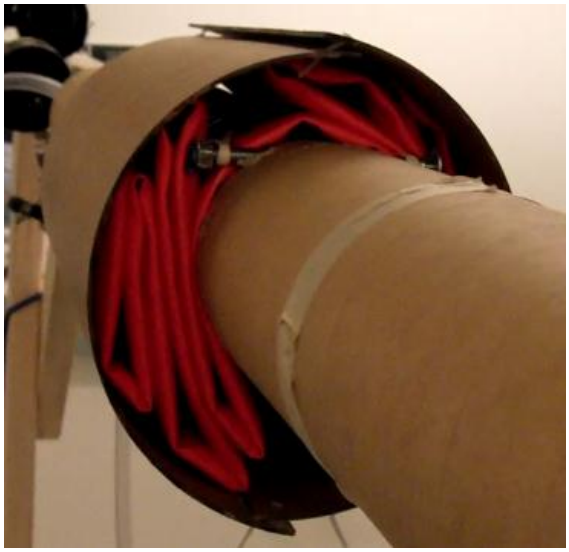

Figure 3.4.4: External Shell Mockup, featuring Z-fold packing method

To perform inflation tests, a test rig was developed that would allow the students to perform static inflation tests, as well as dynamic inflation tests. The dynamic inflation tests were performed by having the wing stowed inside the shell, and the test rig loaded into the back of a truck. The aircraft mockup was exposed to the free stream, as the truck traveled down a smooth street. Once the truck reached its target velocity, the wing was deployed. A camera was mounted to the test rig, and was used to monitor pressure as well as the aircraft attitude during deployment. The inflation rate was controlled by throttling the flow rate of air from a compressor, via a built in regulator. The rate of inflation was limited by the output of the air compressor, and therefore rapid inflation tests (less than 1 second until the wing is fully pressurized) could not be performed at the time. A vacuum pump was utilized in between inflation tests to remove the air from the inflatable wing, and return it to its initial packed conditions. The experimental setup is shown below in Figure 3.4.5.

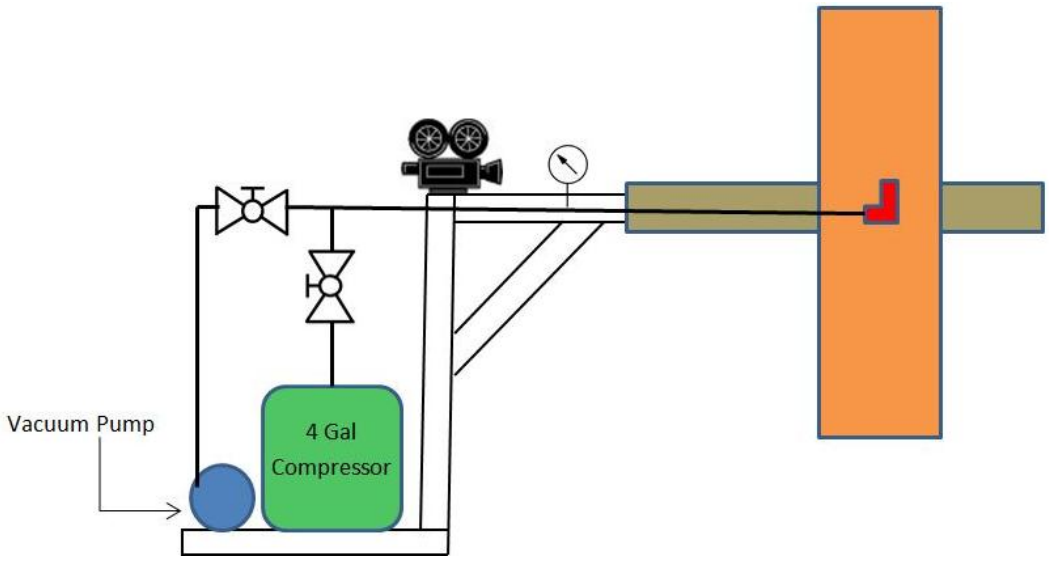

Figure 3.4.5: Inflation Rate Experiment Setup

The student performed deployment tests at static conditions as well as dynamic tests. The dynamic tests were conducted with the truck traveling at 15 mph into a head wind, that varied from 17 to 19 knots (19 to 22mph), for a relative velocity of approximately 35 mph. This speed is slightly lower than our predicted max cruise speed of 50 mph, meaning that any unsteady affects would be amplified during flight. From the students testing, it became very obvious that the Z-fold method would be the most reliable and more importantly, less hazardous to the aircraft as it transitions during flight. The wrap method provided a lot of unnecessary stress on the aircraft mockup, and produced significant damage to the body, limiting the amount of testing that could be conducted. The Z-fold and Roll method were both able to deploy from the aircraft without causing damage, or putting the aircraft into an undesirable attitude, though from both the static and dynamic tests, it was seen that the Z fold method produced the least head pressure, and thus was able to deploy faster. Some of the footage from the dynamic deployment tests are shown below in Figures 3.4.6, 3.4.7, and 3.4.8, as well as the data collected from these tests, in Table 3.4.1.

	Folding Method		
	Z Fold	wrap	roll
Avg shell deployment time	0:00	0:01	0:01
Avg wing rigid time	0:07	0:09	0:10
	all units in seconds		

Table 3.4.1: Dynamic Inflation Test Results

Figure 3.4.6: Z-Fold Dynamic Inflation Test

Figure 3.4.7: Wrap Method Dynamic Inflation Test

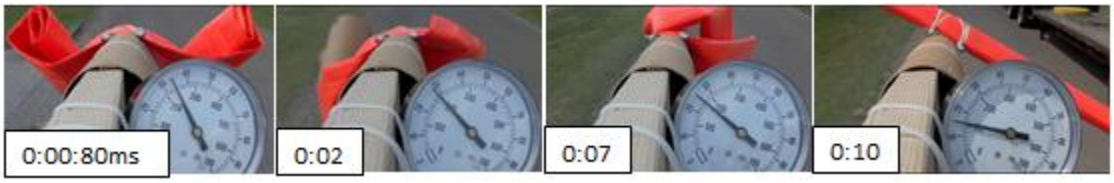

Figure 3.4.8: Roll Method Dynamic Inflation Test

During the dynamic deployment tests, the student witnessed how the unsteady aerodynamic affects played an important role as the aircraft deployed it wings at low flow rate. The inflatable wing would contort and fold in odd ways, and often flail around in the wind. These inflation tests using a slow inflation rate resemble the results seen in previous wind tunnel tests, conducted by OSU [2]. From these dynamic tests, it became obvious that a very rapid inflation

time would be required in order to prevent the aircraft from entering hazardous attitudes and damaging the aircraft.

Using the video footage taken during testing, the student was able to calculate the roll rate of the aircraft during deployment, and how the inflation process affected this roll rate. From the students calculations a deployment rate of approximately 0.75 to 1.0 seconds maximum would be most ideal. This rapid inflation would allow the aircraft deploy its wings without being exposed to significant unsteady affects, and would help to ensure the safety of the vehicle. In order to calculate the rolling rate, Equations 3.4.1 and 3.4.2 were used, while the results obtained from the video footage and analysis are shown in Table 3.4.2.

$$L = C_{l,roll} Q S l \qquad \text{Equation 3.4.1}$$

$$C_{l,roll} = \frac{-2p}{S b u_0} \int_0^{b/2} c_{l_\alpha} \, c y^2 \, dy \qquad \text{Equation 3.4.2}$$

ρ	0.002377	slugs/ft^3			Initial		Final		
v	35	mph			ti	0:26	tf	0:27	
v	51.33333	ft/s			θi	0	θf	73	deg
q	3.131698	lb/ft^2			Δt	1	sec		
					Δθ	1.27409	radians		
cl	0.194444				radius	36	inches		
L	3.80587	lb		θdot	ω	1.27409	s^-1		
rolling moment									
cl	-0.03241	theoretical			cl	-0.01108	Nelson Eq 3.96		
					roll moment experimental				

Table 3.4.2: Roll Moment Coefficient, Theoretical (left) and Experimental (Right)

The footage taken during testing as well as the compressor specifications was used in order to obtain an approximation for the inflatable wing's volume. The student was able to calculate the compressor's flow rate, and use the inflation time from the videos to develop these

estimations. The equations used for these estimations are shown below, in Equations 3.4.3 and 3.4.4.

$$P_1V_1 = P_2V_2 \qquad \text{Equation 3.4.3}$$

$$P_1CFM_1 = P_2CFM_2 \qquad \text{Equation 3.4.4}$$

Now that the student was able to calculate the volume, and flow rate of the compressor, and also knew approximately what inflation time was required, the student was able to reuse the same equations discussed previously, to find out the CFM that would be required to fill the volume within a certain time frame. The student found that in order to conduct sub-one second inflation tests, a compressor rated for 8 CFM at 90 psi (or better) would be required. A compressor with these ratings is often fairly large and expensive. The results from the volume estimation, compressor flow rate information, and desired inflation rate calculations are tabulated below (Table 3.4.3). For more information on these inflation tests, analysis, and results, see the report *Deployment Methods of Inflatable Wings in Mid-Flight*.

3	cfm	@	90	psi	Compressor data	
2.331829	cfm	@	120	psi	test pressure	
↓						
67.15667	in^3 per second					
0.001101	m^3 per second					
Avg time to get to 8 psi, fully inflated				16	second	
		air volume		1074.507	in^3	
	desired inflation time			0.75	second	
	necessary flowrate			1432.676	in^3/sec	
desired flowrate		1074.507	in^3 per second			
		37.30926	cfm	@	8	psi
		8.087902	cfm	@	90	psi

Table 3.4.3: Wing Volume and Flow Rate Calculations and Results

From these deployment tests the student found that the Z-fold method would provide the most reliable and fastest deployment, while minimizing unsteady aerodynamic affects, and

minimizing the possibility of damaging the aircraft during flight. In addition, the student found that a near instantaneous inflation rate would be most ideal. These results and findings mirror the aircraft and inflation systems used by ILC Dover in the FASM/Quicklook project, as well as NASA's I2000 aircraft [9] [7]. With these details worked out, the design of the aircraft began to take shape, and the student was able to turn their attention to the designing of the inflation system that would be used in the inflatable wing UAV.

CHAPTER IV

INFLATATION SYSTEM DEVELOPMENT

4.1 INFLATION SYSTEM METHODS

In order to develop an effective inflation system, one must consider the aircraft's operation, flight duration, required pressure, and leak rate of the inflatable wing, as well as the plumbing used between the two components. The student began the design process by benchmarking and comparing the inflation systems used in the ILC Dover Quicklook/FASM program, NASA I2000, previous research conducted at OSU, as well as the knowledge and previous experience obtained through the years of high powered rocketry flights.

Discussions of each of these systems were described fully in Chapter 2 Literature Review, but a discussion of the advantages and disadvantages are discussed here as well. In the NASA I2000 inflation system a very high pressure (1800 psig) vessel was used to store the inflation system gas, and during their testing, it was found that they could only inflate the wing 180 psig when their wing was rated to be pressurized up to 300 psig [7]. It is this researcher's belief that the cause for this problem was that their relief valve was integrated very closely to the exit of the high pressure tank. When an inflation system is designed to inflate the wing rapidly, a high pressure vessel must be used, and the air must be allowed to fill the inflatable wings up to their designed pressure before any air is released. When the relief valve is next to the exit of the pressure vessel, a lot of air is lost as soon as the inflation system is actuated. This is because the air flowing out of the pressure vessel is at a high pressure, higher than the setting for the relief valve, and therefore the relief valve is opened and releases the gas out of the system. In general it is my belief that it is better to have a relief valve as far down-stream (such as built into the wing-tips) or not included at all, if possible. This is because the inflation system gas is moving at such a

high flow rate and high pressure when the system is initially actuated, that too much inflation gas is lost, which requires a larger than necessary pressure tank, which can increase the system weight significantly.

The actuation system used in I2000 to release the inflatable wings and trigger the inflation process was extremely complicated. A pneumatic release pin with multiple valves, and a separate pressure vessel was used to release the inflatable wings, when something as simple as a Velcro strap, or pop-off straps could have been used instead (as shown in the research conducted at OSU) [7] [2]. In addition, with all of the tubes, connection points, and valves built into the system, there is a high chance for leakage to occur at any one of the points.

The I2000 inflation system had several advantages over other inflation systems studied. The ability to easily refill the high pressure tank used for the inflating the main wing allows for more testing, and a better understanding of the capabilities of the inflation system. In addition, the servo-actuated spool valve (small enough to fit and function in such an aircraft) that ultimately controlled the inflation process was quite ingenious. I only wish that more information was available on this device.

The Quicklook/FASM aircraft inflation system is an elegantly simple way to solve such a complex problem. The problems that were experienced with the inflation system burning through some of the inflatable materials seems like something that could be resolved, given the time to redesign the system and develop a second version. In addition, this system has a huge advantage, in that very little volume is taken up by the system, and almost all of the mass in the inflation system goes directly into producing the necessary gas to inflate the wings. The biggest draw back from this system is the chemical nature of the gas generator. Each time the system is tests, a new chemical gas generator must be produced. This surely must have caused limitations on the amount of testing that could be conducted. From the diagram of the gas generator system, it is

apparent that a small , electric-match was used to initiate the burning of the chemical gas generator.

In the research conducted at OSU, a small pump was primarily used to provide a slow inflation process. As discussed earlier, a high rate of inflation is desired and any pump that would be able to inflate an inflatable wing in less than a second is simply too large and heave to be used in an aircraft. The report also looked into using a paintball gun canister to provide the inflation gas for the inflatable wing, similar to how the NASA I2000 system works. The problem with using a paintball tank is that the smallest available size is 13 cubic inches and 3000 psig and is 2 inches in diameter, which provides way more gas than necessary to inflate the wing being used for this project. The wasted gas and volume, in addition to added weight (most paintball tanks are made of steel, or steel wrapped in carbon fiber) provides too much of a constraint on the design of the aircraft and is highly inefficient.

Once the Rouse Tech CD3 system and pyro-valve technology was looked into closely, some interesting advantages and disadvantages were discovered. Co2 canisters come in a multitude of standard sizes ranging from 8 grams 126 gram canisters. In addition, two or more canisters can be utilized in order to provide the exact amount of Co2 necessary to inflate a volume. Co2 cylinders are also readily available in many stores, and easy to purchase online. However Co2 canisters are still quite heavy, being made of steel, though if the precise amount of Co2 (grams) needed is found, then there is very little wasted space and weight, as compared to paintball tanks, or the I2000 pressure vessels. In addition, once the precise amount of Co2 is found inflate a volume, then the need for a relief valve is completely removed, since there exists just enough gas in the cartridge to inflate the volume completely to its operational pressure. If the leak rate of the inflatable wing or inflation system is poor, then another system could be added to provide the make-up gas needed to keep the wing inflated throughout its flight. Furthermore,

pyro-valves are so light weight, and require such little energy to actuate that it makes the system very appealing. The only downside to using a pyro-valve as a wing inflation system as that it must be cleaned in between uses, meanwhile the black powder used in the system is readily available at gun stores, or rocket launches, and the e-matches can be easily home made with materials found in stores, or can be purchased online, or at rocket launches. Meanwhile, there exists only a small chance that any damage to the inflatable structure could occur from the heat of the black powder charge, or the freezing temperature from a Co2 cartridge being instantly emptied.

Once each one of these systems were studied, the best option became very apparent. A system similar to the Rouse Tech CD3 should be used, though it required a complete redesign in order to channel and direct the Co2 gases, and mitigate leakages in the inflation system. A system that utilizes a pyro-valve for its inflation system provides high reliability, with minimal risk from fire or otherwise, minimal power requirements, while requiring a reasonably small weight and volume. In addition, by piercing a Co2 cartridge all of the gas is expended almost immediately, which would provide the near instantaneous inflation rate of the inflatable wing that is desired.

4.2 PROOF OF CONCEPT

In order to develop a pyro-valve inflation system, the concept would first have to be proven. The student started first by making a new exterior shell (lathed using 1” diameter aluminum), and re-using the same piercer and e-match holder from the Rouse Tech CD3 system. The inflatable wing from ILC Dover initially had a one-way, plastic valve attached to the wing, therefore the same type of plastic valve was used on the pyro-valve I developed to see if it would be able to withstand the pressures from the Co2 cartridge. The first iteration of the inflation system, prior to the experiment is shown below, in Figure 4.2.1.

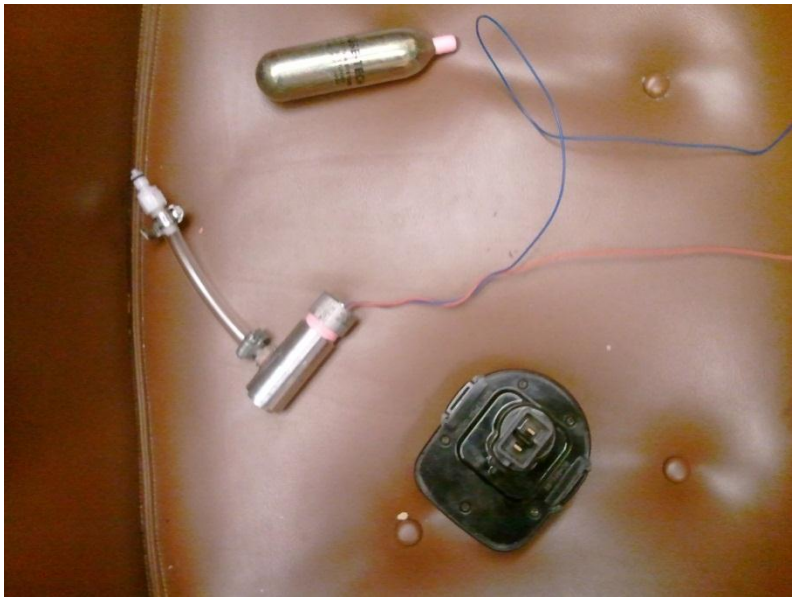

Figure 4.2.1: First Pyro-Valve Inflation System made

The inflation system was prepped in the same way as the Rouse-Tech system is, and was connected to a small test-sized inflatable wing. The purpose of the first test was not to see if the inflatable wing would fully inflate, but rather to see if the inflation system would work. The experimental setup and results from the first test of this system are shown below in Figures 4.2.2 and 4.2.3 respectively.

Figure 4.2.2: First Pyro-valve Experiment setup

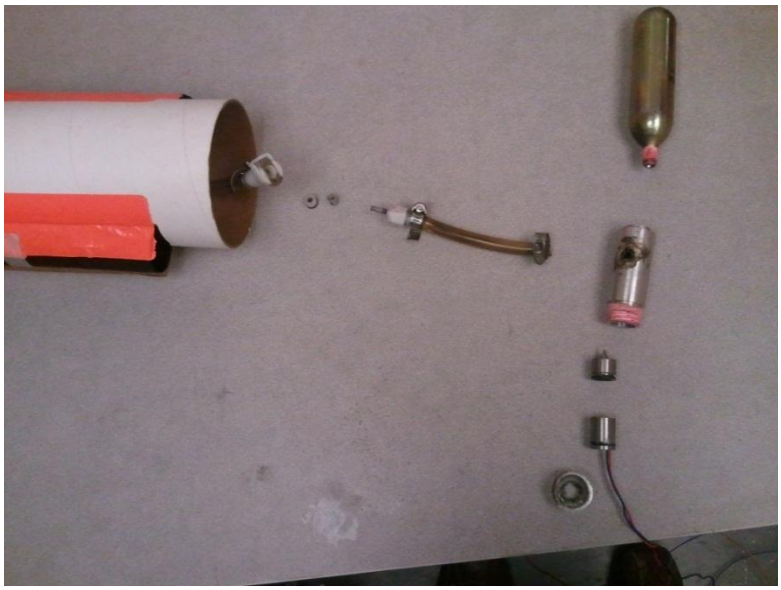

Figure 4.2.3: First Pyro-valve Experiment results

As seen in the images above, the first pyro-valve test was a failure. The pyro-valve was able to ignite the black powder, and propel the piercer with enough force to open the Co2 cartridge. The plastic connections on the pyro-valve were destroyed instantly when the Co2 gas was released and the wing did not inflate. Furthermore, part of the plastic valve was left inside of the exterior shell and could not be removed.

Work then began on another inflation system; one with metal fittings that would be able to withstand the pressure from the Co2 cartridge. Brass fittings were selected for this second iteration of the design, as they are readily available, and would certainly be able to handle the pressure from the Co2 cartridge. As a result, the brass fittings made this inflation system exceptionally heavy. While the Rouse Tech CD3 system that this inflation system was designed after only weighs 77 grams, the second iteration of the inflation system weighted 270 grams, as shown in Figure 4.2.4.

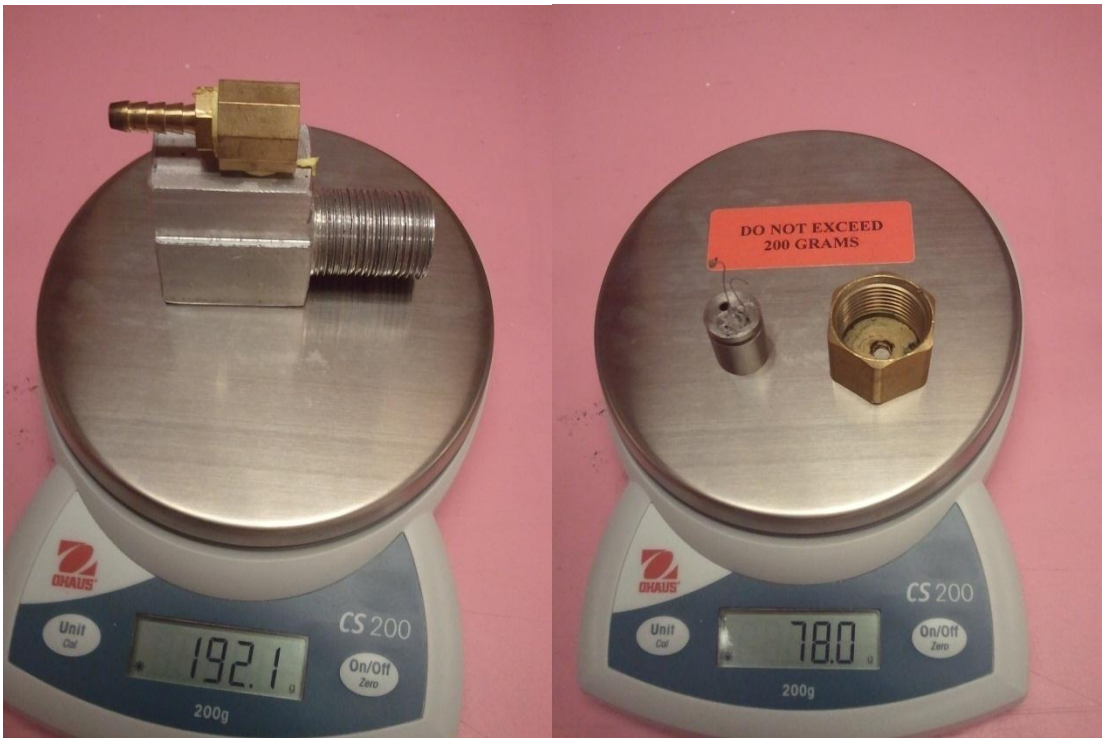

Figure 4.2.4 Second Iteration Inflation System Weight

The second iteration inflation system was tested similarly to the first inflation system. The system was tested using a small, test-size inflatable wing with a Co2 cartridge that was not sized (correct amount of grams of Co2 for the volume and design pressure) for it. The second inflation system was just being tested for proof of concept. Multiple tests had to be conducted, as the piercer got stuck the first couple of tests. These problems were due to the rushed machining, resulting in poor quality. Each time the inflation system was tested, it was prepared with 0.5 grams of black powder and electric match, as shown in Figure 4.2.5.

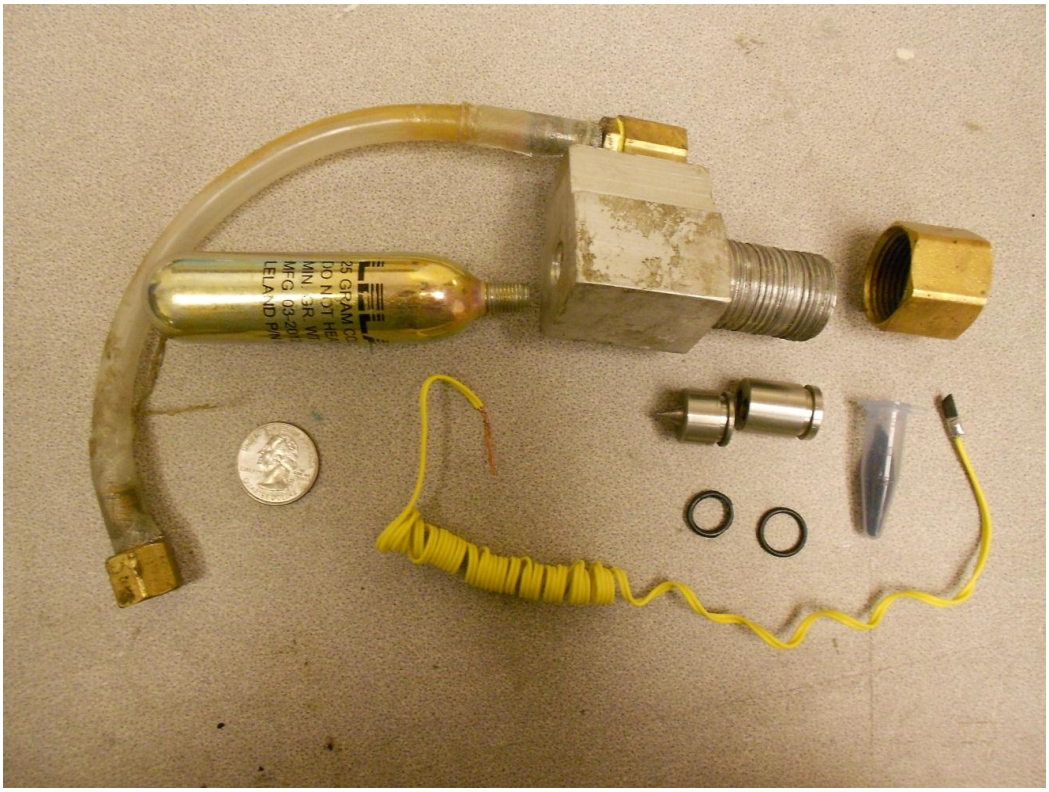

Figure 4.2.5: Second Iteration Inflation system

The second test of the pyro-valve inflation system proved to be successful. The inflation system was able to release the Co2 cartridge gases, and the gases filled the inflatable volume. Now that the concept had been proven, work began on a new inflation system – one that was optimizes for minimal weight, and minimal volume, and built to a better quality with tighter tolerances. Analysis and testing were also conducted on the ILC Dover inflatable wing to find out its precise volume.

4.3 WING VOLUME TESTING

The student elected to not use a relief valve as an uncertain amount of gas would be lost (and potentially prevent the wing from deploying fully) each time the inflation tests were performed. Therefore the precise amount of Co2 necessary to inflate the wing to operational pressure was needed; too much Co2 and the wing could burst, and too little and the wing may not deploy correctly or the aircraft would not be able to generate lift. Before any tests were conducted

on the inflatable wing (potentially harming it) calculations were conducted to estimate its theoretical volume, and thus how much Co2 was needed.

Estimations of the inflatable wing's volume were conducted using several methods. Using the wing loading test data (discussed in section 3.3) and inflatable airbeam equations, the wing volume was estimated to be approximately 1100 cubic inches. The inflatable wing was then designed and constructed in SolidWorks (CAD program) using measurements taken from the wing at its design pressure. The CAD model was then used to estimate the volume and was found to be approximately 1225 cubic inches, as shown in Figure 4.3.1.

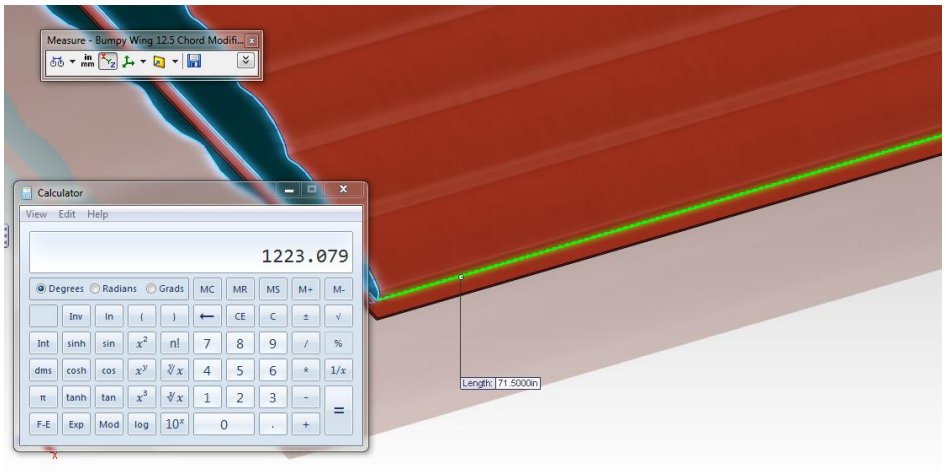

Figure 4.3.1 SolidWorks Volume Estimation

Finally, the volume was again estimated during the early inflation tests of the inflatable wing (discussed in section 3.4) using the mass flow rate of the compressor, and the time it took to inflate the wing to its full volume. From these tests it was found to be approximately 1075 cubic inches.

Once the volume of the inflatable wing is known, with a good degree of accuracy, then the Co2 cartridges could be sized. Sizing how much Co2 is needed to fill the volume is very straight forward. Co2 cartridges are sold according to how many grams of Co2 they contain, as in a 25 gram Co2 cartridge contains 25 grams of Co2. Then to figure out how many grams of Co2 is needed, the ideal gas law is applied. Using the estimated volume of the wing, the operational

working pressure of the wing, ambient temperate (or the temperature of the environment that the wing will fly in), the amount of moles of Co2 needed can be calculated, and from that, how many grams is needed.

$$PV = nRT \qquad \text{Equation 4.3.1}$$

By applying Equation 4.3.1, and by researching the various sized of Co2 cartridges that are sold, a table was developed that describes how much volume a single cartridge, or combination of two cartridges would fill, at ambient temperature and at the design pressure of 8 psi. A copy of this table is provided in Appendix C.

While all of the values and estimations for the volume are fairly close together, the researcher considered it too high of a risk to just size the Co2 canisters for this volume and try it. This is due mostly to the small window of operational pressure for the inflatable wing. The inflatable wing specifications stated that the operational pressure of the wing was between 8 and 10 psig, a window of only 2 psi, while the inflatable wing was estimated to burst at 15 psi. That means, that if these calculations are wrong, or my estimations were off, then there would only be a window of 2 psig before the wing would see damaged.

A method was then developed to directly test how much Co2 the wing would require. This was done by utilizing a Co2 bicycle inflator, The Genuine Innovations Ultraflate Plus, shown in Figure 4.3.2. This device allows a person to screw in a Co2 cartridge into the inflator, creating an air-tight seal, and release air as needed by using the trigger. In addition, the inflator can be screwed onto a bike tire valve, which also makes an air tight seal.

Figure 4.3.2: Ultraflate Plus Bike Tire Inflator

The student then created an adapter that connected the valve on the inflatable wing to a bike tire valve (Schrader valve). A pressure gauge was built into this adapter so that the change in pressure could be monitored as Co2 is added. A picture of the adapter used in this experiment is shown below in Figure 4.3.3.

Figure 4.3.3: Wing Volume Testing with Co2 Cartridges

The experimental procedures used to determine the amount of Co2 required to inflate the wing, as well as its internal volume are shown below.

1. Starting with the wing completely deflated, in its pre-deployment configuration. Screw in a Co2 cartridge (16 grams) into the tire inflator, and measure their combined weight on a scale. Take the initial pressure of the inflatable wing
2. Screw the tire inflator onto the adapter, and inflate the wing, making sure to not go above 10 psi.
3. When the Co2 cartridge runs out of air, disconnect it from the adapter and measure the final weight of the combined Co2 cartridge and tire inflator. Calculate the difference in weight from the final weight to the initial weight.
4. Repeat Steps 1 through 3 until the wing is up to full operational pressure. Calculate the total weight of Co2 used to inflate the wing.

This test was performed twice. The first time was using 16 gram cartridges exclusively. After the first test, the amount of Co2 needed was found with a reasonable amount of accuracy. However each time an empty Co2 cartridge was removed from the tire inflator, a small amount of gas was released into the environment. Therefore, the test was performed again using 25 gram Co2 cartridges, and a single 16 gram (once the target weight of Co2 was close) to reduce the amount of times an empty cartridge would be removed. Once these tests were conducted it was found that the ILC Dover inflatable wing requires 60 grams of Co2 to reach 8 psig. The results from these tests are shown in Appendix D

Once the precise amount of Co2 needed was found, a set of Co2 cartridges was selected that would meet this amount. Co2 cartridges have a wide range of volumes and sizes, but a 60 gram Co2 cartridge does not exist. Therefore, it was determine that two Co2 cartridges would be used to make 60 grams. In the Co2 cartridge market, there exists, 8, 12, 16, 25, 32, and 45 gram cartridges that all have the same 3/8-24 thread size. The student selected a 25 gram and 38 gram Co2 cartridges to be used in the inflation system, providing a total of 63 grams, which would pressurize the wing to 9.4 psi. A 45 gram and 16 gram Co2 cartridge could have been used to

achieve a more accurate 61 total weight of Co2, but a 45 gram cartridge with the 3/8-20 thread size proved difficult to find, and would have made it much more difficult to adapt into the aircraft.

4.4 DESIGN OPTIMIZATION AND CONSTRUCTION

When designing a pyro-valve inflation system, or anything in general, it is important to keep track of the all the limitations that are encountered, whether it's the limitations in the machine used to build the parts, the drill bits and taps available for use, or the size and dimensions of each part that is being used, and how its function limits the design. Once all of these limitations and dimensions are accounted for, building a pyro-valve with a minimal weight and size almost designs itself.

During early experiments, and generally using the Rouse Tech CD3 system, it became very obvious that one of the things that needed to be changed was the e-match holder and the rear cap. Since the rear cap and e-match holder were not integrated into one part, there was ample room in between the parts that allowed air to escape. In addition, during the first two inflation system that I built, specifically the first one, I found it much more difficult and troublesome to have to make external threads on the outside of the casing, as well as making threads on the side of the rear cap. That is why on the second iteration pyro-valve, I elected to use a cap that was purchased rather than make my own. During the designing of this third iteration, after much thought consideration, I realized that I could use an internal plug that threaded to the inside of the casing. This plug would be able to serve the same purpose of holding the e-match and black powder charge, eliminating the e-match holder used in previous designs, while providing an air-tight seal.

Throughout my experience with inflatable structures and the plumbing that is involved in them, one thing became very clear. Using hoses, hose clamps, or pipe fittings with barbed ends is always a bad idea – they leak excessively, and don't provide a reliable seal. Threaded pipe fittings

should be used at all time, whenever possible. However, a problem that was discovered when building the second iteration pyro-valve was the use of brass pipe fittings and how extremely heavy they are in comparison to the aluminum casing. After a lot of searching around town, and online, I finally found a place where aluminum pipe fitting can be purchased. Aluminum pipe fittings are often used in high-performance cars, and in NOS systems, and are available online. These pipe fittings us the standardized AN thread type, which is a US military derived specification, standing for Aeronautical and Navy. Using these pipe fittings proved to be challenging, since the proper taps are sometimes hard to come by, and finding precise specifications and dimensions on the threads and parts was difficult. Specifications on AN thread sizes can be found in Appendix F.

To understand what stresses the pyro-valve casing undergoes during an actuation, a better understanding of Co2 cartridges was required. When Co2 is stored inside of a cartridge it is pressurized to the point at which it becomes a liquid. From the Co2 phase diagram below (Figure 4.4.1), we see that at standard temperature Co2 is a liquid at approximately 900psia. In addition the warning label that is shown on Co2 cartridges warns that a cartridge should not be left out in the sun or in a hot car, as they would explode. This temperature is at about 130 degrees F. On the phase diagram, this temperature corresponds to a super-critical liquid at about 1400psia. When the seal is punctured on a cartridge, pressure is instantly reduced, the liquid Co2 changes phases to gas, the temperature of the gas drops to freezing temperatures, and the gas is released from the cartridge at approximately 450 psi.

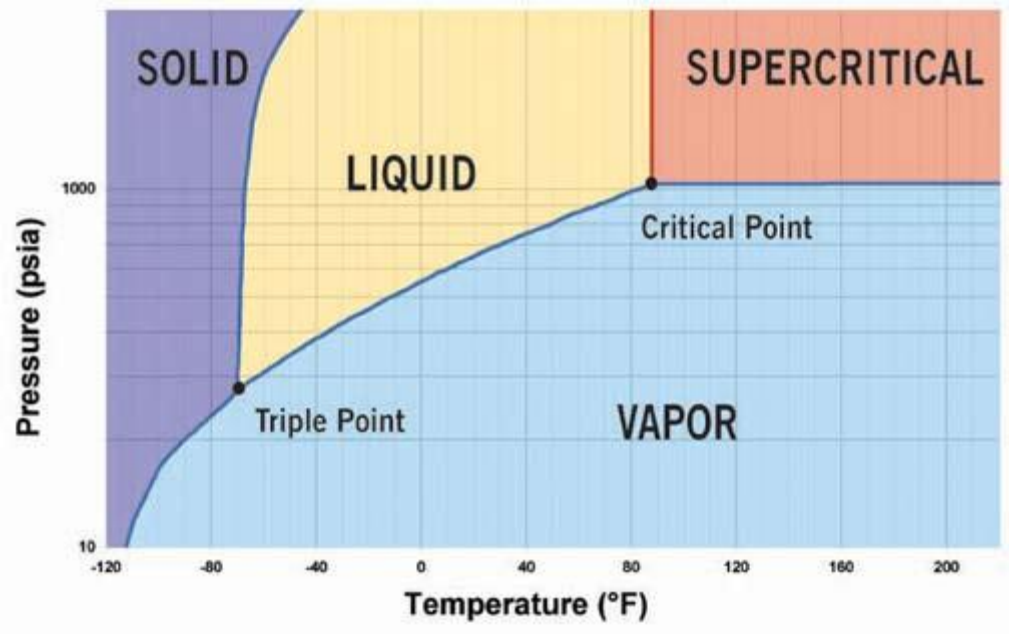

Figure 4.4.1: Co2 phase diagram **[21]**

With this information, the thickness of the casing, including the inside and outside diameter could then be determined. Using the simple pressure vessel equations (Equations 4.4.1 and 4.4.2) the minim required wall thickness could be determined, with an included safety factor of 1.3. Meanwhile, the minimum diameter of the shell is limited by the diameter of the threads on the Co2 cartridge, which are 3/8-24 threads, and by the threads of the AN plug, which for my design was an AN -6 hex plug. A AN -4 Tee is used to connect two pyro-valves together and is used to direct the Co2 gases into the inflatable wing. The drawing for my pyro-valve shell design is also included below in Figure 4.4.2. A small hole was drilled into the hex plug, using the lathe. This hole allows for the wires of the pyro valve to be wired through. The hole was drilled to be just large enough for the wires to pass through.

$$\sigma_t = \frac{pD}{2t}$$ Equation 4.4.1

$$\sigma_t = \frac{pD}{4t}$$ Equation 4.4.2

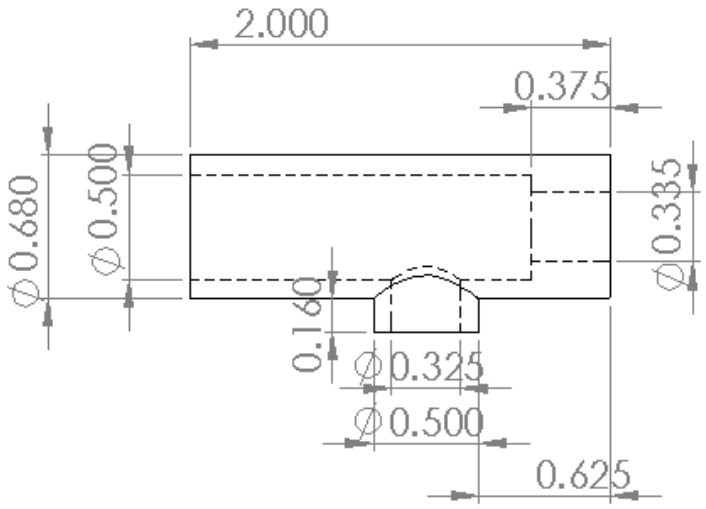

Figure 4.4.2: Pyro-Valve Casing Dimensions

The piercer used in the previous Rouse Tech system was made of stainless steel, since the tip of the piercer would bend and deform if it were made of aluminum. For this reason, the material of the piercer that I developed was kept as stainless steel, while the diameter had to be reduced to reflect the size of the casing. O-ring was used to prevent the piercer from sliding back and forth and accidentally discharging the Co2 canister, and therefore a groove was cut into it to position and hold the O-ring. The dimensions for the piercer are shown below, though it is important to note that the angle of the sharp tip had to be changed to a finer angle during experimentation. This change is reflected in the diagram below (Figure 4.4.3), with the updated dimensions. During early testing it was found that the piercer would sometimes pierce the Co2 cartridge, and then get stuck inside the neck of the cartridge. To resolve this, the piercer tip base was made smaller so that it would not get stuck.

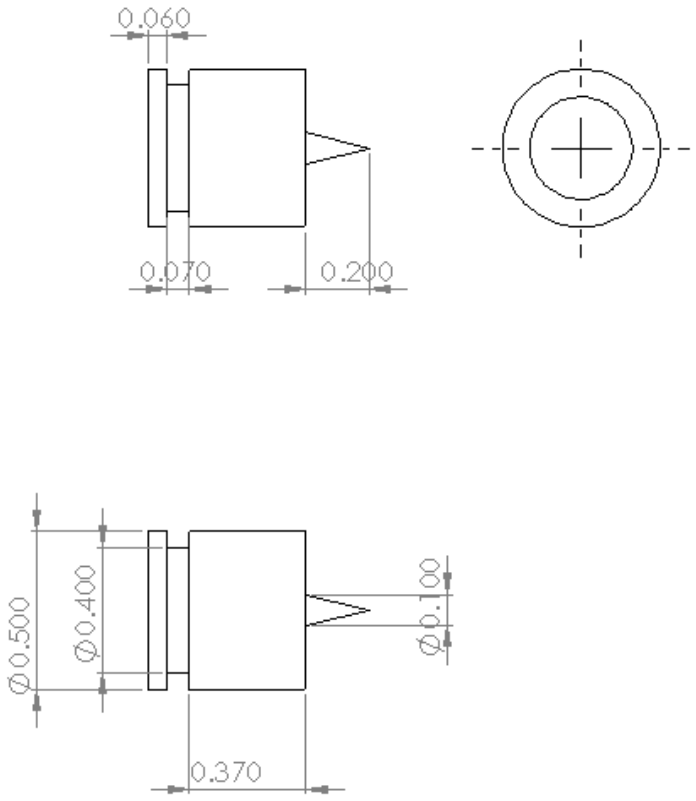

Figure 4.4.3: Pyro-Valve Piercer Dimensions

Throughout the entire design process of the inflation system I always tried to keep the construction process in mind, in order to make it easier to build and tried to minimize the weight. Once parts the AN fittings were ordered and received, dimensions were checked and the parts were ready to be made. A CAD design picture of the final inflation system design is shown in Figure 4.4.4. The 25 gram Co2 cartridge is on top, with the 38 gram cartridge on bottom. The hex plug, tee, and Co2 cartridge can be seen intersecting the walls of the cartridge; this is used to show the size of the threads on these parts, to ensure plenty of material is available for them to thread into. All machining was done myself using the lathe and mill available at the Oklahoma State Design and Manufacturing Laboratory.

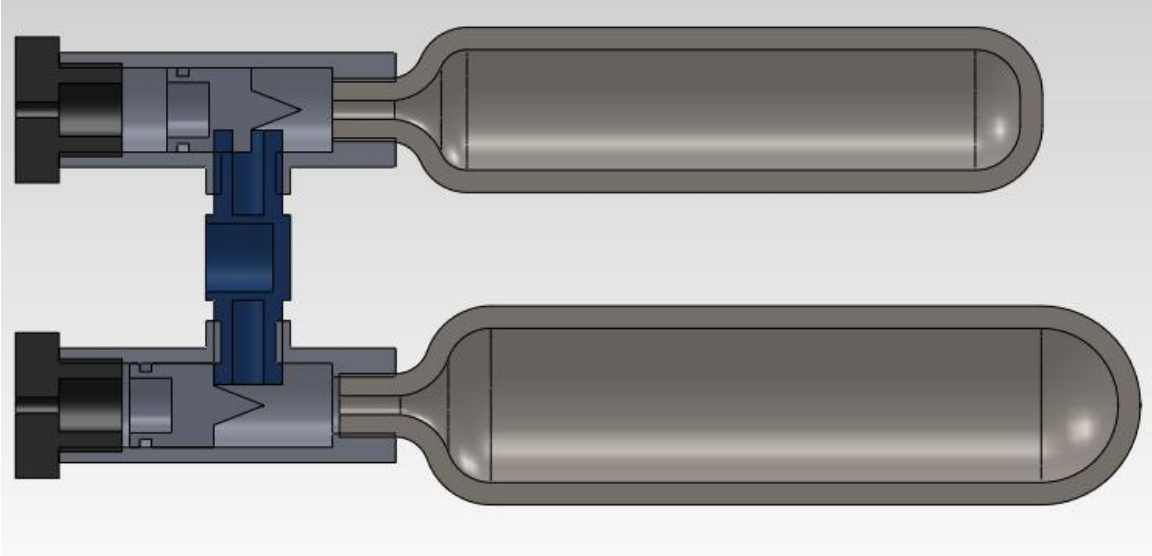

Figure 4.4.4: Inflation System CAD Cut-Away

The two casings of the pyro-valve were made using one inch round-stock of aluminum. The majority of the machining was done on the lathe, including drilling and tapping the holes on either end. Tapping the holes had to be done using the machine, in order to ensure strait threads with minimal error or gaps that could lead to Co2 leaks. The hole on the side of the casing, as well as the tapping for it was done using a mill, after all work was done on the lathe. The tee, as shown in the above picture had threaded ends that protruded too far into the casing, and were machined down to an appropriate length using the mill.

The piercer was made entirely on the lathe and took quite a bit of time and finesse, since the material being machined was made of stainless steel, and the part is so small. The tip of the piercer was particularly challenging. The tip was cut by placing the tool post on the far side of the part, with the tool pointing back, towards the part, while running the machine in reverse at a slow speed. The tool post was positioned at an angle to provide the correct angle of the point of the piercer that was desired. A picture of the assembled, finished parts is shown below in Figure 4.4.5.

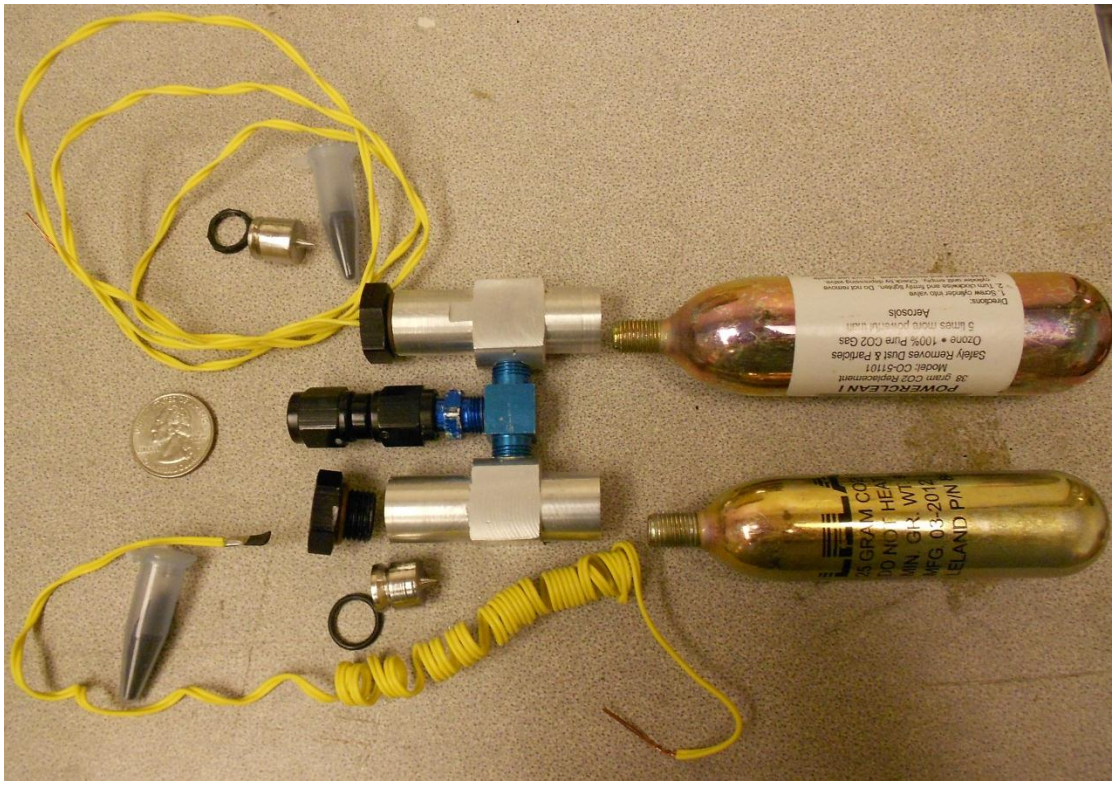

Figure 4.4.5: Completed Inflation System

Once the parts were completed, their final weight was measured and compared against previous version (Figure 4.4.6). The inflation system that I had developed was proven to be smaller and lighter (almost half the weight) than the Rouse Tech CD3 system. Compared against previous iterations of the pyro-valve that I made, the new pyro-valve was also machined to a much better quality, with very tight and accurate tolerances and straight, clean and tight threads, all while being more reliable, smaller, and lighter. In addition, the inflation system I developed was stronger than the Rouse Tech CD3 that it was based on, as it used a higher safety factor for the wall thickness. Pictures comparing the various pyro-valves and inflations systems and their weights are shown below in Figure 4.4.7.

Figure 4.4.6: Pyro-Valve Comparison

Figure 4.4.7: Pyro-Valve Weight Comparison

(From left to right: Rouse Tech CD3, 2nd Iter Pyro-Valve, Final Pyro-Valve)

4.5 INFLATION SYSTEM TESTING

Once the pyro-valve inflation system was completed, inflation testing could commence. Initial inflation tests were conducted on a small, inflatable, pillow-shaped volume made specifically for this purpose. The procedures used to prepare the pyro-valve prior to test are shown in Appendix E. Throughout these inflation tests, one problem with the pyro-valve inflation system presented itself. During one of the tests, the piercer rammed and punctured the Co2 cartridge as designed, but remained stuck in the neck of the cartridge, rather than being shot back

from the pressure of the Co2. It was decided that the base of the sharp point of the piercer was too wide, and caused it to get stuck. The piece was taken back to the lathe, and fixed. No problems with the pyro-valve inflation system have occurred since. After a few successful tests using the inflatable pillow (Figure 4.5.1), with no damage found on either the inflation system or the pillow, testing began on the inflatable wing.

Figure 4.5.1: Inflation Test on Inflatable "Pillow"

Throughout the early inflation testing with the inflatable wing, several problems were encountered. During each test, the extremely high pressure would expose a weakness in the plumbing from the inflation test, going to the wing. Due to the large size of the inflatable wing, and the static air that surrounds it, a large head pressure is created. This head pressure was larger than that of the inflatable pillow, and put more strain on the plumbing. After each inflation test with the inflatable wing, the video footage, inflation system and its plumbing, would be reviewed and inspected for leakages and repaired. In order to remove leaks and reduce head pressure from the plumbing, high pressure hosing was used, and the hose section that connected from the inflation system to the wing was shortened to its minimum length. In addition, any threaded parts

used plumber tape, made specifically for gas systems, and the hoses pieces were eventually epoxied in place, as it would ensure no leaks would occur and maintain high strength. A picture from one of these early inflation tests is shown below in Figure 4.5.2, depicting the various problems with leaks found during each test. None of these early tests were conducted with the full amount of Co2 (the 38 and 25 gram Co2 cartridges) as Co2 cartridges become expensive after a few tests.

Figure 4.5.2: Early Inflation Test
(Leak in the pressure gauge plumbing)

After several inflation tests, finding leaks and repairing them, the student conducted a few more inflation tests, again not using the full amount of Co2. These tests proved successful, as no leaks were found or observed and the wing was partially inflated from the small volume of Co2. A test was then conducted on the inflatable wing, using both pyro-valves, the full volume of Co2: a 25 gram and 38 gram Co2 cartridge for a total of 63 grams of Co2. The test proved very successful, as the wing inflated to its full pressure. A small leak was observed in one of the threaded connections. The leak in the threads was determined to be caused by thermal shrinking

from the freezing temperatures of the Co2 cartridge as it was punctured. A time-lapse of the inflation is shown in Figure 4.5.3. Water can be seen condensing on the pipes from the freezing temperatures.

Figure 4.5.3: Inflation Test Time-lapse

CHAPTER V

AIRCRAFT DESIGN AND CONSTRUCTION

5.1 CONCEPTUAL DESIGN

Developing a Hybrid Rocket/UAV provides some interesting complications; most notably the location of both the center of pressure, and center of gravity changes significantly in midflight between the rocket and UAV flight modes. In both cases the center of gravity must be ahead of the center of pressure to fly stabile, however in the rocket phase, there is a solid rocket motor that changes the center of gravity of the entire vehicle fairly significantly, due to its heavy weight at the aft portion of the vehicle. In addition, since the inflatable wing is stowed in an enclosed area and deployed in mid-flight, the center of pressure changes significantly from the rocket phase to the airplane's flight. The student took great care when designing the vehicle to incorporate the changing CP and CG so that the vehicle would fly correctly in both flight modes and be able to transition in mid-flight between phases.

In the early design phase of this project, the student used the Tomahawk Cruise missile and inflatable aircraft as a benchmark to help develop initial sizing estimates for components, as well as the location of the components. The design phase is a very iterative process, where small changes can have significant effect on the design. As the design began to take shape, some features became necessary to make the vehicle successful. It was decided early on that the aircraft phase of the vehicle would utilize an electric motor, rather than one that required fuel. This is because using fuel, or having a fuel leak in a system that incorporates a rocket booster and black powder ejection charges could prove to be dangerous and catastrophic, but also because small hobby-size gas motors often cannot be started in mid-flight and are more complicated.

As a rocket, symmetrical fins around the diameter of the body are necessary to keep the aircraft from arching over to one side or the other, while airplanes often have tail stabilizers that are non-symmetrical around the body. In the early design phase, the concept of having two separate stabilizing fins for the two different phases of the vehicle was considered. One of the initial ideas was to incorporate a lower rocket booster with symmetrical stabilizing fins that would fall away as the vehicle transitioned to an aircraft. Meanwhile the aircraft would have deployable (such a spring loaded, or folding) control surfaces or inflatable control surfaces. This idea was eventually discarded since early calculations and estimates showed that the aircraft vehicle would be tail heavy and require a long nose to counter-balance it, which added significant weight. Therefore it was decided that the control surfaces for the aircraft and the stabilizing fins for the rocket would be one and the same; requiring symmetrical rudders on the top and bottom, in addition to horizontal stabilizers that are mounted along the centerline. In addition, since the rocket fins and the aircraft stabilizers are the same item, the airfoils for these stabilizers must be symmetrical, in order to prevent undesired flight paths during the rocket launch.

With this decision to incorporate symmetrical aircraft stabilizers, the next problem became figuring out how to land the aircraft. In some of the previous inflatable aircraft research conducted by Dr. Jacob, as well as the Tomahawk cruise missile design, a parachute system has been used. For inflatable aircraft research, this has been used as a back-up system in the event of sudden air-loss in the wing. Since parachute recovery systems is something that I was very familiar with in high powered rocketry, it was seen as a simple and elegant solution, rather than having to deal with folding, retractable landing gear that would be very heavy and long, due to the symmetrical stabilizers. The parachute recovery system was included in the design of the aircraft, since it would provide an emergency means of landing in the case of some significant failure in the system. In addition it would provide a landing system for the aircraft as it finished

its flight phase. When the aircraft prepares for landing, it would pitch up and climb to reduce its velocity, then deploy the parachute and glide down to safety.

During the early design of the aircraft, the shape of the aircraft nose came into question. It was decided that the aircraft body would be made of phenolic cardboard tubes, since a symmetrical body was needed, and these tubes, commonly used in high powered rocketry were available for use. The shaped of the nose, or nose cone for this aircraft was determined by studying the Tomahawk cruise missile, other subsonic missiles, and by studying missile design. From my research, an elliptical nose cone produces the least induced drag, for an aircraft traveling in the sub-sonic regime and is therefore the most efficient nosecone for this hybrid rocket/UAV [22]. However, an elliptical nose cone could not be found in the 4 inch diameter size that was needed for this project, so the next closest nose cone was used; a nosecone style resembling the Sidewinder missile nosecone, shown in Figure 5.1.1.

Figure 5.1.1: Elliptical Nose Cone (left) [23] and Sidewinder Nose Cone (right)

5.2 AIRCRAFT CONFIGURATIONS AND SELECTION

In the early design stages, the student considered three basic aircraft configurations, including a Pusher, Tractor, and EDF (Electric Ducted Fan) aircraft configuration. In these early designs, a lower rocket booster section would be adapted to the aircraft section, and deployed prior to the wing deployment. Each aircraft configuration had some unique characteristic that would provide its own design challenges. In the EDF configuration, the majority of all electronics is located near, or at the nose of the aircraft, which can lead to an over-stable design; a problem that does not occur often. At the very tip of the nose of the aircraft, a First person view (FPV) camera (and additional equipment) could be mounted for piloting the aircraft in real-world combat scenarios where the UAV would likely be used as a kamikaze aircraft. However, for the purpose of this project, a recovery parachute is located in the nose of the aircraft instead. As mentioned previously, early designs utilized an additional, lower rocket booster section that would integrate with the aircraft section. In the case of the EDF configuration, this would allow for the addition of a "thrust –tube" which a device often used in many remote-controlled EDF aircraft. A thrust-tube is essentially just a tube that is approximately the diameter of the EDF shroud on one end, and approximately the same cross-sectional area of the fan-sweep area at the other end. This tapered tube acts as a converging nozzle for the airflow and helps to squeeze out a little bit extra thrust from the EDF; hence the name, thrust-tube. In later designs, it was decided that a thrust-tube would not be used, but instead the EDF tube would perform the dual-roll of also acting as a mounting location for the rocket booster section. Using the EDF tube to hold the rocket motor mount reduces the amount of weight being launched significantly, while reducing the potential thrust output of the EDF motor.

In both of the Tractor and Pusher aircraft configurations, a folding prop was used for propulsion. In the pusher configuration, the folding propeller would be concealed by the fall-away rocket booster section. In the tractor configuration, the prop would be concealed inside the

nose cone of the aircraft, which would require the nose cone to be jettisoned in mid-flight at approximately the same time the wing is deployed. As part of the NAR safety rules, no rocket is allowed to fly that has parts (heavy enough to hurt anyone or anything) coming down without an appropriate decelerator. Therefore, the nose cone that is jettisoned, would have to have a parachute, and that parachute could easily become tangled in the nearby electric motor and prop. As discussed earlier, a parachute recovery system was decidedly included into the aircraft. Though, it is not shown in the tractor or pusher aircraft configuration pictures above, the parachute bay was decided to be located near the quarter-chord of the inflatable wing, in order to keep the parachute lines out of the way of the electric motor, and since it would be providing deceleration at the approximate CG of the aircraft. After further analysis, it was discovered that with the inflatable wing, inflation system, and wing mount all located approximately at the same location as the proposed parachute recovery system, there would be insufficient space for an appropriately sized parachute.

In preliminary propulsion analysis many different electric motor, ESC, propeller, and battery configurations were tested and analyzed using the online performance calculator provided by Castle Creations, eventually after testing enough configurations, the most efficient configuration was found [24]. The "optimal" propulsion units found for the various aircraft configurations are described here. In the propulsion analysis, an electric motor and prop combination was found that could provide the necessary power for the pusher and tractor aircraft configurations. A Hacker A20-22l electric motor with a 10x6 carbon folding prop was selected, which produces over 2.35 lb of thrust. Meanwhile, OSU had a set of three different EDF motors that were available for use. All three EDF motors are made by Lander and had a KV rating of 2185, 2399, and 3900. The manufacturer specifies the thrust output of each of these EDF motors as 1.6 kg, 1.7 kg, and 1.1 kg respectively. Each EDF motor was analyzed using the Design Program I developed, and the design that produced the most thrust relative to the aircraft's weight

was selected. The EDF selected was the Lander LEDF68-1A21 , with a kv rating of 2185 and a thrust output of 1.6 kg. After selecting a motor, and Electronic Speed Controller (ESC) was chosen. For the tractor/pusher configuration, a Castle Creations Phoenix Ice 25 was selected, while a Castle Creations Phoenix Ice 50 was selected for the EDF configuration.

With the motors and ESC's selected for the various configurations, the student moved on to battery selection. The student sized the batteries with the goal of having a flight time of approximately 15 minutes. Using LiPo batteries currently available on the market, the student selected a battery for the tractor/pusher configuration. The student found that a 2500 mah 3S Lipo rated for 20/30 C would provide a flight time of approximately 14.5 minutes for the selected Hacker motor and ESC combination. The EDF motor batter was then selected. After reading the manufacturer's specifications on this motor, it was found that it could run on a 5S and 6S battery, but would only achieve its maximum thrust using 6S. In order to handle the amps that the EDF motor is capable of pulling, a battery rated at 45C was selected, and in order to meet that 15 minute flight time, a 4400 mah battery capacity was selected. The propulsion unit, as well as the ESC and battery used in this aircraft are shown below in Figure 5.2.1.

Figure 5.2.1: EDF Configuration Propulsion System

Preliminary weight estimations were made for each of the three configurations, and using the program described in section 5.3. From these weight estimations, it was found that the difference in weight between the three configurations was nearly negligible. All three configurations had an initial theoretical weight estimation of approximately 8.6 lbs with a variance of ± 0.2 lb. However, due to the construction process, added materials and parts, the gross weight estimation was more accurately decided to be approximately 10 lbs. The EDF configuration has by far the largest battery selected in order to provide a flight time of 15 minutes, however both the battery and the EDF are located relatively close to the CG of the aircraft (the quarter-chord), when compared to the tractor and pusher configuration. In these configurations, since the motor is placed either at the nose, or the tail of the aircraft, a comparable counter balance is added in order to keep the CG located at the quarter chord. In early design

simulations, this added nose length or tail length proved to provide substantial weight, making the weight of the three aircraft configurations about the same.

After conducting preliminary designs of the aircraft configuration, an EDF based design was selected. It is well known that propeller driven aircraft have better performance than electric ducted fans at this size of an aircraft, and at lower velocities, however the propeller based designs also carry increased risk. As discussed previously, it was decided that a parachute would be used in case of emergency situations and used for recovering the aircraft. Using a pusher or tractor configuration carries the added risk of one of the parachute lines getting tangled in the prop or motor shaft of the propulsion system, while the EDF would be enclosed inside the aircraft, preventing this situation. The importance of having a successful parachute recovery system in this aircraft far outweighs the loss in performance using an EDF propulsion system rather than prop-based system. In addition, complications with the tractor and pusher configuration designs made the EDF configuration design the clear choice with it elegantly simple layout. Once this aircraft configuration was decided upon, the aircraft design underwent a series of iterations designed to optimize the performance of the aircraft and reduce the weight of the aircraft.

5.3 DESIGN OPTIMIZATION AND IN-DEPTH ANALYSIS

Once a weight estimations were established, general parts, shapes and sizes of components were known and a general idea of the propulsion unit's capabilities were understood, further analysis could be conducted. A drag build-up of the subcomponents was calculated, which included the drag of the fuselage, horizontal and vertical stabilizers, and the wing. Using this information, the amount of thrust necessary to overcome this drag and perform the mission was determined. The iterative process of re-selecting components, re-estimating the weight, stability of the aircraft, and drag build-up was then performed until the design reached a steady-state. A program was created to help speed up this process, and minimize the weight of the aircraft .

The program I developed is based on a brute-force iterative design process. The program takes inputs parameters about each component used in the aircraft, such as the motor's weight, CG location, and where it is generally located with respect to the wing's quarter-chord. Other components with similar inputs include servos, the ESC, the battery, nose-cone, and inflation system. In addition, the densities of parts with unknown sizes are included. These inputs include the density (per unit length) of the rocket airframe, EDF tube, and wires, as well as the density (per square inch) of the material used to make the horizontal and vertical stabilizers. The length of these parts as well as their CG locations are determined in the program, while the CG of the aircraft is forced to be near the quarter-chord by determining the length of the nose to counter balance the tail weight.

The user inputs an upper and lower bounds for an appropriate tail length, Lh (the length from the quarter-chord of the main wing, to the quarter chord of the stabilizers), and an appropriate nose length, Ln (the length from the quarter chord to the tip of the nose). Initial estimates for the horizontal tail volume (Vh), the neutral point, static margin, and aspect ratio of the tail were calculated using equations from *Flight Stability and Automatic Control.* A tail volume around 0.4 was decided upon, to give the aircraft a static margin of approximately 0.35. The tail volume and aspect ratio of the tail are then input into the design program, where the weight of the stabilizers and aircraft can be calculated. A flow chart of the Design Programs process is shown below in Figure 5.3.1. The calculations for the initial aircraft stability and tail volume sizing are shown in Appendix G. In addition, the program code and layout are shown in Appendix H.

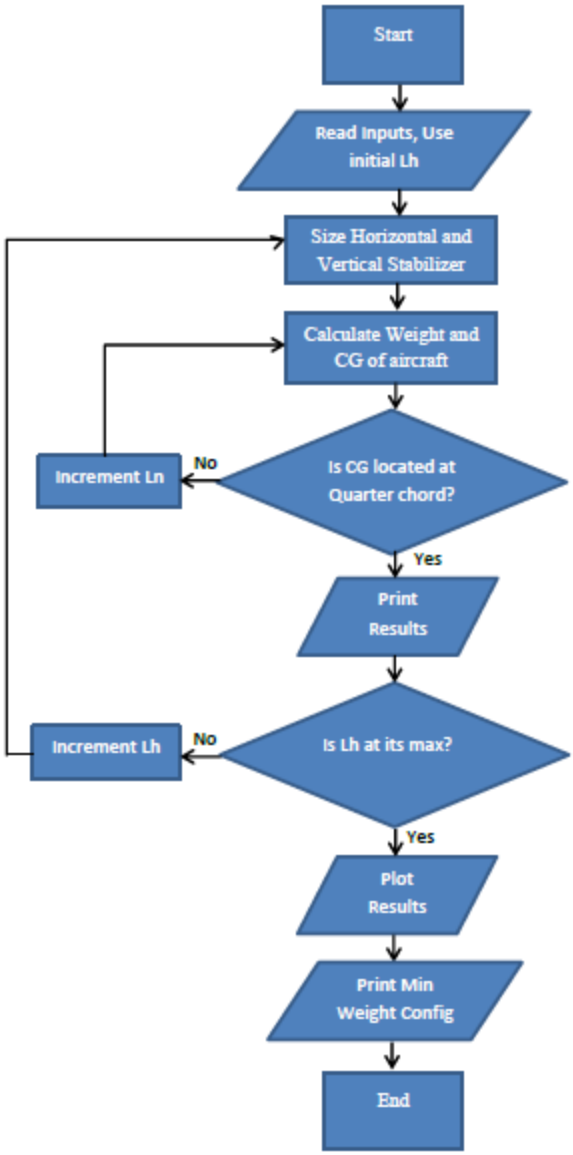

Figure 5.3.1: Aircraft Design Program Flow Chart

The size and dimensions of some of the key components were determined were determined by using this program. The program utilizes the basic center of mass equation, and calculates what the nose length must be in order to balance the CG at the quarter chord of the main wing. The program was adapted for the pusher, tractor, and EDF aircraft configurations, by simply moving components (within the program, and by through internal calculations) to their relative position, and calculating the CG. For example, on the tractor configuration, the motor is

always going to be at the nose of the aircraft, and for the pusher configuration, the motor is always at the tail of the aircraft, so the CG balancing equations within the program are edited to reflect these variances. As mentioned previously, this program provides a pretty thorough weight estimation of all three aircraft configurations. Since the EDF configuration was selected for the final design, the results from the EDF design program are shown below. A range of tail lengths were tested and the corresponding nose length to balance the CG was found. From these results, a design was selected that is close to the minimum theoretical weight, shown in Table 5.3.1, and Figure 5.3.2 below.

Winning Design																Selected Design				
Vh	0.4326		Hchord	10												Vh	0.48	Hchord	10	in
Ln	23.75	in	Hspan	20												ln (inches	24.75	Hspan	20	in
Lh	27	in	Lfuse	55.09161	in											lh (inches	27	Lfuse	59.25	in
Shor	204.9158	in^2	(minus nose cone)													Shor (in^2	200			
Wstab	322.7087	grams	=	0.711451	lbs											Wstab (gr	284.7575			
Wfuse	622.8107	grams	=	1.373062	lbs											Wfuse (gr	665.5261			
Wtotal	4029.931	grams	=	8.884478	lbs											Wtotal (g	4034.696			
Xcg	0.122497	in														Xcg	0.096596			
																Wtotal (lb	8.894981			

Iteration #	0	1	2	3	4	5	6	7	8	9	10	11	12	13	14	15	16	17	18
Vh	0.4326	0.4326	0.4326	0.4326	0.4326	0.4326	0.4326	0.4326	0.4326	0.4326	0.4326	0.4326	0.4326	0.4326	0.4326	0.4326	0.4326	0.4326	0.4326
ln (inches)	22.75	22.75	22.75	22.75	22.75	22.75	23	23	23	23	23	23.25	23.25	23.25	23.25	23.25	23.5	23.5	23.5
lh (inches)	18	18.25	18.5	18.75	19	19.25	19.5	19.75	20	20.25	20.5	20.75	21	21.25	21.5	21.75	22	22.25	22.5
Shor (in^2)	270.375	266.6712	263.0676	259.56	256.1447	252.8182	249.5769	246.4177	243.3375	240.3333	237.4024	234.5422	231.75	229.0235	226.3605	223.7586	221.2159	218.7303	216.3
Wstab (grams)	423.1774	417.5007	411.9766	406.599	401.3622	396.2607	391.2893	386.443	381.7172	377.1075	372.6096	368.2195	363.9333	359.7473	355.6582	351.6625	347.7572	343.939	340.2053
Wfuse (grams)	559.2613	561.41	563.5725	565.7483	567.937	570.1381	575.1776	577.4024	579.6386	581.8858	584.1436	589.2379	591.516	593.8037	596.1009	598.4073	603.5488	605.8727	608.2049
Wtotal (grams)	4066.851	4063.323	4059.961	4056.759	4053.711	4050.811	4050.879	4048.257	4045.768	4043.405	4041.165	4041.869	4039.861	4037.963	4036.171	4034.482	4035.718	4034.224	4032.822
Xcg	0.038707	0.053506	0.068896	0.084864	0.101396	0.118479	0.040509	0.058586	0.077183	0.096289	0.115896	0.04001	0.060525	0.081515	0.10297	0.124883	0.050936	0.07369	0.096882
Wtotal (lbs)	8.965871	8.958093	8.950682	8.943623	8.936903	8.930509	8.930659	8.92488	8.919391	8.914183	8.909244	8.910797	8.906369	8.902185	8.898234	8.89451	8.897235	8.893941	8.890851

Table 5.3.1: EDF Aircraft Configuration Optimization Program

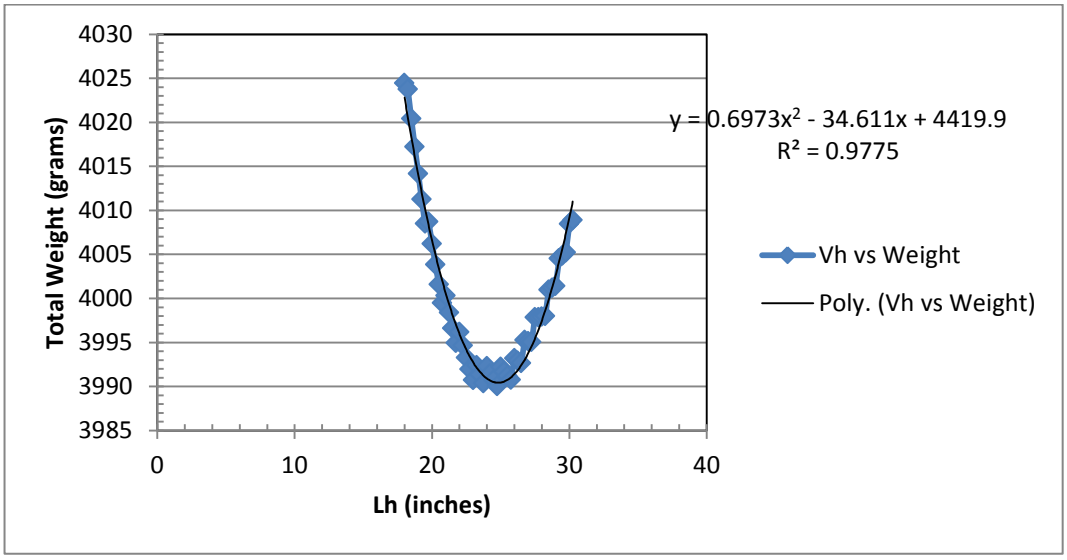

Figure 5.3.2: EDF Aircraft Optimization Results

The general known characteristics of the inflatable wing used, and the performance of the propulsion unit can also be put into the aircraft to perform further analysis. With the general size and shape of all components on the aircraft, including the size and shape of the wings, stabilizers, nose cone, etc. a drag analysis was performed in order to determine each components zero-lift drag, as well as the overall aircraft's zero-lift drag, and the drag as a function of dynamic pressure for each component and the overall aircraft. From this analysis, the following results were found, shown in Table 5.3.2 and Figure 5.3.3. The program used in order for these calculations, and the code behind it can be found in Appendix I.

Complete Aircraft (- Wing)	
D/q (ft^2):	0.072591906
Cdo:	0.006049326
Complete Aircraft (w/ Wing	
D/q (ft^2):	0.116256723
Cdo (total):	0.00968806

C_{Do} Breakdown	
Fuselage:	0.0019
Wing:	0.00843
Horizontal Tail:	0.003
Vertical Tail:	0.0014
Total	0.0097

Table 5.3.2: Drag Analysis Results

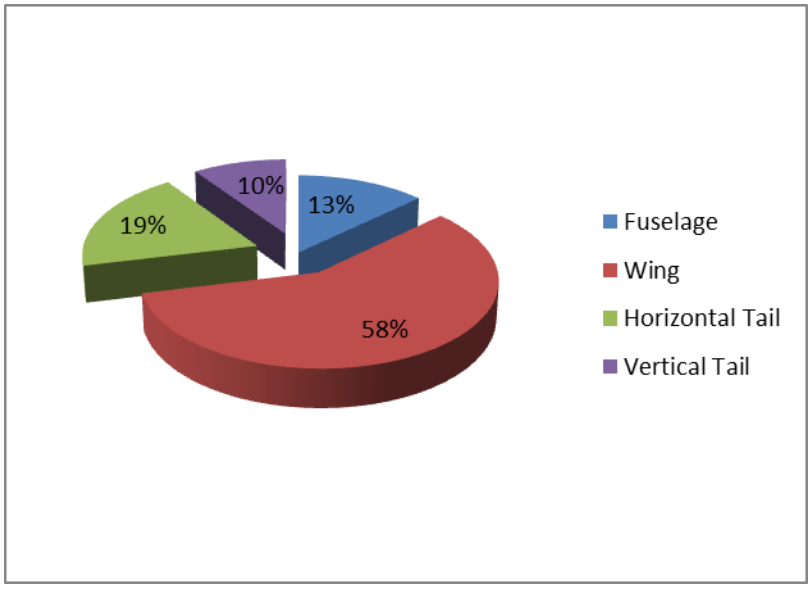

Figure 5.3.3: Zero-Lift Drag Breakdown

Using the drag analysis data, an early thrust requirement analysis was performed. The thrust analysis showed that the aircraft would require approximately 0.7 lb of thrust to maintain steady, level flight; far less than the 3.5 lbs of thrust output that the manufacturer specifies for the EDF being used. From this accumulation of data, the 3D wing data was also calculated. The 2D airfoil data and the specifications for the inflatable wing, and the aircraft's drag characteristics were used to calculate the wing's performance corrected for aspect ratio. A graph reflecting this data is shown in Figure 5.3.4, while a table of the data can be found in Appendix J.

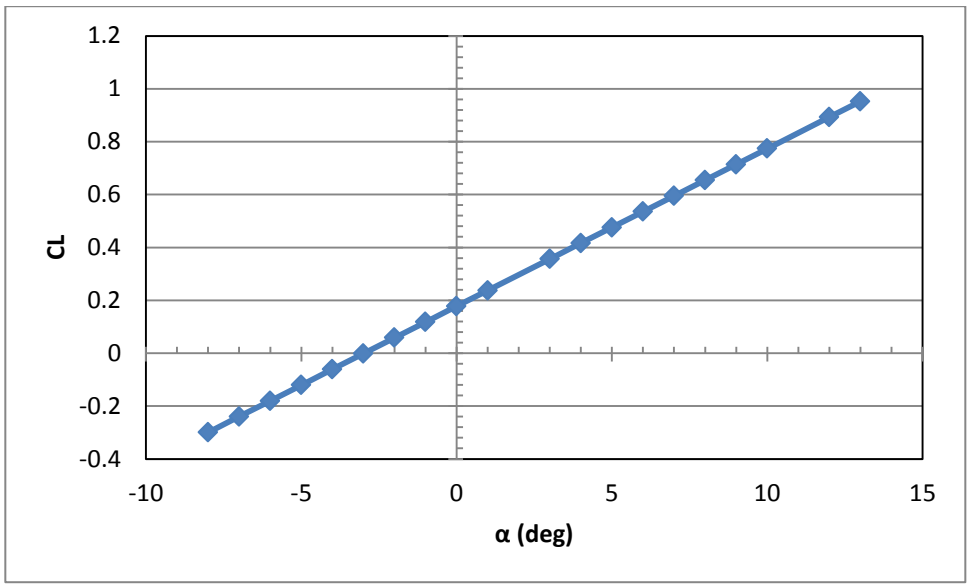

Figure 5.3.4: Wing Airfoil Data Corrected for 3D effects

As discussed in the preliminary design, the tail airfoil had to be a symmetrical airfoil. Typical rocket fins in high powered rocketry are approximately 1/8th to 1/4 inch thick material to prevent excessive drag, while maintaining structural integrity. The material selected for the aircraft fins is a composite material composed of 1 layer of carbon fiber, 1/8 inch thick balsa, and 1 layer of Kevlar, measuring approximately 0.14 inches thick. In order to simulate the use of this material, the control surfaces were modeled as NACA 0006 airfoils. The tail airfoil data corrected for 3D effects can be found in Appendix J.1.

Using the propulsion data, and the specifications of the aircraft, analysis was conducted on the propulsion system, predicting the performance of the aircraft. The results from these analyses can be found in Appendix J.3. From the analysis, it was found that the minimum required thrust is less than 1 lb, while the EDF motor produces approximately 3.5 lbs of thrust. A diagram showing the aircraft's thrust requirements is displayed below, in Figure 5.3.5. Some analysis also went into the designing of an EDF thrust-tube, but once it was decided that the EDF tube would be used as a housing for the rocket motor, analysis stopped and is therefore not included in this report.

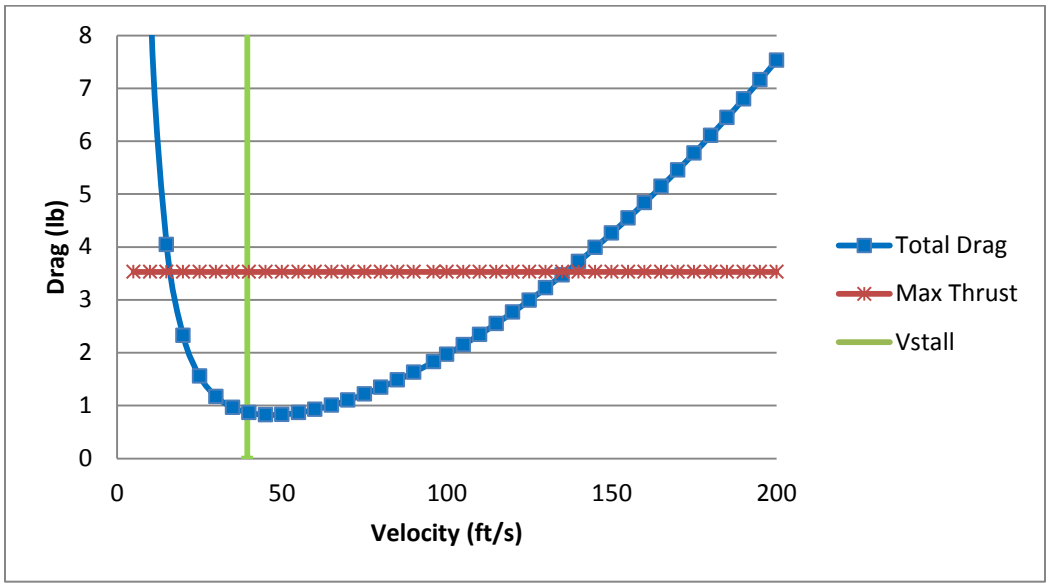

Figure 5.3.5: Thrust Requirements

Once the performance of the aircraft's propulsion unit was studied, work the focused on the verification of the aircraft's stability in flight sizing the control surfaces and servos used to actuate the control surfaces. Xfoil, a popular design program for airfoil analysis, was used to calculate the necessary control surface size, and the amount of torque placed on the servo. Using Xfoil, the force per unit span of the stabilizers was found, then through analysis, the hinge moment was calculated, and the torque required from the servo was found. The operations used to find the force per unit span in Xfoil are shown in Figure 5.3.6. From these analysis, it was found

that a servo capable producing a torque of 25 oz*inches (Servos are often sold using these units) was needed for the horizontal stabilizer and a servo rated for 13 oz*inches was needed for the rudders, which are approximately have the size of the horizontal stabilizers. Using the calculated torque ratings, servos were selected. Two HiTech HS-82MG servos were selected to control each of the horizontal stabilizers, while two HiTech HS-55MG servos are used to control the rudder actuations. The Xfoil analysis can be seen in the figure below, while the in-depth analysis of the servo sizing can be found in the Appendix J.4 and J.5.

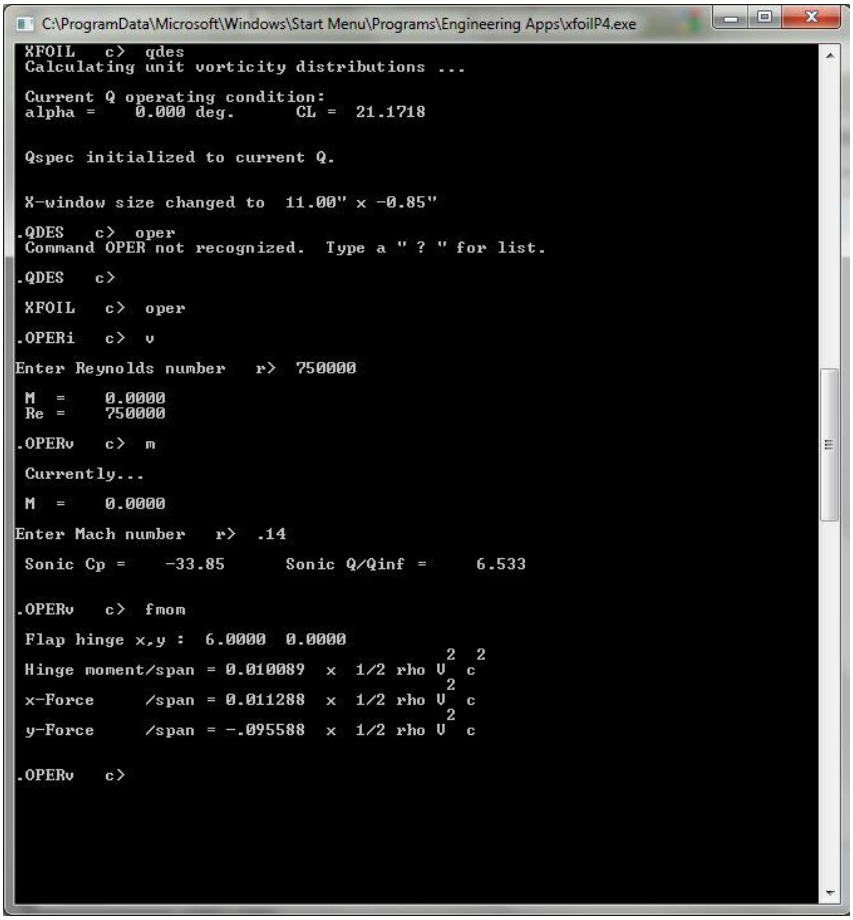

Figure 5.3.6: Control Surface Servo Sizing

Once the control surfaces and servos were calculated, the effects of these surfaces on the stability of the aircraft were calculated. In addition, the servo deflection angle that trims the aircraft to steady, level flight was calculated. Again, the horizontal stabilizer cannot be anything

other than a symmetrical airfoil due to the rocket boost phase, and because of this control surface must be used to trim the aircraft for level flight. From the stability calculations, it was found that a deflection angle of approximately 2 degrees down would trim the aircraft for steady flight. The effects from the control surfaces on the stability of the aircraft were calculated, and a graph depicting the results is shown below in Figure 5.3.7.

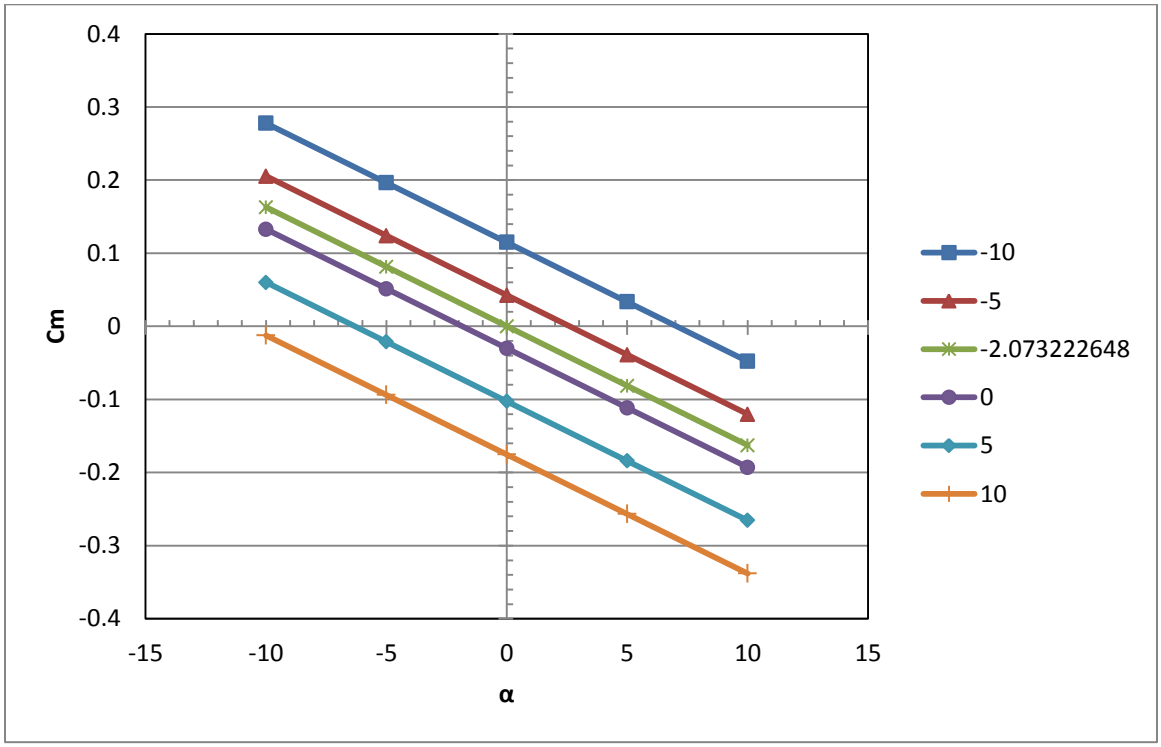

Figure 5.3.7: Static Stability with Flap Deflection

A program, commonly used in high powered rocketry, called RockSim was used to perform simulations of the aircraft as it launched. The program helped the student to visualize the CG and CP of the aircraft, and measure its stability as rocket, while all previous analysis has been focused on the stability of the vehicle as an aircraft. After building the rocket in RockSim, it became apparent that the rocket would be over-stable, which could cause the aircraft to try and over-compensate when it is perturbed by a gust of wind, producing a “fish-tail” like motion. This over-stability could be corrected, but would require adding significant weight to the rocket booster section and motor mount (all of which would be ejected after boost phase), which would

substantially reduce the altitude that the aircraft achieves during the rocket booster phase. It was decided to not add weight as very little could be benefited from this added stability. An Aerotech J350 solid rocket motor was selected for this aircraft, due to the altitude range predicted by the simulations, and the limited amount of motor casings available at OSU. Figures showing the RockSim representation of the aircraft (Figure 5.3.8), and the aircraft during a simulation (Figure 5.3.9) are shown below.

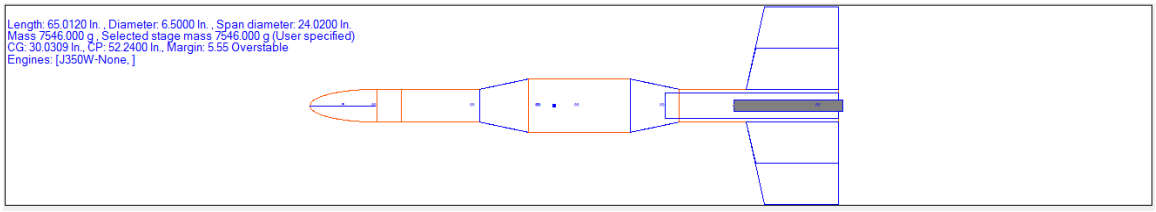

Figure 5.3.8: RockSim Model of Aircraft

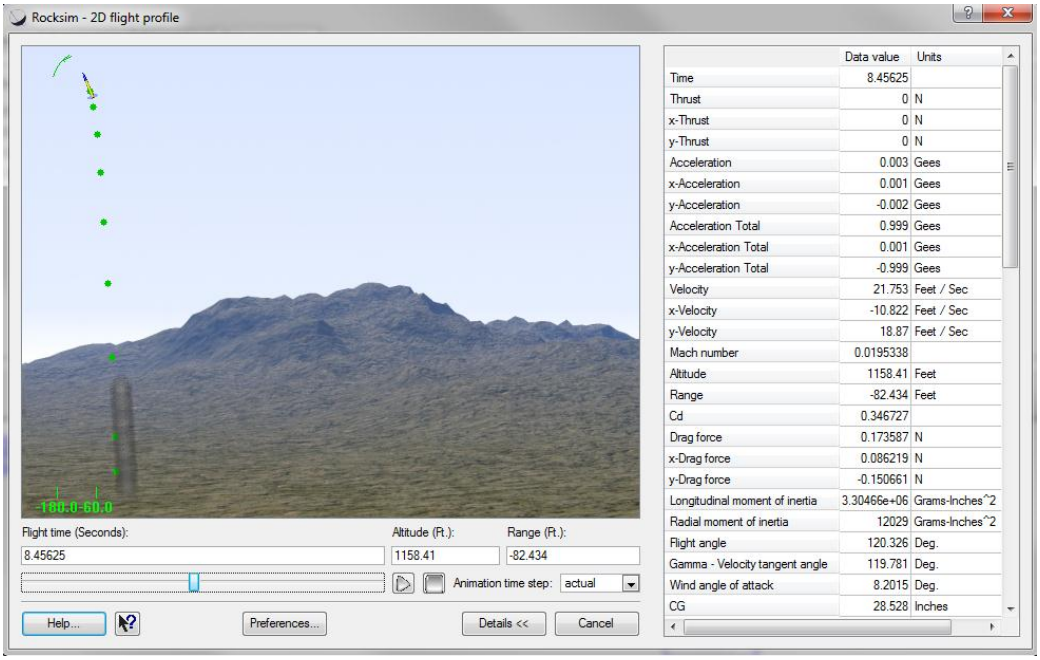

Figure 5.3.9 RockSim Simulation

Using RockSim and theoretical analysis, the coefficient of drag (Cd) was estimated for the aircraft. Using the equation shown below, the Cd of the aircraft and the resulting altitude can be computed. The equation takes into consideration the changing thrust of the rocket motor, as

well as the changing mass and velocity of the aircraft throughout its flight. The thrust curve data used in these calculations are readily available online from the manufacturer of the rocket motor. Early calculations for the air vehicle produced an approximate coefficient of drag of 0.65.

$$T_i = C_D \frac{1}{2} \rho {V_i}^2 A + M_i g - \left({dm}/{dt}\right) gt \qquad \text{Equation5.3.1}$$

The aircraft was designed and modeled in SolidWorks, helping the student find any issues with sub-components and assemblies, and visualize the problem and resolve them prior to construction. The aircraft was modeled according to the specifications calculated in the Aircraft Design Program I created, as well as the specifications from the propulsion and stability analyses. The overview of the aircraft in CAD is shown below.

The diagrams below (Figures 5.3.10 and 5.3.11) provide an overview of the fully designed aircraft and how all of the parts are assembled together, though some items were left out of the CAD assembly. It was calculated that a parachute ranging from 60 inches to 72 inches in diameter would be needed to bring the aircraft down safely. The parachute used is for flight testing was a Sky-Angle Classic 60, and is not pictured in the CAD. In addition, the launch guides, wiring, and other small components are also not featured in the CAD design.

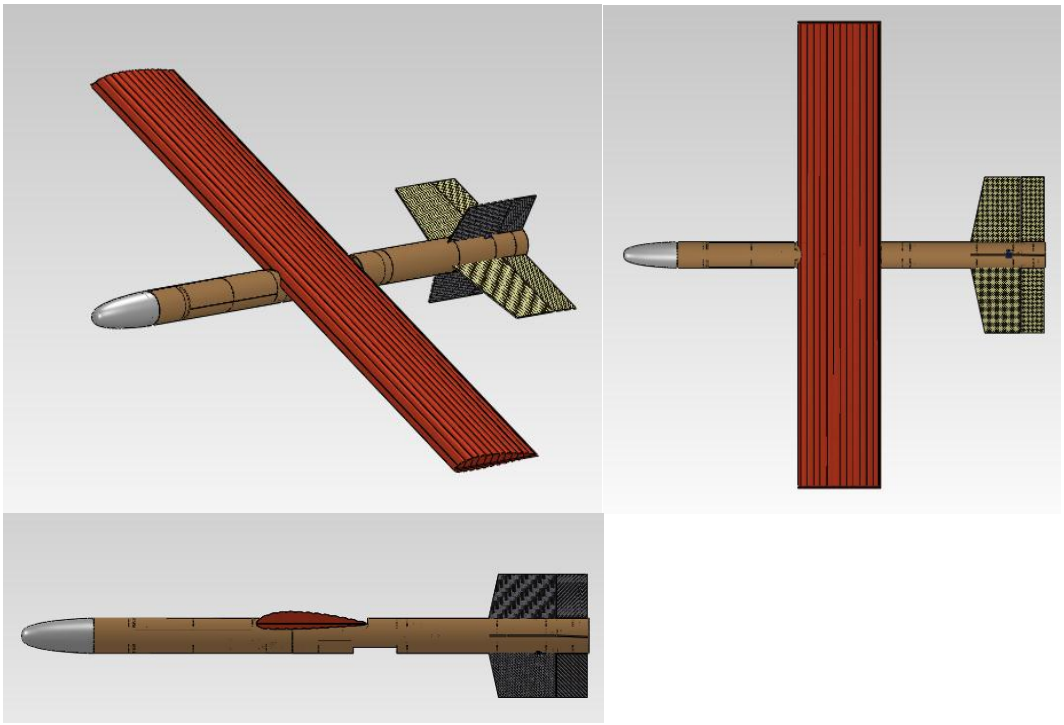

Figure 5.3.10: UAV in Flight Configuration

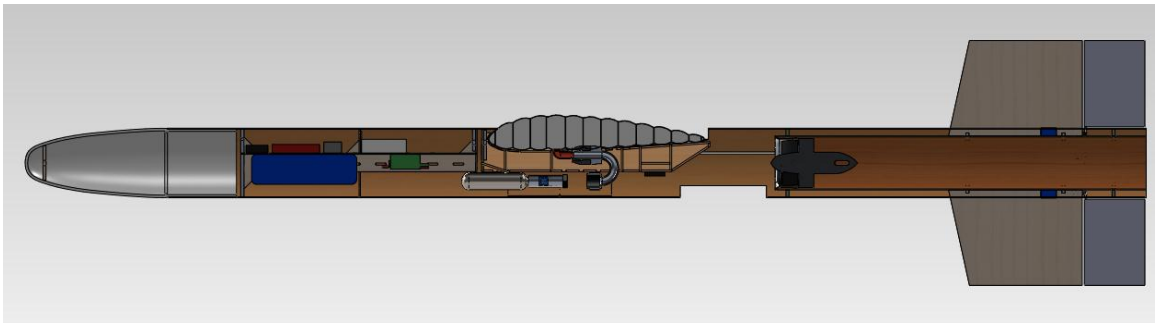

Figure 5.3.11: UAV in Flight Configuration Cut-Away

From these views of the Aircraft CAD in flight, it is easy to see that the vehicle looks right as an aircraft. The EDF is located partially behind the inflatable wing, and ducts are cut out of the aircraft body frame on the top and bottom the aircraft to provide airflow to the EDF. A wing mount is built-up that provides room for the inflation system internally, and allows the plumbing to pass through to the inflatable wing. In addition, an electronic-bay was designed and

built in CAD that would provide a mounting place for all of the electronics used for RC flight, and for deploying the inflatable wings and ejecting the rocket motor.

In the pictures below (Figures 5.3.12, 5.3.13, and 5.3.14), the aircraft when it is in its launch configuration is shown. The aircraft stands vertically on the launch pad, and uses launch-guides to control the aircraft during take-off. A composite shell was designed and built using CAD, and is used to hold the inflatable wing internally during the rocket launch. Once the aircraft reaches apogee, the rocket booster is ejected and the inflatable wings are deployed, as the external shell returns to the ground under parachute.

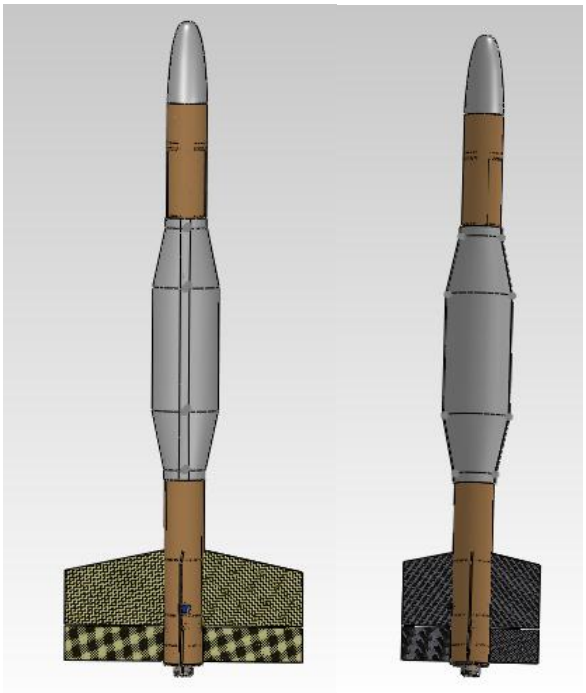

Figure 5.3.12: UAV in Launch Configuration

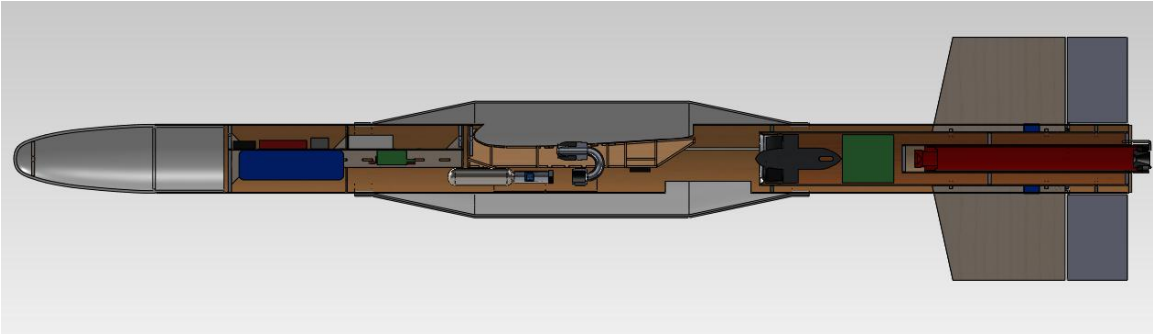

Figure 5.3.13: UAV in Launch Configuration Cut-Away

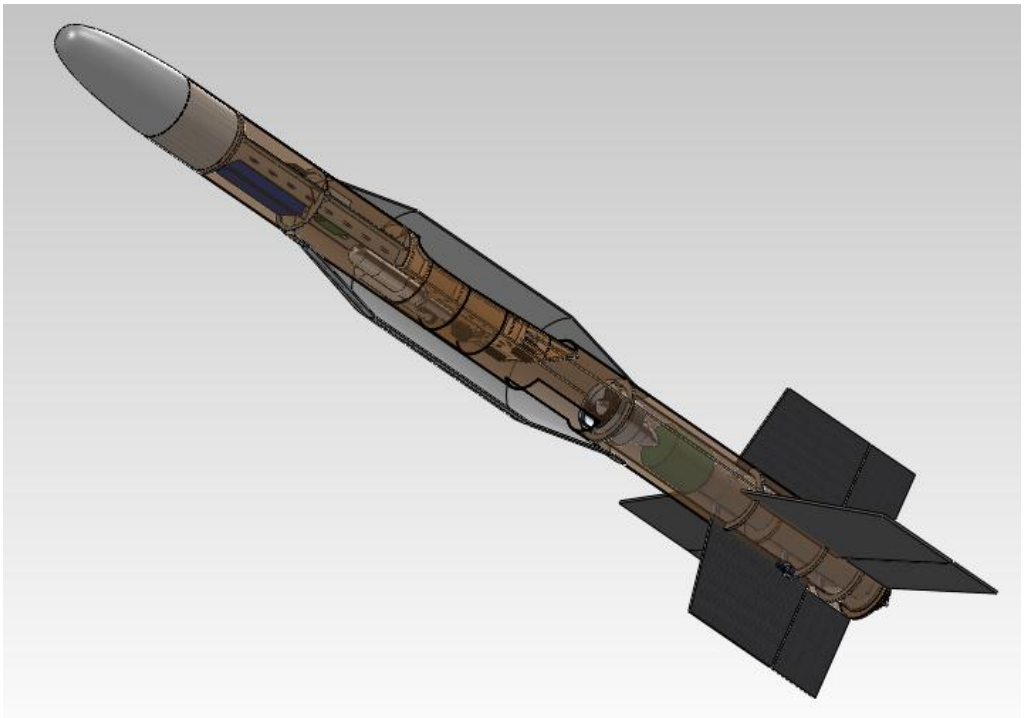

Figure 5.3.14: UAV Internals

5.4 CONSTRUCTION

Once the aircraft was designed, and thorough analysis was conducted, construction could proceed. Components such as the electronics bay, wing mount, and exterior shell required significant effort to design and fabricate. These items are discussed in detail in this section. The main body of the aircraft utilizes high powered rocketry phenolic cardboard tube that is commonly available. The inlets for the EDF duct, and the location for the wing mount were cut

into these tubes. The EDF inlets were placed in a location that would be concealed by the exterior shell during the rocket booster phase. In addition, access hatches were cut on the belly of the aircraft where the inflation system is located so that the inflation system could be attached to the inflatable wing (Figure 5.4.1 - Right). An access hatch was also cut into the aircraft body frame just ahead of the wing mount, on the top of the aircraft. This hatch allows the student to place a bolt through the electronics bay and into the wing mount (Figure 5.4.1 - Left). Bolts also run through the side wall of the aircraft body, into the electronics bay. The electronics bay requires significant structural support, since the main recovery parachute attaches to it.

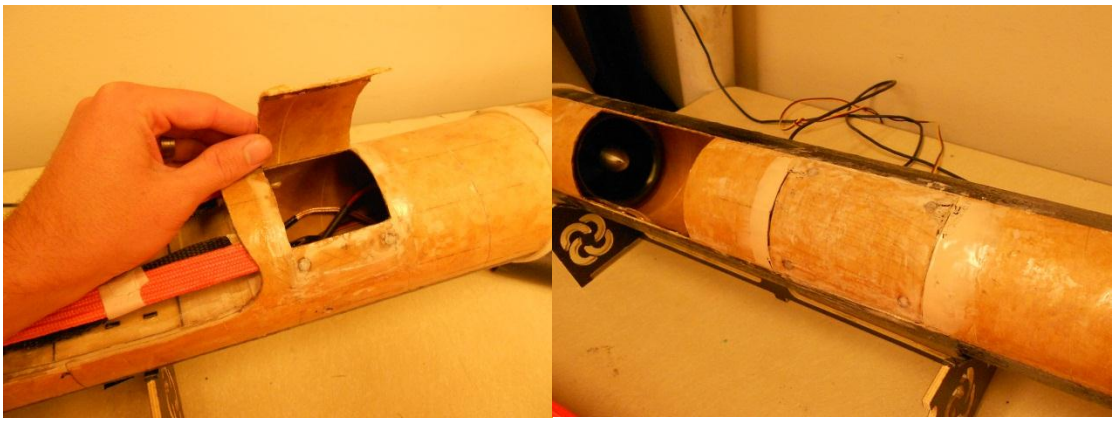

Figure 5.4.1 Access Hatches on Aircraft

In the CAD model shown in the previous section, bulk-heads and centering rings can be seen towards the aft of the aircraft, connecting the stabilizers to the aircraft, and supporting the EDF tube. These bulk heads were cut out of birch plywood on a laser-cuter. The bulkheads are advertised to be 1/8 inch thick, but are actually about 0.18 inches thick. Similar bulkheads and centering rings are used in the construction of the rocket motor mount. The rocket motor used for the booster section is an Aerotech J350 solid rocket motor, which is a standard motor diameter of 38 mm. The rocket motor mount tube is made of phenolic cardboard tube, and was cut to the length shown in the CAD. The rocket motor mount is designed to fit slightly, and snuggly inside the lip of the aircraft body tube. At the aft of the aircraft body tube, between the EDF tube and the

main body tube, is a e-match with black powder charge that ejects the rocket booster, similar to how parachutes are deployed in high powered rocketry. A rear bulk head is placed behind the stabilizers to prevent damage to components, and direct the black powder gases. The rocket motor mount is shown below with the J350 motor casing in Figure 5.4.2. The casing fits inside the mount, and is held in place with three L-shaped screws. The motor mount has a 24" parachute that brings the motor mount and motor down safely once it is ejected in midflight.

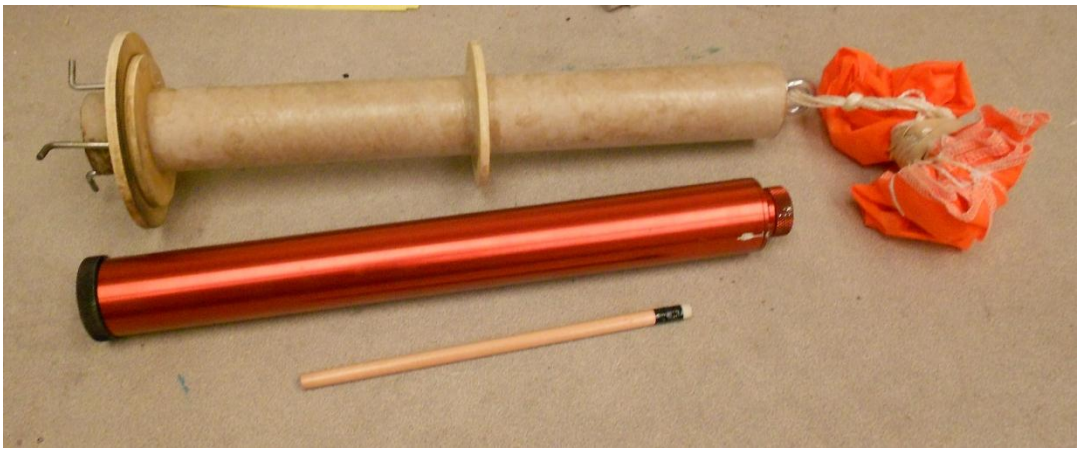

Figure 5.4.2 Rocket Booster Motor Mount

The material used for the horizontal and vertical stabilizers is a composite material with carbon fiber, balsa, and Kevlar. Three sheets of 1/8 " x 36" x 4" balsa were CA'ed together to provide a single sheet that is 1/8" x 36" x 12" using common balsa wood aircraft construction techniques. The grain of the balsa is oriented so that the grain runs across the span of the stabilizers. The Kevlar used in the layup was 5.0 oz. /sq. yd. while the carbon fiber had a density of 5.7 oz./ sq. yd.. Both the Kevlar, and the carbon fiber were oriented diagonally to the balsa. and were laid-up on a glass surface and vacuumed to -20 mm of Hg. the lay-up was left to cure for 24 hours. G-code was produced using SurfCAM for the horizontal and vertical stabilizers, and the parts were CNC'ed out of the stock material. The carbon and balsa layers are cut at the hinge locations, leaving just the Kevlar layer, acting as the hinge between the stabilizer and the control surface. A set of the horizontal and vertical stabilizers are shown in Figure 5.4.3.

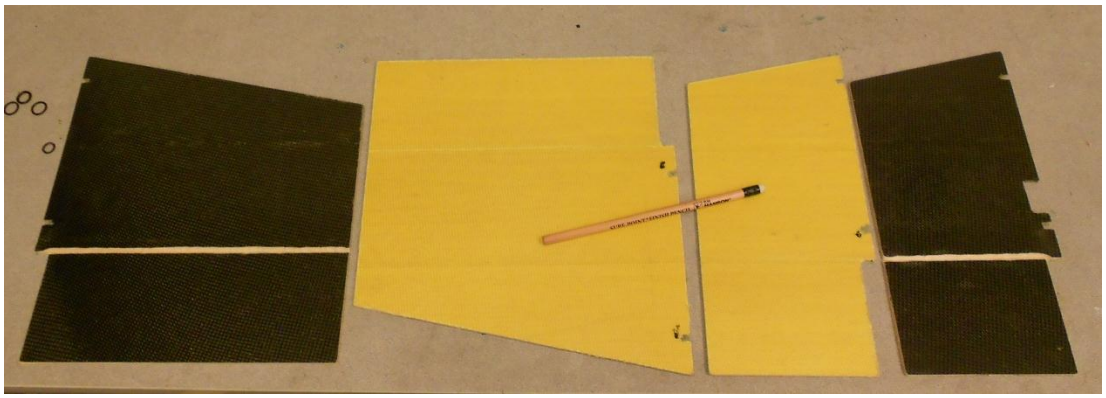

Figure 5.4.3: CNC Cut Composite Stabilizers

The material used to make the majority of the wing mount and the electronics bay also used composite materials. The core material was 1/16th inch birch plywood, while a layer of 1.4 oz./sq. yd. fiberglass oriented diagonally sandwiched the core material. The material was laid-up on a glass surface, in the same manner as the stabilizers material. This material was then cut out using a laser cutter, to produce the parts that easily fit and snap together. Once in place, parts were epoxied. A lot of work went into the design and CAD of both the electronics bay, and the wing mount. Both assemblies were designed to be easily cut out on the laser cutter, then assembled together like a kit. Many notches and slots are cut into parts on both assemblies to ensure that parts were oriented at right angles and to ensure that the parts were precisely places to ensure that the completed assembly would reflect the CAD design. The CAD of these two assemblies are shown below (Figures 5.4.4 and 5.4.5), depicting the inter-connecting parts on each.

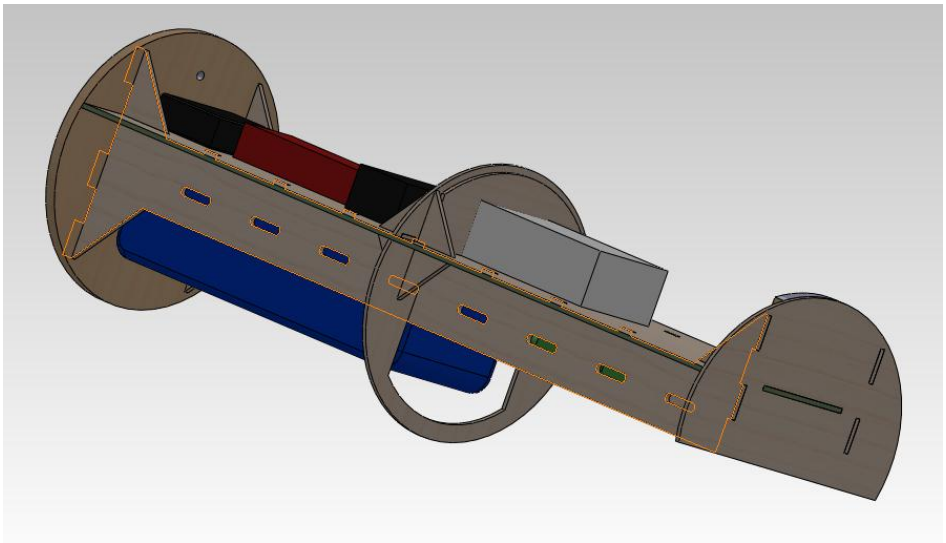

Figure 5.4.4: Avionics Bay CAD Assembly

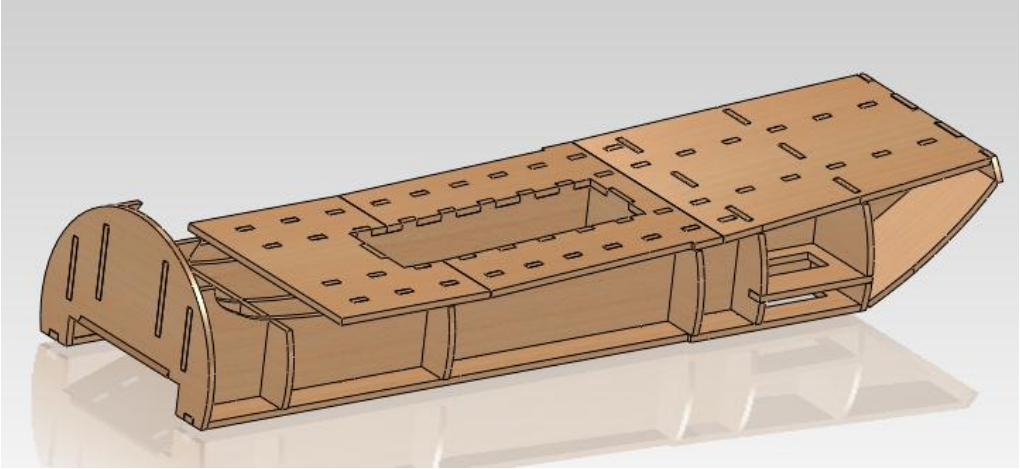

Figure 5.4.5: Wing Mount CAD Assembly

The avionics bay is a very important component, in terms of the aircraft's overall design. Not only is this component used to hold the electronics, including the Altimeter, ESC, batteries, and RC receiver, it also contains the U-bolt where the main parachute is attached. In most cases in high powered rocketry, the primary bulkhead with the main parachute U-bolt is epoxied in place, however, on this aircraft it was not possible to do this, since access is needed to so many different electronics. Instead, the avionics bay was made to be removable, and capable of sliding in and out of the aircraft. Once in place, a 7/16" bolt connects the avionics bay to the wing mount,

which is epoxied in place. In addition, small screws run through the aircraft body tube, into the avionics bay in six different positions, to ensure that the avionics bay remains attached to the aircraft during flight and when the parachute is deployed. A section of 0.18” thick birch plywood is located at the front of the avionics bay, where the U-bolt connects and at the rear where the avionics bay connects to the wing mount. The completed electronics bay is shown below, in Figure 5.4.6.

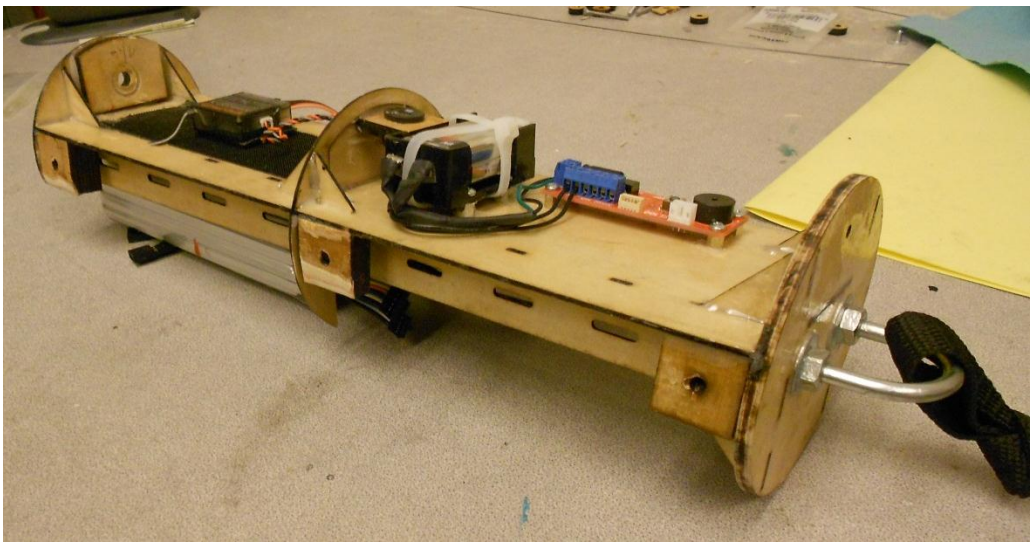

Figure 5.4.6: Avionics Bay

In order to control events such as the inflatable wing deployment, and rocket booster being ejected, a Perfect Flight altimeter is used. Altimeters are commonly used in high powered rocketry to trigger events such as the parachute deployment. In this case, the altimeter is programed to wait until the aircraft reaches apogee, then the internal relay triggers the black powder charges in the inflation system, which in-turn inflate the wings and remove the exterior shell surrounding them. In addition, another relay is used to eject the rocket motor mount when the aircraft reaches apogee using another black powder charge. The thrust of the EDF and the control surfaces are controlled using a Spektrum transmitter/receiver. These components are shown mounted to the avionics bay in their launch configuration in Figure 5.4.6. In order for the

pilot to control when the main parachute is ejected, a remote controlled relays was purchased, and wired together. The RC relay plugs into one of the auxiliary channels on the Spektrum receiver, while the power that is controlled by the relay comes from the main aircraft battery. The relay is connected to a black powder charge that jettisons the aircraft nose cone, and deploys the parachute recovery system. The completed RC relay system is shown below in Figure 5.4.7, being tested.

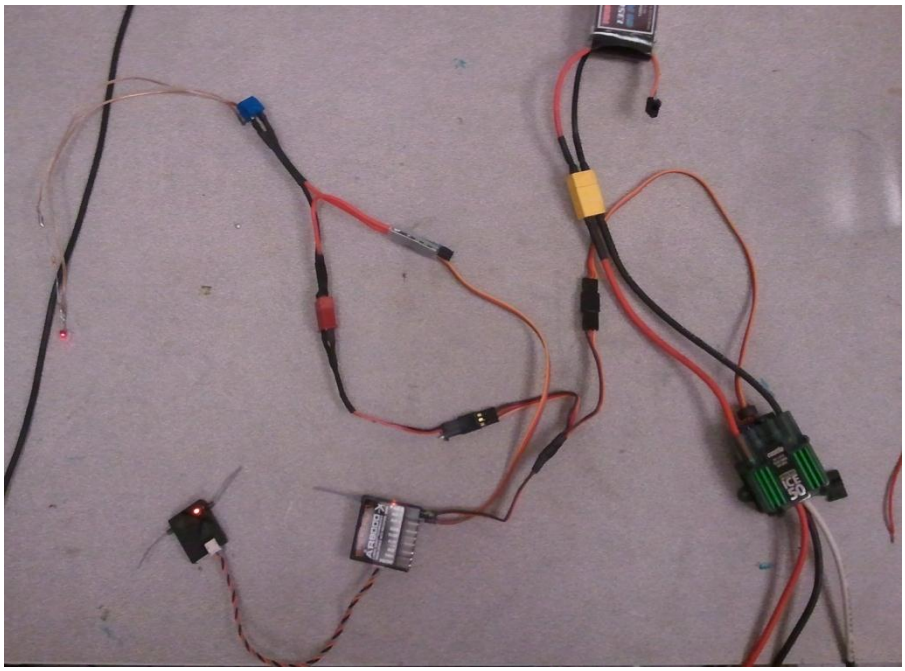

Figure 5.4.7: RC Relay Parachute Deployment System

The wing mount on this aircraft utilizes nylon and elastic straps to keep the wing in place. Traditional methods of screwing or bolting a wing onto the aircraft cannot be used since the wing is an inflatable volume, and because it inflates in mid-flight. Because of these limitations, a wing mount was created that follows the contours of the inflatable wing's airfoil precisely, so that when the wing deploys in flight, it will have a tendency to orient its self into the correct position. The elastic straps were placed on this wing mount to maintain control of the wing as it's volume and shape changes. The elastic straps help the wing to stay in position prior to inflation, during

the inflation process, and once it is inflated. However, due to the straps flexible nature, they would be unable to keep the wing in place when the aircraft is banking. Therefore, non-flexible nylon straps were also epoxied onto the wing mount. These nylon straps are rated for a working load up to 2000 lbs, are more than strong enough for any forces that the wing will place on the aircraft. The majority of the wing mount is made using 1/16" birch plywood and fiberglass composite, however in order to match the very small curvature of the leading edge of the airfoil, balsa wood was used. 1/8" balsa was soaked in water until it became pliable and was bent to match the contour cut into the wing mount. The balsa was then CA'ed in place and sanded to meet the thickness of the birch plywood composite. The completed wing mount installed into the aircraft body is shown in Figure 5.4.8.

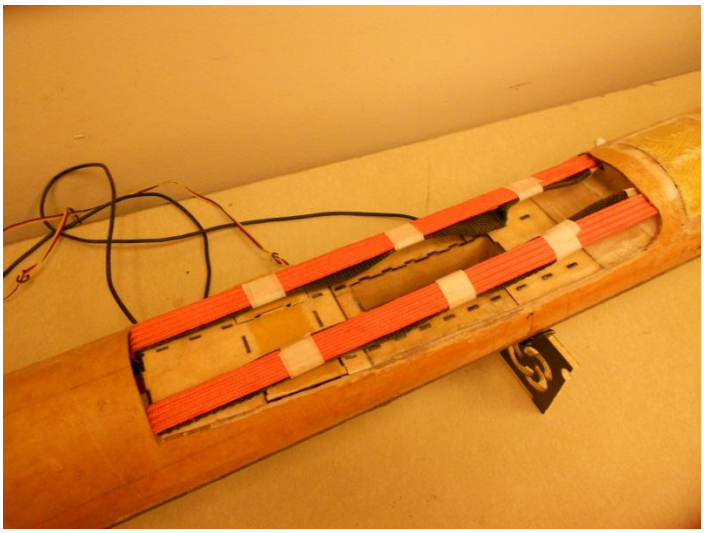

Figure 5.4.8: Wing Mount Installed

The servos for the aircraft's vertical stabilizers are mounted at the rear of the aircraft, in the rudders themselves. Meanwhile, the horizontal stabilizer servos are located in the wing mount, with control lines running to the rear of the aircraft. A place for these servos was designed in the CAD, and once the wing mount was constructed, the servos were attached via screws. An access hatch is placed on the top of the wing mount, located under the inflatable wings, so that the servos can be maintained and settings can be adjusted if needed. Figures 5.4.9 and 5.4.10 show

how the servos were attached to the wing mount, and how they are accessed once the wing mount is installed in the aircraft.

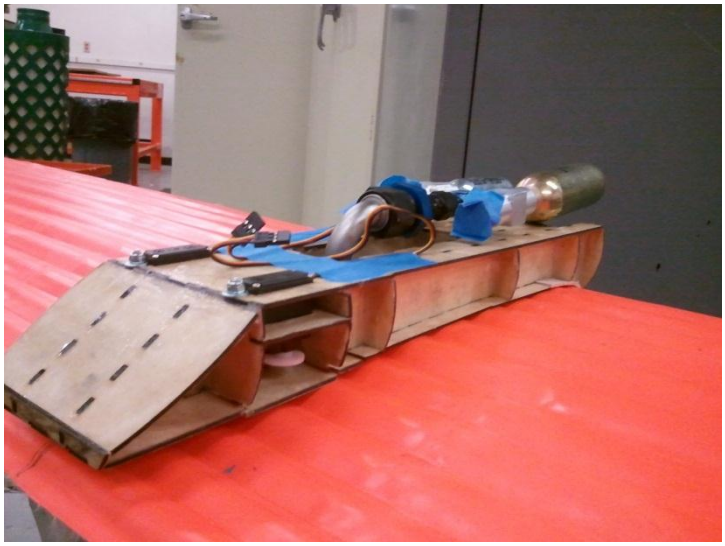

Figure 5.4.9 Wing Mount Assembly

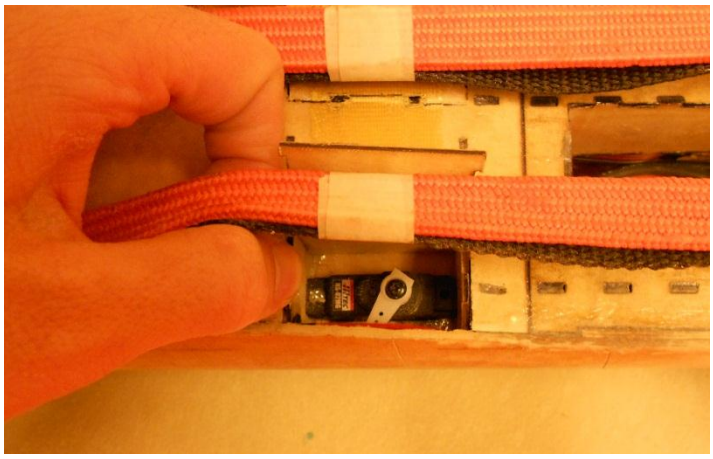

Figure 5.4.10: Wing Mount Servo Hatch

The exterior shell that keeps the inflatable wings enclosed during the rocket boost phase was made using a composite mold. A female plug was designed in SolidWorks, G-coded in SurfCAM and cut out of medium density fiber board (MDF) using a 3-axis CNC machine (Figure 5.4.11 – Left). The exterior shell is designed to be a symmetrical, semi-circle with a built in lip that allows the two halves to fit together. By making the two shell halves symmetrical, only one

mold needed to be made. The MDF female plug was made out of six sheets, each ¾" thick. The exterior shell is approximately 6.5 inches in diameter, making each shell-halve about 3.25 inches tall. Due to constraints in the CNC machines capability, and the length of milling-tools available, the plug was CNC'ed in two halves then joined together. Each half of the plug was comprised of three sheets of MDF that were joined together using wood glue. Notches were drilled into each half by the CNC machine to align the plug halves. Once each plug halve was CNC'ed, they were aligned using pegs that fit into the drilled notches, and then joined with wood glue, clamped and left to cure overnight. The finishing bit used on the final pass in the CNC process had a tip radius of 1/8th inch, and is unable to get into some of the sharp corners. Once the female plug halves were joined, the plug was sanded to remove these errors, and make the halves meet up smoothly. A thin coat of epoxy was then spread onto the female plug, to fill in micro-voids and prevent the MDF from absorbing paint and epoxy during the subsequent procedures (Figure 5.4.11 – Right). The epoxy coat was then sanded until the surface became smooth, using 400 grit sand paper.

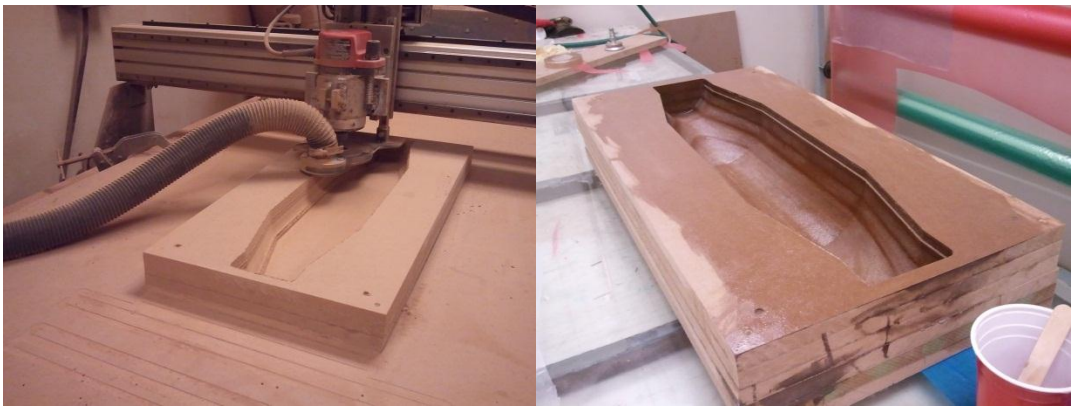

Figure 5.4.11: Exterior Shell Female Plug Construction

An MDF wall was built around the top of the plug. This wall allows for epoxy to be poured into the mold, and for a solid base to be made. A latex primer coat was then painted over the female plug, and sanded. This step was repeated twice to form a mirror-like finish that would prevent epoxy from seeping into any part of the MDF plug. The mold was then waxed, using automotive wax, and then a few coats of release were painted onto the mold. The wax and release

are used to create a very thin membrane-like layer between the plug and the mold that epoxy cannot stick to, and allows the mold to be separated from the plug once it is cured.

With the MDF plug fully prepared, the male mold was created. A gel-like epoxy was painted on first, creating the top face of the mold, then several alternating layers of heavy tooling fiberglass and gel-coat epoxy were added to create a stiff exterior with a clean, glass-like surface. The epoxy was allowed to cure over-night, and then the interior of the shell was filled with a gypsum based plaster cement. The gypsum cement was used for its ability to create a strong structure, without shrinking. Once the cement had cured, the MDF wall was dismantled, and the mold was removed from the plug. The pictures below (Figure 5.4.12) depict this progress, showing the female plug on the left with the built up MDF wall, and the female mod created from it on the right.

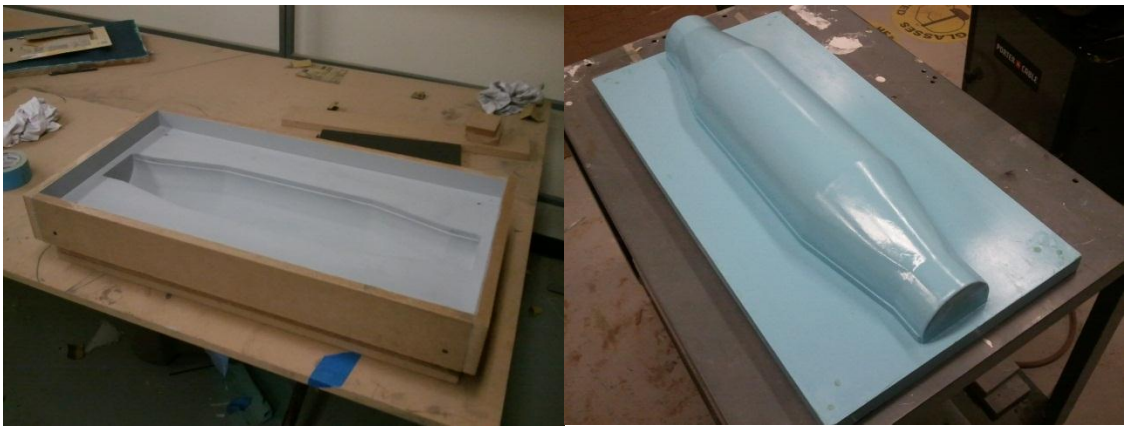

Figure 5.4.12: Exterior Shell Male Mold Construction

Now, with the male mold completed, a composite exterior shell could be made. In order to lay-up an exterior shell half on onto the mold, the mold was waxed, and released. The first attempt at making an exterior shell half was made using a layer of fiberglass, carbon fiber strips running the length of the shell, sections of foam core, and then another layer of fiberglass. The fiberglass used was 1.6 oz./sq. yd. while the carbon fiber was uni-directional carbon toe. The foam core pieces were cut using a 2D template made from the SolidWorks model. The foam was

then heated and applied onto the mold, in an attempt to make them form to the shapes of the mold. However, the curves on the mold proved to be too small of a radius for the foam to bend to, so the heat-forming process was abandoned. Nevertheless, an exterior shell half was laid-up on the mold, using the layers previously described. When the shell-half had cured and was removed, it was found that the foam pieces did not fit into their proper positions, and had moved while preparing the lay-up. The exterior shell half was very light, but was unusable, so a new method was devised.

The second attempt at making an exterior shell half utilized an inner and outer layer of 1.6 oz./sq. yd. fiberglass, for smoothness. The internal layers of the lay-up included one layer of heavy tooling glass, a layer of carbon fiber, Kevlar strips around the edges, followed by another layer of tooling fiberglass. The sharp edge that makes up the lip of the exterior shell was injected with an epoxy mixture, containing colloidal silica; a high-strength gap filler. By removing the foam core pieces in the second layup, the process became much easier, however when the part was removed from the mold the following day, it was found to be much heavier than the first iteration, weighing in at 320 grams. Since the exterior shell is designed to fall away in mid-flight and will not be present as the aircraft flies around using the inflatable wings, this added weight was considered acceptable. Despite the shell-half's heavy weight, the part turned out very clean and stiff, and conformed to the mold precisely. Therefore, a second shell-half was made using this same method to complete the exterior shell. Figure 5.4.13 shows the two different exterior shells that were made using the two different processes. The shell-half in the foreground shows the first attempt at making a shell, with the large gaps between foam core pieces clearly shown, while the shell-half behind it shows the second attempt at making an exterior shell.

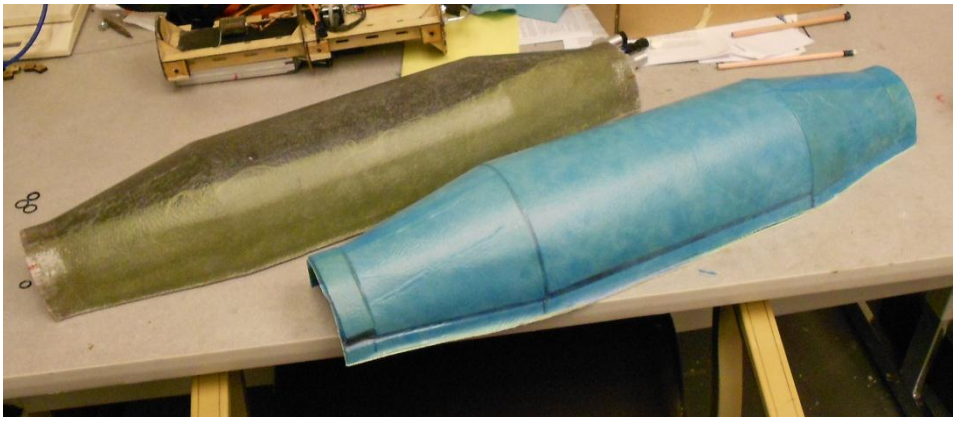

Figure 5.4.13 Exterior Shell Attempts

Once the two exterior shell halves were completed, steps were made to ensure that the pieces would fit snuggly on the aircraft exterior and would not move during the rocket boos-phase. The excess material on the exterior shells was cut off using a band saw and Dremel tool. When the shell-halves were placed on the aircraft body tube, it was found that there was a small void at the top of the semi-circle on both pieces, indicating that there were problems with the female mold. In order to fill these voids, a section of the aircraft and shells was coated with a layer of release and the shell-halves were placed on the body tube. The voids were then filled epoxy mixed with colloidal silica, and left to cure overnight. When the parts were inspected the next day, it was found that the problem had been resolved. Two holes were drilled into the exterior shells to allow for a shear pin to connect the two pieces. Figure 5.4.14 shows one of the exterior shell halves after these adjustments had been made.

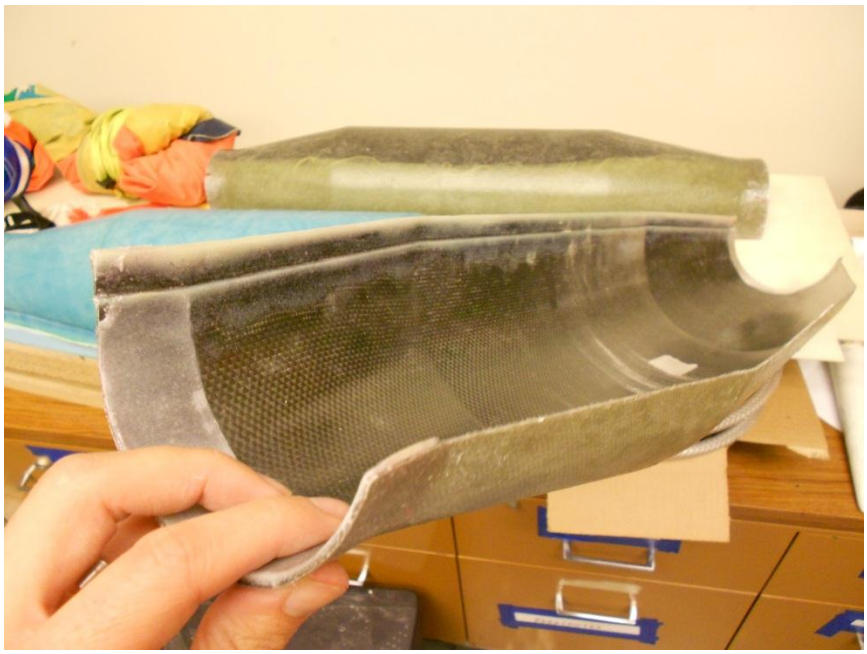

Figure 5.4.14: Exterior Shell Voids Corrected

Shear pins are small, nylon bolts that can easily be sheared, and destroyed when a strong force is exerted. These shear pins are commonly used in high powered rocketry to keep parachute sections contained, and to keep them from prematurely deploying. Shear pins were used on this aircraft to keep the nosecone attached to the rocket body, prior to parachute deployment. They were also used on the exterior shell to keep the two halves together prior to wing deployment. A picture of the shear pins used is shown in Figure 5.4.15 next to a penny for size comparison.

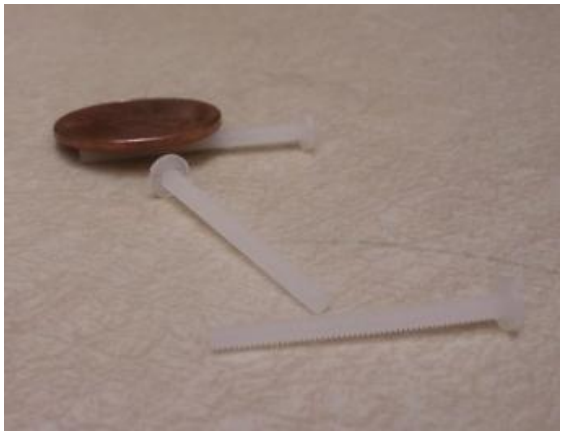

Figure 5.4.15: Shear Pins

Once the voids were fixed on the exterior shell, and the shell halves were able to be mounted together via shear pin, fillets were made on the aircraft to hold the shell in place during launch. The exterior shell and parts of the aircraft was coated in a layer of release to ensure that the epoxy would not stick in areas that it wasn't supposed to. The exterior shell was then placed in the desired location and orientation, with the lips of the shells parallel with the aircraft rudders. With the shell in place, epoxy mixed with colloidal silica was placed on the aircraft body, forming a fillet that followed the precise shape and contours of the exterior shell. With these modifications and measures in place, the student felt comfortable that the aircraft shell would not move or become detached from the aircraft prior to wing deployment. Figure 5.4.16 shows the aircraft after these modifications had been conducted.

Figure 5.4.16: Exterior Shell Mounted on Aircraft

CHAPTER VI

AIRCRAFT EXPERIMENTS

6.1 WING DEPLOYMENT TEST

Once the majority of the aircraft had been constructed, it was decided that a wing deployment test should be conducted using the designed wing mount, exterior shell, and inflation system. The deployment test incorporated all major components of the aircraft, and was conducted at static conditions. This served as a good indication of the inflatable wing's deployment and the inflation system's performance.

The inflation system was prepared, as discussed in Appendix E, using a 25 and 38 gram Co2 cartridge. The inflatable wing was connected to a vacuum pump prior to packing the inflatable wing into the exterior shell. The wing was then connected to the inflation system, and the wings were folded using the Z-fold configuration. The exterior shell was then placed around the folded wings, and held in place using shear pins. Once the aircraft and inflation system were prepared, the vehicle was moved to the test stand for the deployment test. For this deployment test efforts were made to support the nose and tail of the aircraft with the test stand, while leaving the midsection (where the inflatable wing, exterior shell, and inflation system are located) uninhibited in order to simulate in-flight characteristics. High speed cameras were placed at the rear and starboard of the aircraft, allowing a closer look into the wing's deployment. Once the aircraft, test bench, and high speed cameras were ready the deployment test was conducted. Figure 6.1.1 shows the rear view of the aircraft during this inflation test.

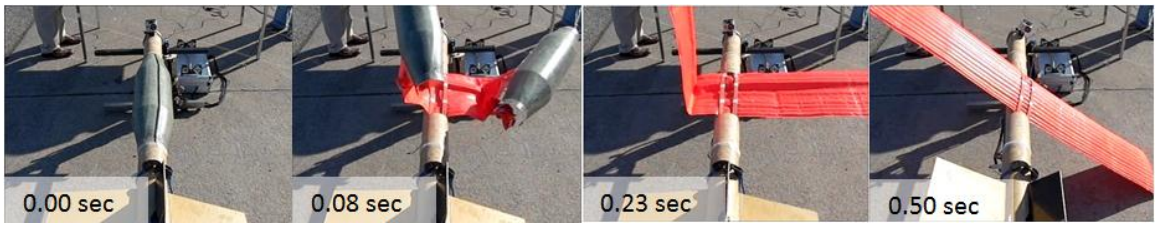

Figure 6.1.1: Wing Deployment Test

In the wing deployment test, the high speed footage showed that the inflatable wings deployed asymmetrically in approximately half a second. While the asymmetrical deployment is undesirable, the author believes that it would be nearly impossible to ensure absolute symmetrical deployment of the inflatable wings. During the inflation test, the starboard wing, that inflated first, hit the ground, causing the aircraft to recoil from the force. Despite this, no damage was seen on the aircraft, or the inflatable wing. Overall, the deployment test was very successful, since it demonstrated that the inflatable wing could deploy from the exterior shell, and the inflation system worked as designed.

6.2 AIRCRAFT FLIGHT TEST – FIRST LAUNCH

The first launch for this aircraft was designed to test some of the functions of the aircraft and the vehicles capabilities on launch, without risking the inflatable wing. It was decided that a flight test using the rocket booster should be done first, prior to testing the full aircraft in order to find problems and resolve them, should they arise. The goals of this first test were as follows:

- Fly the aircraft with the exterior shell in place, but without the inflatable wing, to test the shell's capability to stay attached to the aircraft during launch
- Test the Perfect Flight altimeter's capability to deploy the rocket booster section
- Test the parachute deployment, to ensure the aircraft can be recovered safely
- Test the Spektrum RC transmitter, and ensure that the aircraft maintains connection to the receiver throughout the flight by running the EDF motor during decent.

The aircraft was flown using the Aerotech J350, as described previously. The inflatable wing was not installed for this first flight, and neither was the inflation system, however the exterior shell was placed on the rocket and held in place using only the shear pins that would be holding the shell on during a real flight test. Prior to launch, the aircraft was weighed to find its final, constructed weight. The weight of the aircraft , without the inflation system or wing, in its take-off configuration on the day of the launch was 11.85 lbs. With the rocket booster section ejected, the aircraft weighed 10.51 lbs. This weight was a bit troubling, as weight predictions had this vehicles weight estimated to be approximately 10 lbs with the inflatable wing, when the aircraft is flying. Analysis was performed again to measure the effects of the aircraft heavier weight. RockSim initially had estimated that the rocket would cruise to an altitude of 2455 feet at the lower weight, and only 1855 feet at the heavier weight. An altitude of at least 1000 feet is preferred for a rocket of this size, therefore the estimated altitude was deemed acceptable for launch. The results from this simulation can be found in the appendices. Initially, a parachute measuring 40 inches in diameter was planned on being used when the weight estimations put the aircraft at a max weight of 10 lbs, however once the weight of the aircraft was found to be heavier, a larger parachute had to be used. A Sky Angle Classic 60 inch parachute was selected for the aircraft, having a predicted decent rate of 18 ft/s [25]. In high powered rocketry, a decent rate of 20 ft/s is considered high, while a decent rate between 15 ft/s and 17 ft/s is typical.

In order to test that the exterior shell would hold in place during a final launch, the exterior shell was prepared in the same manner. The shell was placed in its position around the aircraft body tube, and shear pins were inserted into the holes in the shell. In order for this portion of the test to be successful, the aircraft would have to be launched, and the exterior shell would have to stay in place throughout the duration of the launch, and return undamaged. Preparation of the exterior shell prior to launch is shown in Figure 6.2.1.

To test the parachute deployment and rocket booster section deployment, the perfect flight altimeter was used. During a full vehicle flight, typically the inflatable wing would be deployed at apogee. However, since there was no inflatable wing being used for this launch, the parachute was set to be deployed at apogee, while the rocket booster section was set to eject at 300 feet, to make it easily retrievable. The deployment charge used for the main parachute contained 1 gram of black powder, while the rocket booster ejection charge was only 0.5 grams of black powder. Both the parachute and rocket booster ejection were tested on the ground outside the DML days before the launch, to find the appropriate amount of black powder to be used, and ensure that both portions deployed correctly.

Figure 6.2.1: Aircraft Being Prepared for Launch

In order to test the Spektrum transmitter's ability to maintain connections throughout the flight, the EDF propulsion system was prepared and connected to the Spektrum receiver. When the rocket booster section was ejected at 300 feet, a person controlling the transmitter would throttle up and down the EDF to ensure connection. Then, once the aircraft came closer to the ground, the EDF would be put in full throttle so that it could potentially (though not likely) produce thrust, helping to slow its decent. It wasn't likely that the EDF would actually produce any thrust, since the exterior shell was left on the aircraft throughout the launch, making the EDF inlets closed off.

The first launch was performed in Leonard, OK at a sod farm that is commonly used by the Tulsa Area Rocketry Association for high powered rocket launch events. The flight was conducted at approximately 3 pm on October 14, 2012 with max wind speeds at 20 mph, and gusts up to 25 mph. These wind speeds were far higher than we like to launch at, but rocket launch events only take place once a month, so we were forced to launch that day due to time constraints. Pictures of the aircraft during launch are shown in Figure 6.2.2.

Figure 6.2.2: Aircraft during launch

The rocket launch was very successful. The parachute deployment charge was fired at apogee, but due to the packing method used on the parachute prior to launch, it took a few moments for the parachute to unpack its self and fully deploy. The aircraft reached an altitude of 1280 feet AGL at apogee, and had a maximum velocity of approximately 300 feet per second. The rocket booster section also successful deployed at precisely 300feet AGL, as shown in Figure 6.2.3. As the aircraft took off from the launch rail, it turned into the wind as it flew, the parachute deployed and the rocket drifted unit it landed less than 200 feet away from the launch rail that it took off from. Due to its close proximity to the launch rail, the aircraft was not able to be recovered immediately, as there were other rockets being launched at the time. Because of this, the aircraft drug on the ground by its parachute from high gusting winds for a short distance. Once the rocket booster section was ejected, the student controlled the thrust of the EDF from the safe zone of the rocket launch. The transmitter/receiver maintained connection throughout the flight, and the student was able to run the EDF once the aircraft was close to landing. The wine of the EDF could be heard due to the rockets relatively near-by landing. The exterior shell stayed on the aircraft throughout the entire duration of the flight, and no major damage occurred to the aircraft. The aircraft landed with the bottom rudder hitting the ground first, causing some damage to it. Since the aircraft was drug on the ground for a short distance, some dirt and debris was found inside the opening, where the main parachute is stowed.

Figure 6.2.3: Aircraft Recovery

Once the aircraft was returned to the laboratory, data was retrieved from the onboard altimeter for analysis. The altimeter data clearly shows that the parachute was deployed at apogee and significant decelerations was not experienced by the aircraft until approximately 4.3 seconds later. In addition, the altimeter data shows when the EDF was run during the launch. Since there was no inlet for the EDF to suck air in from, it created a small pressure difference inside the aircraft, causing the altimeter to report incorrect altitude readings much higher than the aircraft actually was. This information is important to know, because if the EDF is accidently throttled prior to apogee, and prior to the wing deployment, it could cause the wings to deploy too early, which could damage the aircraft. Great care is taken in subsequent flights to prevent this accident from ever occurring. A simulation in RockSim was conducted after the launch, using the same launch conditions as was experienced on the day of the launch. The results from the simulation

were compared against the altimeter data, and are shown in Figures 6.2.4 and 6.2.5.The raw data from the altimeter and the results from the simulation can be found in Appendix K.

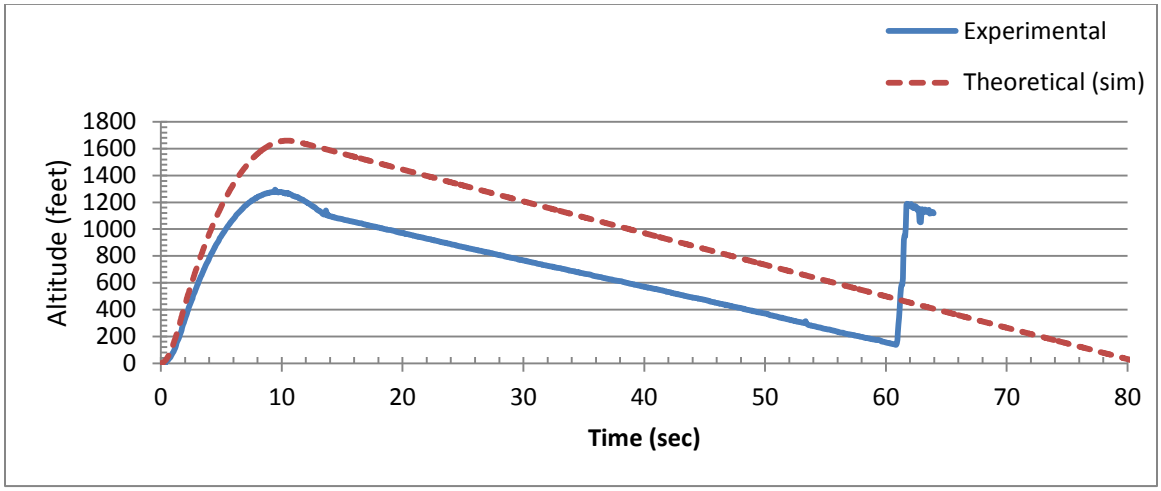

Figure 6.2.4: Flight Results Comparison - Altitude

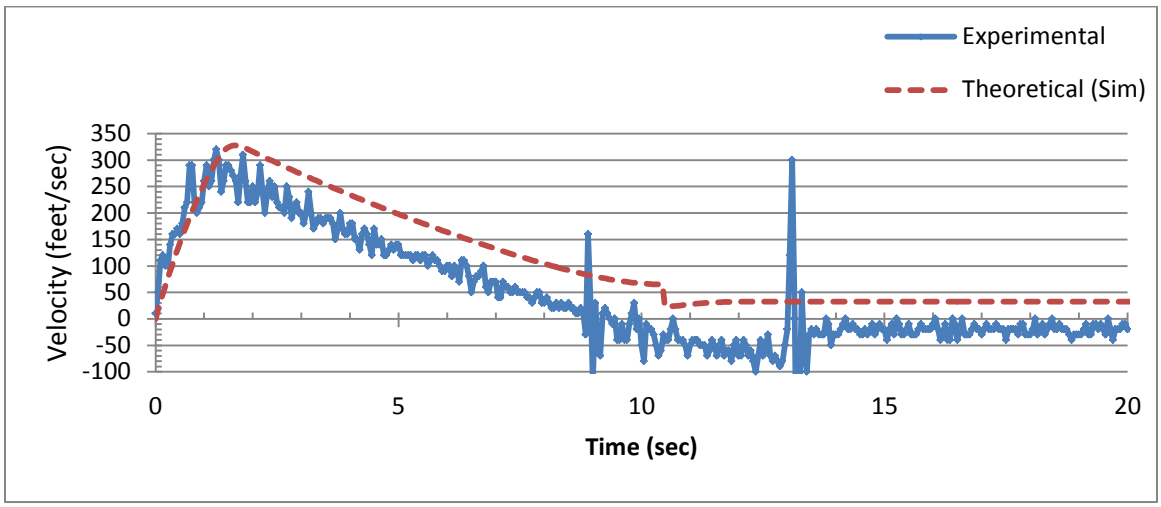

Figure 6.2.5: Flight Results Comparison - Velocity

The packing method for the main parachute will be modified for future tests flights, once an appropriate packing method is found that will allow the parachute to unpack and deploy more quickly. The aircraft reached an altitude of 1280 feet, while the simulation prior to launch estimated that the aircraft would reach over 1800 feet. Due to the high winds that the aircraft was

flown in (approximately 10 to 20 mph), this loss of altitude is not surprising. Efforts will be made to conduct future flight tests earlier in the morning, with much lower wind speeds. Ultimately, the first flight was a resounding success, proving the aircraft's capabilities. All goals that were set for this first launch were achieved, and a significant step forward was made, on its way to a full aircraft flight demonstration.

6.3 AIRCRAFT FLIGHT TEST – FULL SYSTEM

The second flight test evaluated the entire aircraft, and encompassed the entire flight operation of the vehicle. With the success of the first launch, and deployment tests, there was a high level of confidence for the full aircraft flight test. In this flight test, it was expected that the aircraft would launch (as in previous flight) from a launch rail. Once the aircraft reached apogee, the inflatable wings would deploy, and the booster section would eject. The pilot would then be able to fly the aircraft as they would a typical RC aircraft. The goals for this second flight test are shown below.

- Perform a mid-air and in-flight deployment of the inflatable wing.
- Perform a mid-flight deployment of the booster section
- Collect on-board data of the aircraft, including accelerations, roll rates, airspeed velocity, GPS data, and barometric sensor data.
- With the wings deployed, maintain flight stability and fly the aircraft in a simulated loiter scenario.
- Reliable parachute deployment with redundancy in case of failures.

For this flight test, the aircraft was prepared the night before the launch, as there is a lot of work that is involved that takes a long time. The rocket booster and e-matches were built and installed the night before. The inflatable wing was vacuumed and installed with the inflation system into the rocket. The wings were then folded and stored inside of the exterior shell, and all

wiring inside the vehicle was checked the night before the launch. The rocket booster used for this launch was an Aerotech J350; the same as the first launch.

In the first flight, the parachute deployment took longer than what was preferred. Therefore for this launch, the parachute charge was changed to 1.25 grams, while the rocket booster deployment charges were changed to 0.75, representing a 0.25 gram increase for each black powder charge. These new, larger parachute and rocket booster charges were tested on the ground prior to launch day, and were shown to be successful.

Prior to launch, the aircraft was weighed for both its launch configuration, and in-flight aircraft configuration. On the launch pad, the with the rocket motor installed , the aircraft weighed approximately 15lbs, while in-flight as an aircraft, the vehicle weighed 12lbs. Using the flight data from the previous launch, a coefficient of drag for the aircraft was found, where the simulation closely resembled the results of the previous flight test. From these simulations, a Cd of 0.75 was selected. Using this Cd and the weight of the aircraft, RockSim simulations were conducted, with an estimated wind speed ranging from 15 to 25 mph. From these simulations, it was expected that the aircraft would reach an altitude between 850ft to 900ft. In the previous launch, an older Sky Angle Classic 60 inch parachute was used for recovery, and from the flight, gave the aircraft a decent rate of approximately 18 to 21 ft/s (estimated decent rate prior to launch was 18ft/s). For this launch a newer Sky Angle Classic 60 inch parachute with less wear was used. Simulations for the aircraft, using the in-flight weight, put the decent rate at approximately18.4 ft/s. Therefore, realistically, it was expected that the decent rate may be as high as 22 ft/s.

Prior to this launch, it was decided to include a couple additional pieces of hardware that would allow for on-board data collection and video. The hardware used was an Ardupilot Mega (APM) 2.5 with an optional airspeed sensor, while on board video was provided by two Muvi Micro cameras. Due to this late decision, last minute changes had to be made to the aircraft and

avionics bay in order to include the hardware. The airspeed sensor pitot-static tube was mounted approximately half an inch off of the surface of the aircraft body, located on the top of the aircraft. While this location is not ideal for a pitot-static tube, it is the best that could be accommodated, given the short timeline. Two Muvi cameras were mounted to the exterior of the aircraft. One camera was mounted to a launch rail in order to provide a forward facing camera located behind the main wing. The second camera was mounted near the avionics bay, on the belly of the aircraft and provided a side-view from the aircraft during its flight.

For this launch and flight test, extra safety precautions were taken to ensure success. Two Perfect Flight Altimeters with separate switches and battery supplies were used (rather than the one used in the first launch). The first altimeter was programmed to deploy the inflatable wing (via inflation system) at apogee, and provide a back-up rocket booster deployment at an altitude of 750 ft. The second altimeter was programmed to deploy the rocket booster at apogee (primary charge) and provide a back-up main parachute deployment at 150ft in case of radio-loss. There was some concern in programming the altimeter to deploy the parachute, since during the first flight test it was discovered that the EDF motor messes with the barometric pressure sensor. However, from the data collected during the first launch, it seems that the EDF causes the altimeter to read higher altitudes than what is actually true, so it was deemed unlikely that the EDF motor might accidently trigger the parachute deployment. In this launch, the remote controlled parachute deployment system was included, and provided the primary method of deploying the parachute during flight for both recovery and emergency scenarios.

The second flight test, and full system test was conducted at the Oklahoma State University UAV airfield. The flight was conducted at approximately 11:25 AM on Saturday November 24, 2012. At the time of the launch, wind conditions were averaging 12 mph to the North, and it was approximately 50 degrees F outside. Pictures of the aircraft during its flight are shown below in Figures 6.3.1 and 6.3.2.

Figure 6.3.1: Aircraft During Ascent

The flight test was not completely successful; however a lot was learned from this flight. During the rocket boost phase, debris was witnessed falling from the rocket. Soon thereafter it was discovered that the control surfaces on the horizontal stabilizers had fluttered to the point of destruction and had fallen off. The vertical stabilizers also experienced flutter, and received damage, but did not fall off. When the stabilizers had fluttered off, it is estimated that the aircraft was traveling between 160 ft/s and 200 ft/s. The inflatable wings were deployed at apogee as programmed and the exterior shells fell from the aircraft under parachute. Due to the fluttering of the control surfaces, the aircraft did not reach the expected 850ft altitude. Instead the rocket reached an altitude of 660 ft at apogee. The rocket booster was also supposed to be ejected at this point, but failed to do so, while the backup ejection charge for the booster was programmed to fire at 750 feet. The backup charge fired soon after apogee, since the aircraft did not reach an altitude above 750 ft. During the flight, ground video captured the two rocket booster ejection charges firing, but the rocket booster did not eject from either. Instead, the rocket booster did not come out until the aircraft was under parachute and the rocket booster was able to fall out of the aircraft.

When the inflatable wing deployed at apogee, the aircraft was oriented upside-down. So when the inflatable wing was fully inflated, it created lift and the aircraft tried to pull out of the loop-like maneuver. Our pilot, attempted to pull the aircraft out of this state, but since the aircraft had lost its control surface's, he was unable to do so. As the aircraft continued to fall at a high velocity, the inflatable wing buckled, as shown in Figure 6.3.2 (left). It was later discovered that there was a leak in the inflation system where inadequate CA was applied to the hex plug (see Appendix E, Step 4). The leak in the inflation system, coupled with the high velocity caused the wing to buckle in flight. Once it became obvious to the pilot that he could not control the aircraft, and it was approaching the ground quickly, he reacted quickly and deployed the parachute. The parachute deployment occurred quickly and the aircraft was safely under parachute within approximately 1 second; a big improvement over the 4 seconds seen in the first flight. Once it was recovered, it was found that all deployment charges had fired throughout the flight, as designed.

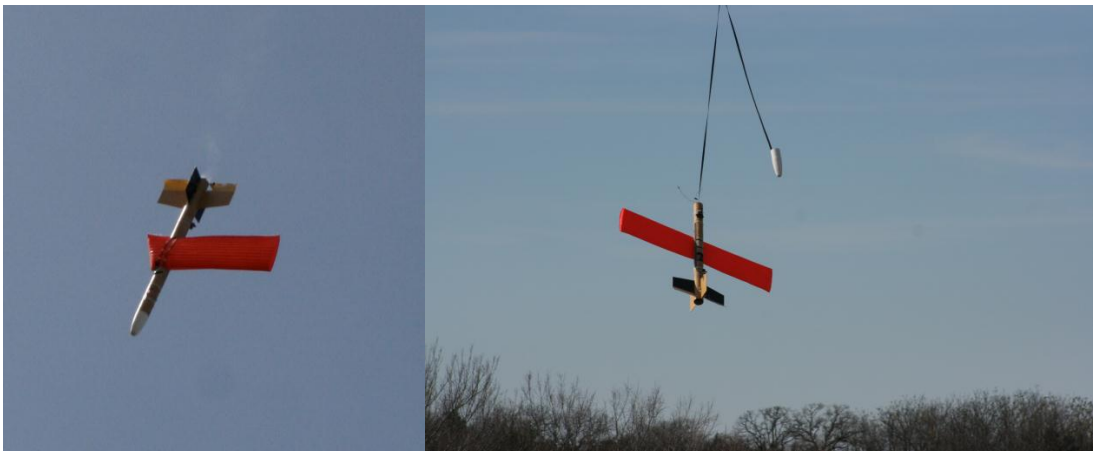

Figure 6.3.2 Aircraft During Descent

Once the aircraft had been recovered the damage was accessed. The left horizontal stabilizer had taken the blow when the aircraft landed under parachute, and therefore received significant (but repairable) damage. As mentioned previously, the horizontal stabilizer control surfaces had fluttered off during the rocket booster phase, while the vertical stabilizers had

received flutter damage as well. It was also found that a crack in the aircraft structure had occurred near the EDF inlet, and it is not clear if this occurred in flight or during landing.

Once the aircraft was recovered, data from the two altimeters and the Ardupilot Mega, was retrieved, while video from server ground-based cameras and the two on-board cameras were retrieved. Both altimeters confirmed that all of the e-matches had been deployed in flight, while the altitude data from the altimeters and the APM closely resemble each other, as shown in Figure 6.3.3. The airspeed sensor used on the APM experienced issues during flight. The sensor was only able to collect data for approximately 4 seconds of the 30 second flight. From RockSim simulations, it was expected that the aircraft would reach airspeeds up to 200 ft/s, but due to the fluttering issues, the aircraft obviously did not reach these velocities. The airspeed sensor measured a maximum of 160 ft/s which is fairly reasonable, but obviously a lot of airspeed data is missing. Altimeter and Accelerometer data collected throughout the flight, while more data, and graphs with more information can be found in Appendix L.

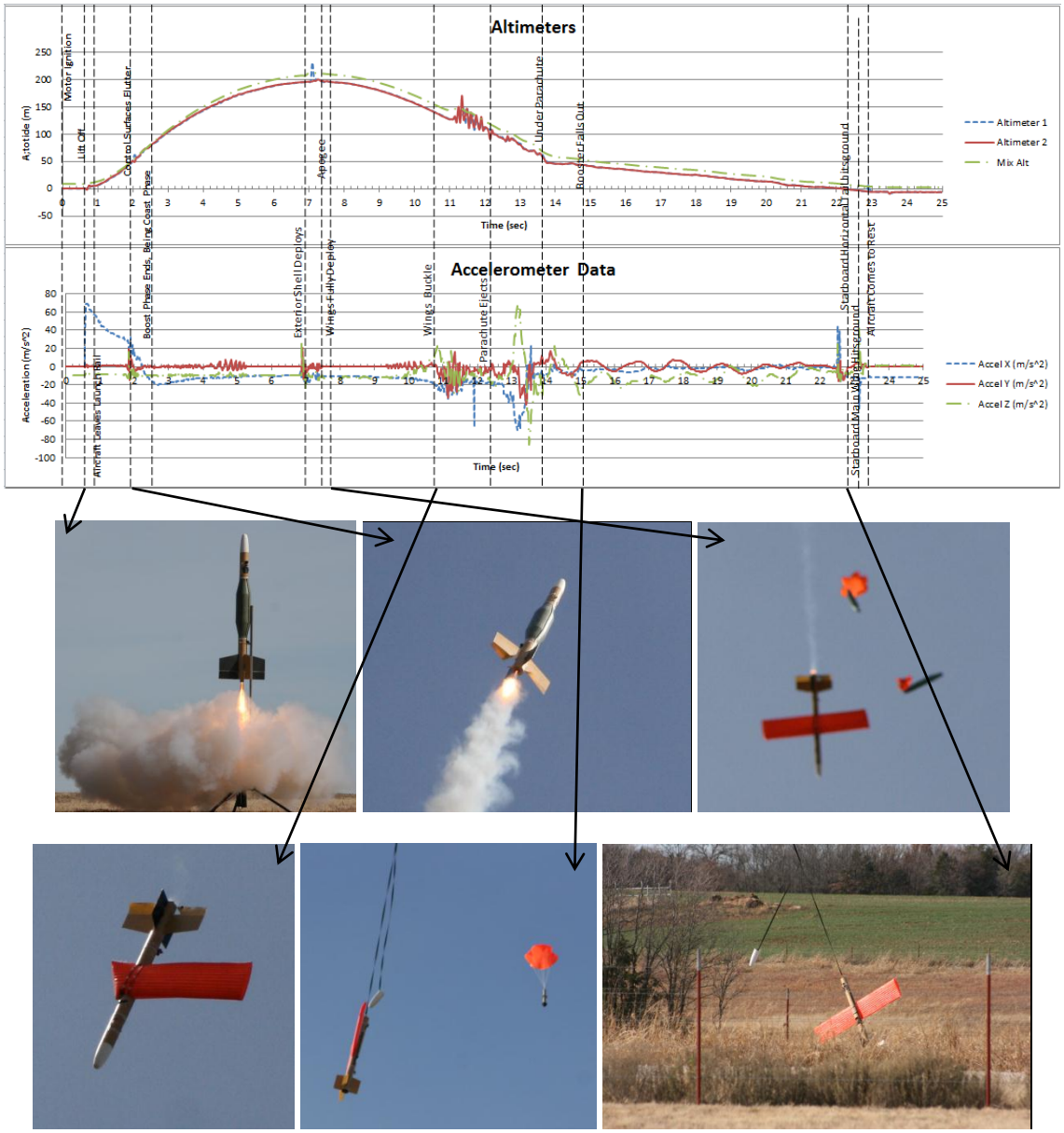

Figure 6.3.3: Flight Data and Events

Once this data was analyzed, further RockSim simulations were performed in order to determine how much drag the aircraft experienced from the fluttering of the control surfaces. From the previous flight test, it was estimated that the aircraft has a Cd of 0.75 while it is in its rocket boost phase. From the data in Figure 6.3.3 we see that the two altimeters, which utilize barometric pressure to measure altitude, read 200 meters for apogee, while the Mix Altitude from the APM read 213 meters. The Mix altitude on the APM is an altitude derived from a

combinations of GPS data and barometric pressure data. Using this data, the coefficient of drag was backed out using RockSim, and was found to be a Cd of 1.5; double that of its initial drag.

Using the data from the flight, the student estimated the airspeed of the aircraft when the inflatable wing buckled. Using the three different sets of altitude data, and the RockSim simulations, it was estimated that the aircraft was traveling at approximately 96 ft/s at the time just prior to the wing buckling. Using the airfoil data of the inflatable wing, the student found that the inflatable wing was producing approximately 12.2 lbs of lift. This lift force is approximately equal to the aircraft's weight in-flight, indicating that the aircraft was gliding. Using the aircraft performance analysis data previously calculated for thrust requirements, it was found that the aircraft had a glide slope ratio of 7.0. Once the inflatable wing load was found, the student used the experimental and theoretical data obtained from the wing bending tests, and found that the inflatable wing buckles at 12.2 lbs when it is pressurized to only 2.45 psi. From this analysis, suspicions were confirmed, and the leak in the inflation system directly caused the inflatable wing to buckle, due to the loss in wing pressure.

Despite the aircraft not being able to fly around and perform a simulated loiter mission, this mission is considered fairly successful. Out of all of the things that could have gone wrong with this project, and this flight test, the aircraft functioned quite well. The wing was successfully deployed in mid-flight, all flight events (spare the booster deployment) worked perfectly, and the aircraft was able to be recovered despite having no control. Future efforts will be focused on redesigning and improving this aircraft. One of major design considerations will be the elimination of fluttering in the control surfaces.

CHAPTER VII

CONCLUSIONS AND FUTURE WORK

7.1 CONCLUSIONS

The purpose of this project was to develop an aircraft that incorporated a solid rocket booster and an inflatable wing that would be deployed in midflight. The aircraft's mission was to take off as a rocket using the solid rocket booster, then when the aircraft reached apogee deploy the inflatable wings in mid-flight. Once the wings were deployed, the aircraft could loiter and fly around as a UAV. Developing a UAV with such transformation capabilities is no simple task, and required a lot of analysis, design trade-offs and testing. Ultimately, the aircraft described in this paper was unable to perform the loitering portion of the mission, since the control surfaces were destroyed during boost phase by fluttering, however this aircraft and the testing that went into it made significant steps towards a complete aircraft system with such transformation capabilities.

This inflation system developed in this project proved to be a major success for this project, as previous inflation systems seen in NASA I2000, ILC Dover Quicklook/FASM, and previous OSU research proved to be overly complicated, unreliable, or dangerous in some cases. The inflation system developed in this project can be easily reproduced in-house, by anyone that is competent in using a lathe and mill. The inflation system is small, lightweight, reliable, safe, and provides an excellent method for deploying the inflatable wings in approximately half a second. The inflation system is small enough to fit within the four-inch body tube used on the aircraft, and while the system weighs approximately 100 grams without the Co2 cartridges.

Furthermore, it can easily be initiated by a simple relay system a 9v battery. The inflation system proved to be an excellent method of deploying the inflatable wings in mid-flight, while the only down-side being that it requires some cleaning between uses.

The exterior shell and shear pin used to contain the inflatable wing prior to deployment also proved to be reliable. There was some concern that the exterior shell or shear pin may fail, and cause the inflatable wing to deploy prematurely, but after two flight tests, and static deployment tests, no such failure was ever experienced. Furthermore, the parachute deployment system used in this aircraft also proved to be reliable when it helped to prevent damage to the aircraft in the second flight test. The wing mount developed for this aircraft also worked very well, and provided a method of holding the inflatable wing in the correct orientation, despite the changing volume, and unpredictable dynamics of the inflatable wing during inflation.

7.2 FUTURE WORK

There are several aspects of this aircraft that could be improved for future versions of this aircraft. The first aspect that could use some improvement is the avionics bay. The avionics bay proved to be structurally very sound, and never had any failures. However, it was quite a hassle to manage all of the wires that ran from the aircraft body to the avionics bay. Because the avionics bay is completely removable, and bolts into the airframe, the wires that run to each electronic device had to be long enough to clear the opening of the aircraft, and connect to the avionics bay prior to installing the avionics bay. Because of this, there is a tangle of long wires that have to be stuffed inside of the aircraft body. Ideally, the best solution would be to make an all composite, custom aircraft body, with hatches that bolt onto the aircraft body. This would allow for a static avionics bay that could be built into the composite body along with the wing mount. In addition,

the molds created for the custom aircraft body would allow for quick turn-around time and allow for multiple aircraft to be made more efficiently. However, if the recourses are unavailable to create a custom composite aircraft body, as they were in this project, one could simply redesign the avionics bay section to allow for removable bulkheads instead. A major problem with this avionics bay is that some of the mounting hardware used to hold the bay in place is located inside of the exterior shell when the aircraft is completely assembled. So, if there ever came a time that something inside the avionics bay needed to be changed, such as changing out batteries or moving servo wires, one would essentially have to disassemble the aircraft.

Another area for improvement would be on the plumbing for the inflatable wing and inflation system. During the assembly and flight preparation of the aircraft the inflatable wing need to be deflated and air vacuumed out in order for the wing to fold properly and be stored inside of the exterior shell. Once the wing was deflated, it was connected to the inflation system. The wings were then folded and stored inside of the exterior shell. This process proved to be troublesome and quite a hassle. One major problem was that it was difficult to align the plumbing hardware on the inflatable wing with that of the inflation system. Because of this difficulty, significant air would seep back into the inflatable wing, and the wing would no longer be able to fit inside of the exterior shell. One easy way that this could be resolved would be include a Tee section in the plumbing, where the opening would be easily accessible by the vacuum pump and could be capped and closed off once the wing was fully deflated. This improvement was not included during this project, as insufficient time was available to order the aluminum tee and plug prior to launch. In addition, this addition would have caused problems when trying to put the avionics bay back into the aircraft, as the inflation system would be protruding out.

Obviously, one of the biggest considerations for future would have to be the fluttering of the control surfaces during the rocket booster phase. While this problem was considered during the design construction of the aircraft, very little could be done about it due to a lack of resources, and a lack of experience in dealing with this kind of problem. The fluttering of the control surfaces occurred during the boost phase of the aircraft, when it was traveling approximately 160 to 200 ft/s. In future work, it is recommended that multiple tail sections be made with a variety of materials and construction methods. The tail section should then be tested in the OSU wind tunnel in order to assess the flutter in the control surfaces. These tail sections would need to include the controlling hardware, including servos, control lines, and servo horns, installed on the tail sections in order to accurately represent the aircraft's controlling stabilizers. The controlling hardware needs to be tested just as much as the control surface its self, as slack in the control line, and the drag created by the servo horns and connecting hardware play a major role in the fluttering of the aircraft's control surfaces.

In addition to these tests, it is imperative that a control surface with a stiffer span be used. The control surfaces used in this project were CNC cut out of a stock piece of material that was laid up. The stock material contained a layer of Kevlar, $1/8^{th}$ balsa core, and a layer of carbon fiber. One of the biggest downfalls of these control surfaces was the delamination of the composite materials from the balsa core. In order to resolve this, the core material should be cut out first to the correct dimensions, and the composite materials should then be laid up on top of it, with the edges of the materials joining around the core. Furthermore, while the balsa core proved to be very light weight and capable of surviving the dynamic forces experienced in flight, each time the aircraft landed under parachute one of the stabilizers was destroyed due to the decent rate

of the aircraft. While a larger parachute would also help to resolve this issue, it would also take up more space and may be difficult to accommodate. A core material comprising of $1/8^{th}$ inch birch plywood, or composite materials should be sufficient to handle the loads during the landing of the aircraft, though the effects of the added weight would need to be assessed.

During the second flight test, the rocket booster section had problems deploying, and did not eject at apogee like it should have. It is not entirely clear why the rocket booster did not eject, when the two separate charges fired during flight. Despite the multitude of successful ground tests of the rocket booster ejection, the booster appeared to have become stuck inside the aircraft body after the rocket booster had fired. This problem could be easily fixed by adding stand-offs to the rocket booster motor mount, however more testing would be required to ensure its success. Additional improvements could be made to the motor mount in order to accommodate a variety of rocket motors of various sizes. This could be done by extending the motor mount tube, so that it protrudes from the aircraft body. This would help to push the CG of the aircraft back during the rocket booster phase, making the vehicle less stable, as currently the vehicle is over-stable in this flight mode. Furthermore, a larger diameter motor tube, up to 54mm, could also be used in future improvements, with an adapter being used to allow for smaller 38mm rocket motors. This would allow for more powerful rocket motors to be used, so the rocket could be launched to a variety of altitudes during flight tests.

In the second flight test, the inflatable wing deployed with the aircraft upside-down. To prevent this sort of problem from happening again, the aircraft should be mounted on the launch rail in such a way that when the aircraft weather-cocks into the wind, the aircraft will be oriented in the correct attitude. Furthermore, it is recommended that the student utilize an on-board

autopilot with augmented control. The autopilot should be programmed such that it will control the elevons and keep the aircraft oriented correctly prior to wing deployment. This will ensure that when the inflatable wings deploy, the aircraft is orientated in a favorable attitude. Since the Ardupilot Mega 2.5 was used for data-logging in the second flight, the same hardware could also be used to perform these autopilot functions.

Other improvements to the launch vehicle would include redesigning the inflatable wing mount. During the construction process flaws in the design were found, when the 38 gram Co2 cartridge had inadequate space inside of the aircraft body. Modifications were made to the wing mount in order to resolve this, but in future designs, better care should be taken to accommodate the inflation system.

Once the aircraft was constructed, it was found that the vehicle was over-stable when the aircraft was in flight mode, as the center of gravity was located almost at the leading edge of the aircraft, rather than at the quarter-chord as is desired. During the design process, it was decided that the LiPo battery used for EDF propulsion would be used to alter the CG and balance the aircraft as desired. However, the battery could not be moved far enough back in the aircraft to fix the CG. During the re-designing of the aircraft, better weight estimations should be used to accurately predict the CG of the aircraft. One way that this could be fixed would be to include a larger, more powerful EDF. The aircraft, as it currently stands has a thrust-to-weight ratio of approximately 0.3. While this ratio is appropriate for “trainer” type aircraft, it may be under powered for the needs of this aircraft. Unfortunately, during the second flight test the propulsion system never saw use, as the aircraft could not be flown, so whether the aircraft is underpowered as speculated, it has not been tested.

Currently there is also one more flight test in preparation as of the release of this report. The next flight test will be conducted without any control surfaces on the stabilizers, and will utilize the same airframe. The horizontal stabilizer that received damage upon landing in the previous flight will be replaced. The primary goal of this flight will be to conduct another mid-flight inflatable wing deployment. Extra care will be taken during the preparation of the inflation system and inflatable wing to ensure that there are no leaks, so that the inflatable wing will not deflate during flight as seen in the previous flight test. The vehicle's solid rocket booster will be an Aerotech J350, and the aircraft will have on-board video and data acquisition. The on-board video cameras will be mounted in order to obtain the best view of the wing deployment in flight. This flight test data and footage will be featured in a report written by this author for the AIAA 51st Aerospace Sciences Meeting (ASM) Conference.

With the success of the first flight test, and the limited success found in the second, there has been a lot of information and experience gathered in this project. As far as we know, this aircraft is the only aircraft that has ever captured on-board in-flight inflatable wing deployment. Furthermore, the development of this new inflation system will help future programs and aircraft to achieve in-flight inflation. This aircraft has served as a good first step towards a fully functional hybrid rocket-UAV, with a vast amount of data, video, and experience obtained throughout this project.

CHAPTER VIII

APPENDICIES

A. UNDERGRADUATE SPACECRAFT DESIGN PROJECTS

As part of a project for undergraduate students in Spacecraft Design class, an early aircraft was developed by a team of students at OSU. This rocket incorporated a small inflatable wing that was deployed at apogee. The inflation system uses the Rouse Tech system, enclosed inside of a PVC container. The inflation system proved to be dangerous during early testing. During it's flight, the rocket was able to deploy the inflatable wings and experienced significant structural failures. This model was never meant to actually be able to fly as a UAV, and the author does not believe that any significant analysis went into any of the subcomponents, or in the stability of the rocket/aircraft. Because of these factors, no aspect of this aircraft's design was incorporated into the UAV discussed in this report. The author used this project as an example and learned from their short-fallings.

(Aircraft Prior to flight, left. Onboard video capture, middle. Aircraft remains during decent)

The author of this report also participated in a undergraduate Spacecraft Design Project of another year. For their project, the student teams were told to develop a rocket that enclosed a small UAV. This UAV was deployed mid-flight, and had to fly from to a predetermined "home" position, using GPS navigation. The author, Cory Sudduth, was lead engineer for one of these teams. From the pictures below, one can see the rocket prior to launch (top, left) and the UAV (top, right) as the GPS navigation system is being installed. The bottom picture shows the rocket and UAV at the moment of deployment. The rocket system had an upper and lower section, each with its own parachute as shown in the picture. During this rocket launch, the system performed as designed. The rocket successfully separated the upper and lower sections, and deployed their parachutes, while deploying the UAV payload. The UAV system flew to its home GPS location and loitered until it landed at its home location.

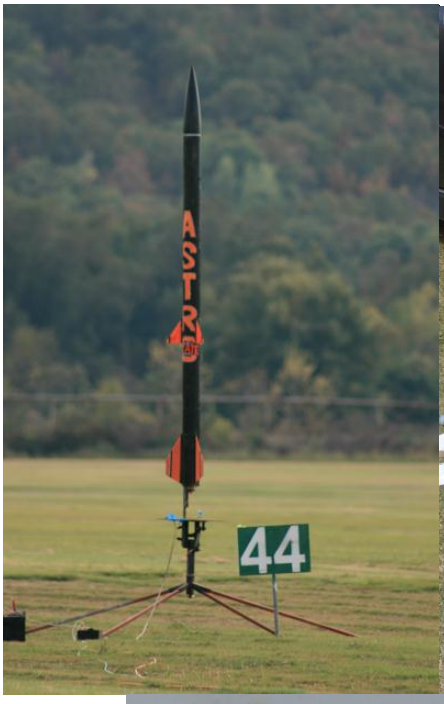
ASTR
44

B. WING LOADING TEST DATA

Wing Loading Test, 8psi

Load (lb)	Deflection (in)	Dihedral Angle (deg)	Moment (lb*ft)	
0	0	0	0	
2.5	0.125	0.403484735	1.848958333	
5	0.25	0.806929455	3.697916667	
7.5	0.375	1.210294169	5.546875	
10	0.5	1.613538933	7.395833333	
12.5	0.625	2.016623875	9.244791667	
15	0.75	2.419509217	11.09375	
17.5	0.875	2.8221553	12.94270833	
20	1.125	3.626571784	14.79166667	
22.5	1.25	4.028263666	16.640625	
25	1.375	4.429559299	18.48958333	
27.5	1.5	4.830419958	20.33854167	
30	1.625	5.230807176	22.1875	
32.5	1.875	6.030008808	24.03645833	
35	2.375	7.621071309	25.88541667	
37.5	#VALUE!	#VALUE!	27.734375	Buckle

Wing Loading Test, 10psi

Load (lb)	Deflection (in)	Dihedral Angle (deg)	Moment (lb*ft)	
0	0	0	0	
2.5	0.0625	0.201746119	1.848958333	
5	0.125	0.40349474	3.697916667	
7.5	0.25	0.807009493	5.546875	
10	0.4375	1.412362948	7.395833333	
12.5	0.5	1.614179142	9.244791667	
15	0.625	2.017874143	11.09375	
17.5	0.75	2.421669387	12.94270833	
20	0.875	2.825585021	14.79166667	
22.5	1.0625	3.431728409	16.640625	
25	1.125	3.633858325	18.48958333	
27.5	1.25	4.038256596	20.33854167	
30	1.375	4.442856478	22.1875	
32.5	1.625	5.252743211	24.03645833	
35	1.875	6.063683871	25.88541667	
37.5	2.0625	6.672681546	27.734375	
40	2	6.46960161	29.58333333	
42.5	2.125	6.875845726	31.43229167	
45	2.375	7.689398296	33.28125	
47.5	2.625	8.504513681	35.13020833	
50	2.875	9.32136691	36.97916667	
52.5	#VALUE!	#VALUE!	38.828125	Buckle

C. CO2 CARTRIDGE SIZING TABLE

C02													
Molar Mass		44.01	gram/mole							Inflatable Wing			
		Gauge Pressure		Absolute Pressure						Design Pressure	8	psi	
Pressure		0	psi	1	atm					Burst Pressure	15	psi	
		Ambient Temperature		Absolute Temperature									
Temperature		70	°F	294.2611111	K					From Volume estimation of the wing on next page; Maximum obtainable pressure / loading factor for each canister			
R, Gas constant		0.0821	L*atm/K*mol							Minium Pressure Required =	7.538964	psi	
http://www.genuineinnovations.com/custom-valve-technology/oem-gas-cylinders.html										Wing Volume=	1285	in^3	
http://www.pbnation.com/showthread.php?t=3185252													
		Internal Volume				Inflated Volume @ Spec Conditions							
C02 Catridge (grams)		(ml)	(in^3)	Weight (grams)	Weight (lb)	Moles C02	(Liters or m^3)	(in^3)		Gauge Pressure (psi)	Loading Factor, n		
8	grams	10	0.610237441	24.5	0.054013254	0.181776869	4.389242328	267.848		-11.63269549	-1.54301		
12	grams	14	0.854332417	41.1	0.09060999	0.272665303	6.583863491	401.772		-10.10106884	-1.33985		
16	grams	16	0.976379906	58	0.127868112	0.363553738	8.778484655	535.696		-8.569442181	-1.13669		
20	grams	12+8 gram canisters		65.6	0.144623244	0.454442172	10.97310582	669.62		-7.037815527	-0.93353		
24	grams	12+12 gram canister		82.2	0.181219979	0.545330607	13.16772698	803.544		-5.506188872	-0.73036		
25	grams	32	1.952759811	100	0.220462262	0.568052715	13.71638227	837.025		-5.123282208	-0.67957		
28	grams	12 + 16 gram canisters		99.1	0.218478102	0.636219041	15.36234815	937.468		-3.974562217	-0.5272		
33	grams	8+25 gram canisters		124.5	0.274475516	0.749829584	18.1056246	1104.873		-2.060028899	-0.27325		
37	grams	12+25 gram canisters		141.1	0.311072252	0.840718019	20.30024577	1238.797		-0.528402244	-0.07009		
38	grams	52	3.173234693	130.4	0.28748279	0.863440127	20.84890106	1272.278		-0.145495581	-0.0193		
41	grams	16+25 gram canisters		158	0.348330374	0.931606453	22.49486693	1372.721		1.00322441	0.133072		
45	grams	62	3.783472134	185	0.407855185	1.022494888	24.68948809	1506.645		2.534851065	0.336233		
46	grams	8+38 gram canisters		154.9	0.341496044	1.045216996	25.23814338	1540.126		2.917757729	0.387024		
50	grams	12+38 gram canisters		171.5	0.378092779	1.136105431	27.43276455	1674.05		4.449384383	0.590185		
53	grams	8+45 gram canisters		209.5	0.461868439	1.204271756	29.07873042	1774.493		5.598104374	0.742556		
54	grams	16+38 gram canisters		188.4	0.415350902	1.226993865	29.62738571	1807.974		5.981011038	0.793347		
57	grams	12+45 gram canister		226.1	0.498465174	1.295160191	31.27335158	1908.417		7.129731029	0.945718		
60	**grams**	**from testing**				1.363326517	32.91931746	2008.86		8.27845102	1.098089		
61	grams	16+45 gram canister		243	0.535723297	1.386048625	33.46797275	2042.341		8.661357684	1.148879		
63	grams	25+38 gram canisters		230.4	0.507945052	1.431492843	34.56528333	2109.303		9.427171011	1.25046		
70	grams	25+45 gram canister		285	0.628317447	1.590547603	38.40587037	2343.67		12.10751766	1.605992		
76	grams	38+38 gram canister		260.8	0.574965579	1.726880254	41.69780211	2544.556		14.40495764	1.910734		
83	grams	38+45 gram canister		315.4	0.695337974	1.885935015	45.53838915	2778.923		17.08530428	2.266267		
88	grams	120	7.322849292	445	0.981057066	1.999545558	48.2816656	2946.328		18.9998376	2.520219		
90	grams	45+45 gram canister		370	0.815710369	2.044989775	49.37897619	3013.29		19.76565093	2.621799		
92	gram*			408	0.899486029	2.090433992	50.47628677	3080.252		20.53146426	2.72338		
96	grams	8+88 gram cartridges		469.5	1.03507032	2.181322427	52.67090793	3214.176		22.06309091	2.926542		
99.22	grams	Paintball Tank		374.2	0.824969784	2.254487616	54.43757797	3321.9848		23.29605037	3.090086		
104	grams	16+88 gram canisters		503	1.108925178	2.363099296	57.06015026	3482.024		25.12634422	3.332864		
113	grams	25+88 gram canister		545	1.201519328	2.567598273	61.99804788	3783.353		28.57250419	3.789978		
113.4	gram	Paintball Tank		385.55	0.849992251	2.576687117	62.21750999	3796.7454		28.72566686	3.810294		
120	grams				0	2.726653033	65.83863491	4017.72		31.25285084	4.14551		
126	gram	38+88 gram canister		575.4	1.268539856	2.862985685	69.13056666	4218.606		33.55029082	4.450252		
	* from the Rouse tech kit - may be difficult to find replacements												
http://www.amazon.com/Crosman-AirSource-pre-filled-disposable-tanks/dp/B0002IL6Y4/ref=sr_1_7?ie=UTF8&qid=1321846563&sr=8-7													
http://www.amazon.com/Crosman-AirSource-pre-filled-disposable-gram/dp/B000W1R1WC/ref=sr_1_13?ie=UTF8&qid=1321846563&sr=8-13													

D. WING VOLUME TESTING DATA

Test 1										
Weight										
Genuine Innovations Ultraflate Plus				EMPTY	64	g				
	Minus lower shell				24	g				
Leland 16g Co2 cartridge, threaded				FULL	62	g				
Cartridge 1										
Leland 16g w Ultraflate Upper				FULL	102	g				
		Initial Pressure			0	psi				
		Final Pressure		~	1	psi				
Leland 16g w Ultraflate Upper				EMPTY	86	g				
			Total Co2 Weight		16	g				
Cartridge 2										
Leland 16g w Ultraflate Upper				FULL	102	g				
		Initial Pressure			1	psi				
		Final Pressure		~	1	psi				
Leland 16g w Ultraflate Upper				EMPTY	86	g				
			Total Co2 Weight		16	g				
Cartridge 3										
Leland 16g w Ultraflate Upper				FULL	102	g				
		Initial Pressure			1	psi				
		Final Pressure		~	5	psi				
Leland 16g w Ultraflate Upper				EMPTY	86	g				
			Total Co2 Weight		16	g				
Cartridge 4										
Leland 16g w Ultraflate Upper				FULL	102	g				
		Initial Pressure			5	psi				
		Final Pressure		~	8	psi	Problems with pressure loss, leaking			
Leland 16g w Ultraflate Upper				EMPTY	92	g	Estimated final weight			
			Total Co2 Weight		10	g				
			Total Grams of Co2		**58**	**±**	**4**	**grams**		

Test 2								
Weight								
Genuine Innovations Ultraflate Plus				EMPTY	64	g		
	Minus lower shell				24	g		
Leland 16g Co2 cartridge, threaded				FULL	62	g		
Leland 25g Co2 cartridge, threaded				FULL	95	g		
Cartridge 1								
Leland 25g w Ultraflate Upper				FULL	136	g		
		Initial Pressure			0	psi		
		Final Pressure		~	1	psi		
Leland 25g w Ultraflate Upper				EMPTY	112	g		
			Total Co2 Weight		24	g		
Cartridge 2								
Leland 25g w Ultraflate Upper				FULL	136	g		
		Initial Pressure			1	psi		
		Final Pressure		~	6.25	psi	wing is rigid	
Leland 25g w Ultraflate Upper				EMPTY	112	g		
			Total Co2 Weight		24	g		
Cartridge 3								
Leland 16g w Ultraflate Upper				FULL	102	g		
		Initial Pressure			6.25	psi		
		Final Pressure		~	8.25	psi		
Leland 16g w Ultraflate Upper				EMPTY	90	g		
			Total Co2 Weight		12	g		
			Total Grams of Co2		**60**	**±**	**2**	**grams**

E. PYRO-VALVE INFLATION SYSTEM PREPARATION

Prior to each inflation test, an e-match was wired through the e-match holder (AN -6 hex plug). The gaps around the wire was filled using thick CA glue, and a small fillet of glue was place around the area to ensure no air would pass through it. The cavity inside the hex plug was filled with 0.5 grams of FFFF black powder (the standard black powder used for high powered rocketry) and a piece of masking tape was used to keep the black powder in place. Plumbers tape was wrapped around all threaded parts, while the piercer and inside of the pyro-valve casing was lubricated using a non-flammable lubricant: white lithium grease. Instructions on preparing and assembling the Inflation system are below.

Step 1: Assemble Parts:

- Thick CA
- CA Accelerant
- Masking tape
- Pipe tape
- Cotton Swabs
- Lithium Grease
- FFFF Black Powder
- Inflation System
- O-rings
- E-matches
- Isopropyl Alcohol
  (for Cleaning afterwards)

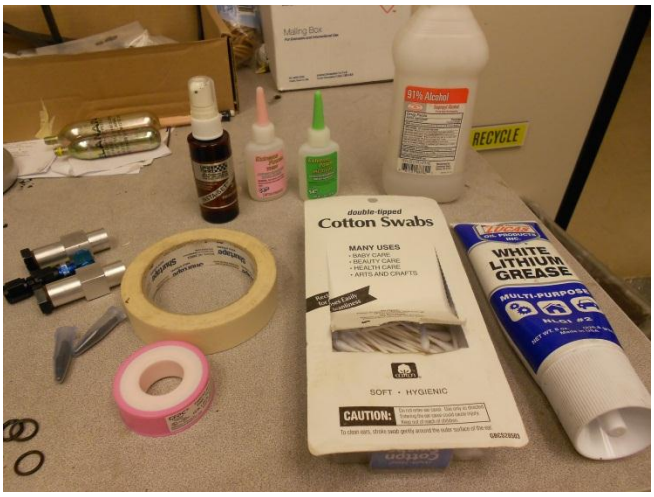

Step 2: Apply grease to the inside shell of the pyro-valve. Put the O-rings onto the piercers and apply grease.

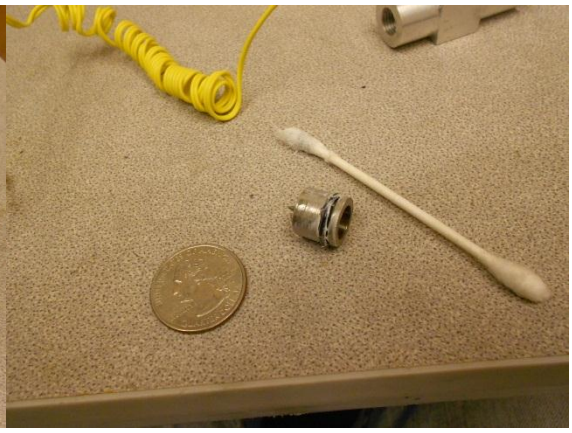

Step 3: Run the wires for the E-match through the drilled hole in the Hex Plug, with the head of the E-match nearly flush with the plug opening.

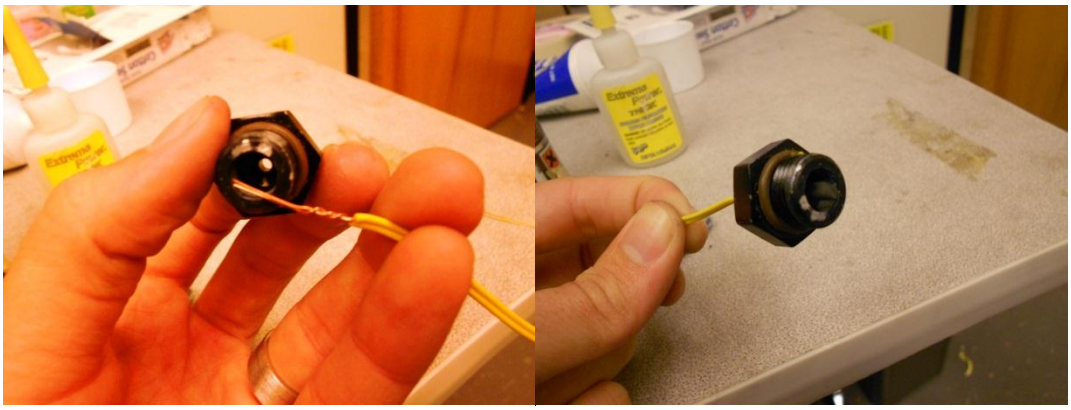

Step 4: CA (using Thick CA) the wire to the Hex plug, making sure to fill the gaps around the wire – preventing air loss. Be careful, as CA produces heat as it cures – which could potentially, however unlikely, ignite the E-match or nearby black powder. Use CA Accelerant if needed. Create a small fillet between the wire and the hex plug

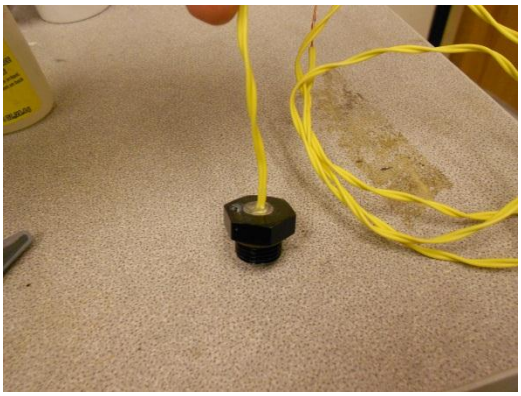

Step 5: Pour 0.5 grams of FFFF black powder into the cavity of the hex plug. Do not use any more than half a gram, as 0.5 grams is more than enough as-is. Then place a piece of masking tape over the top to keep the powder in, and cut off the excess tape with a razor blade. Ensure that there are no grains of black powder on the threads of the plug, as it could detonate when threaded!

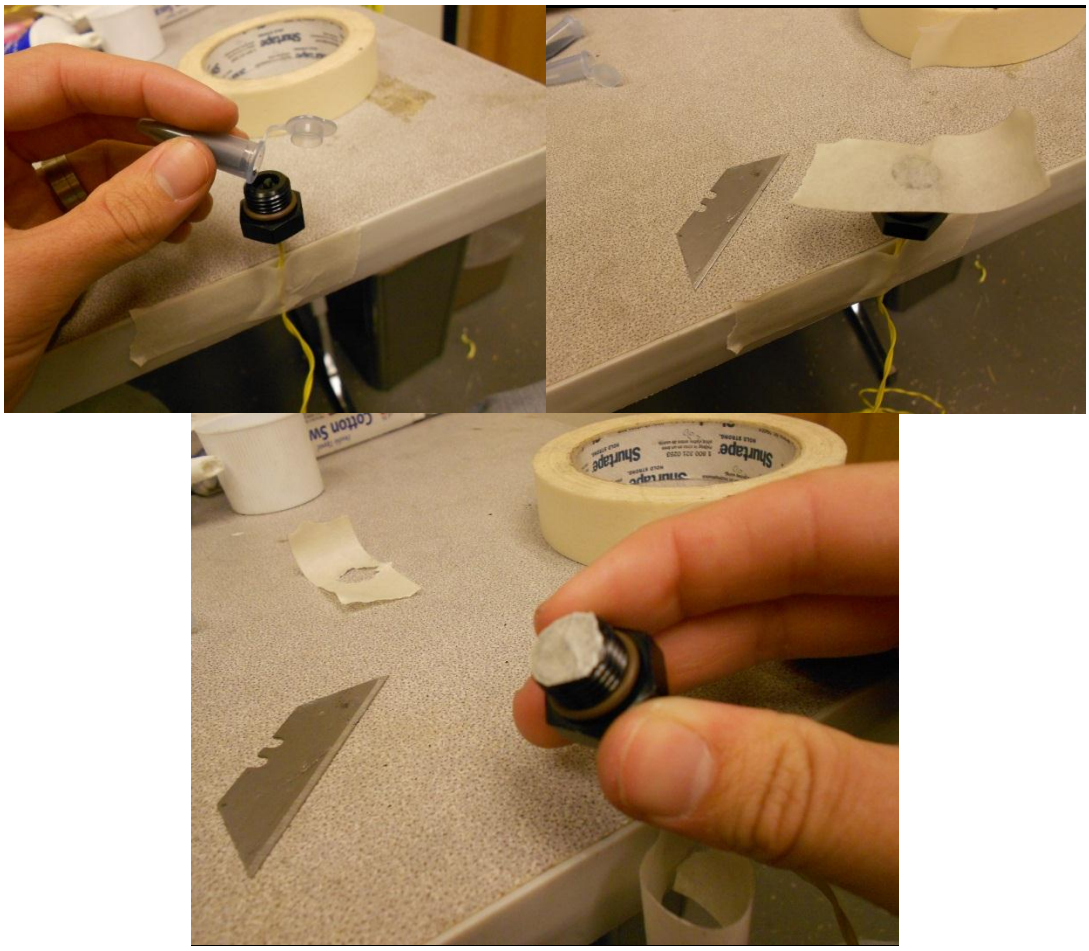

Step 6: Wrap the threads of the hex plug with pipe tape, making sure that some of the pipe tape goes over the edge, to help keep the masking tape on, and the black powder contained. Using a multi-meter, measure the resistance of the e-match to ensure that it is still in working condition and wasn't damaged during this process. Ensure that the multi-meter is configured properly BEFORE attaching the e-match, as voltage from the multi-meter could fire the e-match! The resistance should be between 1.4 and 1.6 ohms. A dead e-match will not have any resistance when checked on a multi-meter. Always keep the wires of the e-match twisted together when the e-match is stored, or not being used immediately. This will help prevent accidentally shorting the wires and discharging the e-match.


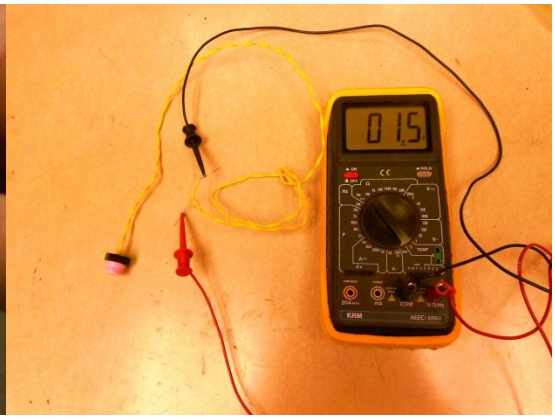

Step 7: Wrap all threaded parts with pipe-tape. The Co2 cartridge and hex plug may need a couple layers to ensure an air-tight fitting with the pyro-valve casing. The threads on the AN parts that are purchased, may only need one layer.

Step 8: Assemble the pyro-valve. Attach the Tee to both pyro-valves, as shown below, with the opening of the tee pointing in the same direction as the opening for the hex plug. This is to ensure that the Co2 cartridges will not have interferences. Put the piercer inside of the pyro-valve shell, just far enough inside to allow the hex plug to fit in behind it. Thread the hex-plug into the casing, and then thread the Co2 cartridges into the casing. Handle the assembled inflation system with care.


Step 9: When you are prepared to perform an inflation test, attach the inflation system to the inflatable wing. The e-matches should be wired in parallel to ensure that they fire at the same time. Each e-match requires about 2 amps to fire.

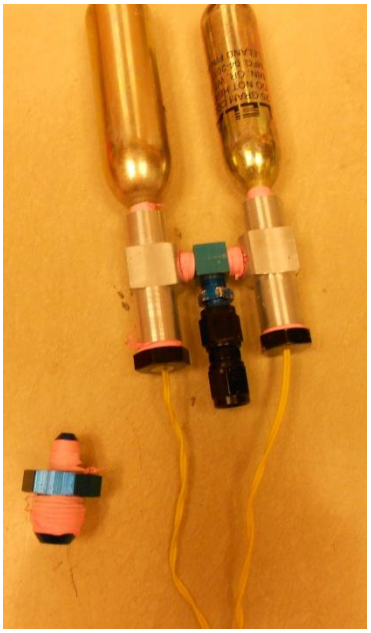

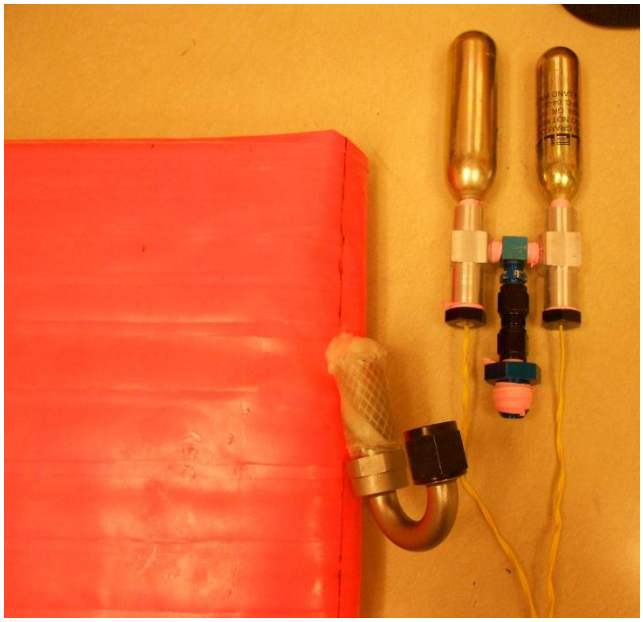

Clean Up: Cleaning the pyro-valve should occur as soon as possible after use, to ensure that contaminates do not leave deposits on parts, or corrode parts of the inflation system. isopropyl alcohol and paper towels can be used to clean the system, as well as baby-wipes. Make sure to thoroughly clean out each part of the inflation system and remove all residue from the black powder. If needed, let the parts soak in 406 cleaner (commonly available at most stores) for an hour, and then clean using the methods previously described. Do not let parts soak in 406 for a long time, as they can start to rust and corrode.

F. AN THREAD SIZE COMPARISON

AN size	-2	-3	-4	-5	-6	-8	-10	-12	-16	-20	-24	-28	-32
Tube OD (Hose ID)	1/8"	3/16"	1/4"	5/16"	3/8"	1/2"	5/8"	3/4"	1"	1-1/4"	1-1/2"	1-3/4"	2"
SAE thread size	5/16-24	3/8-24	7/16-20	1/2-20	9/16-18	3/4-16	7/8-14	1-1/16-12	1-5/16-12	1-5/8-12	1-7/8-12	2-1/4-12	2-1/2-12
Pipe thread size (NPT)		1/8-27	1/4-18		3/8-18	1/2-14		3/4-14					

[26].

G. EARLY AIRCRAFT STABILITY CALCULATIONS

Initial tail sizing (minimum effective)

$c := 12.5$ in $\quad b := 72$ in

$S := c \cdot b = 900$ in^2 $\quad \frac{c}{4} = 3.125$

$ARw := \frac{b^2}{S} = 5.76$ $\quad ARt := 2$

$C_{l\alpha w} := 2\pi =$ ▪ $\quad C_{l\alpha t} := 2\pi$ ▪ per radian

$C_{l\alpha w} := 3.41579$ per radian $\quad C_{l\alpha t} := 6.204$ per radian

$$C_{L\alpha w} := \frac{C_{l\alpha w}}{1 + \frac{C_{l\alpha w}}{\pi \, ARw}} = 2.873 \qquad C_{L\alpha t} := \frac{C_{l\alpha t}}{1 + \frac{C_{l\alpha t}}{\pi \, ARt}} = 3.122$$

Static Margin

$SM := .25$

Equation w/o Downwash

$$ltSt := \left| \frac{-C_{L\alpha w} \cdot SM}{C_{L\alpha t}} \cdot S \cdot c \right| = 2.589 \times 10^3$$

Equation w/ down wash

$$ltSt := -\left[\frac{-SM \cdot C_{l\alpha w}}{C_{l\alpha t} \cdot \left(1 - \frac{2 \cdot C_{L\alpha w}}{\pi \cdot ARw} \right)} \right] \cdot S \cdot c = ▪$$

Neutral Point

$$x_{np} := SM + \frac{c}{4} = 3.375$$

Length between L.E. and c/4 of the tail

$l_t := 27$ $\quad l_t = 27$

Surface Area of the Tail

$$S_t := \frac{ltSt}{l_t} = 95.882 \qquad St := 196.63$$

Span of the Tail

$$b_t := \sqrt{ARt \cdot S_t} = 13.848$$

Average Chord of the tail

$$ct := \frac{S_t}{b_t} = 6.924$$

Horizontal Tail Volume

$$V_H := \frac{l_t \cdot S_t}{c \cdot S} = 0.23$$

Estimated Tail size (Looks right flies right)

$l_t := 27$

$S_t := 200$

$V_H := \frac{l_t \cdot S_t}{c \cdot S} = 0.48$

$SM := V_H \cdot \frac{C_{L\alpha t}}{C_{L\alpha w}} \cdot \left(1 - \frac{2 \cdot C_{L\alpha w}}{\pi \cdot ARw}\right) = 0.356$

Span of the Tail

$b_t := \sqrt{ARt \cdot S_t} = 20$

Average Chord of the tail

$ct := \frac{S_t}{b_t} = 10$

Inner rib chord length assuming tringular tail

$c_{lt} := \frac{2S_t}{b_t} = 20$

Horizontal Tail Volume

$V_H := \frac{l_t \cdot S_t}{c \cdot S} = 0.48$

Neutral Point

$x_{np} := SM + \frac{c}{4} = 3.481$

H. AIRCRAFT OPTIMIZATION PROGRAM

H.1 USER INTERFACE

	1	2	3	4	5	6	7
1							
2			Input				
3			Not used (for future development)				
4							
5		**Component**			**Local Center of Gravity**		
6							
7	Nose Cone						
8	Diameter	4	in		Xcg	1.6875	in
9	Length	6.75	in		Ycg	0	in
10	Weight	292	grams		Zcg	0	in
11							
12	Tail Cone						
13	Dimater	4	in		Xcg	0.5	in
14	Length	2	in		Ycg	0	in
15	Weight	0	grams		Zcg	0	in
16							
17	Wing						
18	Chord (c)	12.5	in		Xcg	6.25	in
19	Span (b)	72	in		Ycg	0	in
20	Area (S)	900	in		Zcg	0	in
21	AR	5.76	in				
22	Weight	1100	grams				

	1	2	3	4	5	6	7	8
23								
24	Motor	Hacker A20-22L		Produces		lb thrust		
25	Diameter	1.1023622	in		Xcg	0.629921	in	
26	Length	1.25984252	in		Ycg	0	in	
27	Weight	203	grams		Zcg	0	in	
28								
29	Prop	Carbon Folding Prop 10 X 6						
30	Diameter	9.65	in		Xcg	0.1	in	
31	Pitch	5			Ycg	0	in	
32	Weight	39.05	grams		Zcg	0	in	
33								
34	Battery							
35	Length	4.094488185	in		Xcg	2.047244	in	
36	Width	1.259842518	in		Ycg	0	in	
37	Height	0.984251968	in		Zcg	0	in	
38	Weight	682	grams					
39								
40	ESC							
41	Length	0.73	in		Xcg	0.365	in	
42	Width	0.16	in		Ycg	0	in	
43	Thickness	0.8	in		Zcg	0	in	
44	Weight	75	grams					

	1	2	3	4	5	6	7	8
45								
46	Servo(s) - tail							
47	Length	0.75	in		Xcg	0.375	in	
48	Width	0.5	in		Ycg	0	in	
49	Thickness	0.75	in		Zcg	0	in	
50	Weight	9	grams					
51	Quantity	4						
52								
53	Autopilot - Arduino Mega							
54	Length	2.952755903	in		Xcg	1.476378	in	
55	Width	1.574803148	in		Ycg	0	in	
56	Thickness	0.75	in		Zcg	0	in	
57	Weight	48	grams					
58								
59	Perfect Flight Altimeter							
60	Length	2.75	in		Xcg	1.375	in	
61	Width	0.9	in		Ycg	0	in	
62	Thickness	0.5	in		Zcg	0	in	
63	Weight	12.76	grams					
64								
65	Camera							
66	Length	3.5	in		Xcg	1.75	in	

	1	2	3	4	5	6	7	8
67	Width	1.5	in		Ycg	0	in	
68	Thickness	1	in		Zcg	0	in	
69	Weight	0	grams					
70								
71	C02 Tank(s)							
72	Diameter	1.5	in		Xcg	3.5	in	
73	Length	7	in		Ycg	0	in	
74	Weight	246	grams		Zcg	0	in	
75	Quantity	1						
76								
77	Pyrovalve(s)							
78	Diameter	1	in		Xcg	1.5	in	
79	Length	3	in		Ycg	0	in	
80	Weight	91	grams		Zcg	0	in	
81	Quantity	1						
82								
83	Parachute - 48" diamter							
84	Diameter	4	in		Xcg	6	in	
85	Length	12	in		Ycg	0	in	
86	Weight	254	grams		Zcg	0	in	

	9	10	11	12	13	14	15	16
1								
2				XCG tolerance			0.125	
3				Change in fuselage length ste			0.25	in
4								
5								
6								
7	Fuselage							
8	Min ln	10	in	length from wing Quarter-Chord to the base of the nose				
9	Max ln	30	in					
10	Min lh	18		length from wing Quarter-Chord to tail Quarter-Chord				
11	Max lh	30	in					
12	Max Total Length	96	in					
13	Density	11.305	grams/in (length)		23.05761	fiberglass		
14	Dimaeter	4	in					
15								
16								
17	Horizontal (initial guess)				Horizontal (Knowns)			
18	Chord (c)	5	in		Vh	0.4326		
19	Semi-span (b/2)	5	in		Density	1	grams/in^2	
20	Span (b)	10	in					
21	Area (S)	50	in					
22	AR	2						

	9	10	11	12	13	14	15	16	17	18	19	20
23												
24	Motor : EDF - 68 mm 2185 kv		Produces thrust (lb	3.5274	Max EDF size = 90mm			LEDF68-1A21				
25	Diameter	2.99	in		Xcg	1.496	in	This is the EDF in the Mars room				
26	Length	2.244	in		Ycg	0	in	http://www.hobbypartz.com/lealalaldufa3.html				
27	Weight	242	grams		Zcg	0	in					
28												
29												
30												
31												
32												
33												
34	Battery	4000 mAh 40c 6s						15 min flight time				
35	Length	5.33	in		Xcg	2.665	in					
36	Width	1.259843	in		Ycg	0	in					
37	Height	0.984252	in		Zcg	0	in					
38	Weight	682	grams									
39												
40	ESC	Castle Creations Pheonix Ice Lite 40										
41	Length	1.8	in		Xcg	0.9	in					
42	Width	0.16	in		Ycg	0	in					
43	Thickness	0.8	in		Zcg	0	in					
44	Weight	75	grams									

	9	10	11	12	13	14	15	16
45								
46	EDF Motor Tube							
47	Diameter	3	in		Xcg	1.5	in	
48	Width	0.5	in		Ycg	1.5	in	
49	Density	5.99	grams/in (length)					

H.2 PUSHER CONFIGURATION RESULTS

	1	2	3	4	5	6	7	8	9	10	11	12	13	14	15	16	17
1		Winning Design															
2	Vh	0.4326		Hchord	9.915553												
3	Ln	24.75	in	Hspan	19.83111												
4	Lh	26	in	Lfuse	66.93666	in											
5	Shor	196.6364	in^2														
6	Wstab	354.4479	grams	=	0.781424	lbs											
7	Wfuse	657.8002	grams	=	1.450201	lbs											
8	Wtotal	4091.058	grams	=	9.019239	lbs											
9	Xcg	0.116756	in														
10																	
11	Iteration #	0	1	2	3	4	5	6	7	8	9	10	11	12	13	14	15
12	Vh	0.4326	0.4326	0.4326	0.4326	0.4326	0.4326	0.4326	0.4326	0.4326	0.4326	0.4326	0.4326	0.4326	0.4326	0.4326	0.4326
13	ln (inches)	23.75	24	24	24	24.25	24.25	24.25	24.5	24.5	24.5	24.5	24.75	24.75	24.75	25	25
14	lh (inches)	18	18.25	18.5	18.75	19	19.25	19.5	19.75	20	20.25	20.5	20.75	21	21.25	21.5	21.75
15	Shor (in^2)	270.375	266.6712	263.0676	259.56	256.1447	252.8182	249.5769	246.4177	243.3375	240.3333	237.4024	234.5422	231.75	229.0235	226.3605	223.7586
16	Wstab (grams)	475.3246	469.2895	463.4143	457.6926	452.1185	446.6864	441.3906	436.2263	431.1884	426.2723	421.4737	416.7883	412.2122	407.7414	403.3724	399.1017
17	Wfuse (grams)	570.5663	575.5413	577.7037	579.8795	584.8945	587.0956	589.3088	594.3599	596.5961	598.8433	601.1011	606.1954	608.4735	610.7612	615.8847	618.191
18	Wtotal (grams)	4124.701	4123.641	4119.928	4116.382	4115.823	4112.592	4109.509	4109.396	4106.595	4103.926	4101.385	4101.794	4099.496	4097.313	4098.067	4096.103
19	Xcg	0.122995	0.062274	0.085704	0.109623	0.049948	0.074717	0.099937	0.041232	0.067242	0.093671	0.120508	0.063035	0.090591	0.118529	0.061883	0.090497

	16	17	18	19	20	21	22	23	24	25	26	27	28	29	30	31	32
10																	
11	16	17	18	19	20	21	22	23	24	25	26	27	28	29	30	31	32
12	0.4326	0.4326	0.4326	0.4326	0.4326	0.4326	0.4326	0.4326	0.4326	0.4326	0.4326	0.4326	0.4326	0.4326	0.4326	0.4326	0.4326
13	25	25.25	25.25	25.25	25.5	25.5	25.75	25.75	25.75	26	26	26	26.25	26.25	26.5	26.5	26.5
14	22	22.25	22.5	22.75	23	23.25	23.5	23.75	24	24.25	24.5	24.75	25	25.25	25.5	25.75	26
15	221.2159	218.7303	216.3	213.9231	211.5978	209.3226	207.0957	204.9158	202.7813	200.6907	198.6429	196.6364	194.67	192.7426	190.8529	189	187.1827
16	394.9261	390.8422	386.8471	382.9379	379.1119	375.3663	371.6987	368.1066	364.5876	361.1396	357.7604	354.4479	351.2001	348.0152	344.8913	341.8267	338.8196
17	620.5063	625.6564	627.9887	630.3291	635.5037	637.8598	643.0497	645.4207	647.7988	653.01	655.4018	657.8002	663.0313	665.4424	670.6859	673.1091	675.5381
18	4094.242	4095.309	4093.646	4092.077	4093.426	4092.036	4093.558	4092.337	4091.196	4092.96	4091.972	4091.058	4093.041	4092.268	4094.387	4093.746	4093.168
19	0.119469	0.063603	0.093212	0.123159	0.068032	0.098582	0.043895	0.075029	0.106471	0.052467	0.084465	0.116756	0.063408	0.096229	0.043273	0.076611	0.11022

	33	34	35	36	37	38	39	40	41	42	43	44	45	46	47	48	49
10																	
11	33	34	35	36	37	38	39	40	41	42	43	44	45	46	47	48	49
12	0.4326	0.4326	0.4326	0.4326	0.4326	0.4326	0.4326	0.4326	0.4326	0.4326	0.4326	0.4326	0.4326	0.4326	0.4326	0.4326	0.4326
13	26.75	26.75	27	27	27	27.25	27.25	27.5	27.5	27.5	27.75	27.75	28	28	28	28.25	28.25
14	26.25	26.5	26.75	27	27.25	27.5	27.75	28	28.25	28.5	28.75	29	29.25	29.5	29.75	30	30.25
15	185.4	183.6509	181.9346	180.25	178.5963	176.9727	175.3784	173.8125	172.2743	170.7632	169.2783	167.819	166.3846	164.9746	163.5882	162.225	160.8843
16	335.8685	332.9718	330.1279	327.3355	324.5931	321.8994	319.2531	316.6529	314.0976	311.586	309.1171	306.6897	304.3028	301.9554	299.6464	297.375	295.1402
17	680.7991	683.2394	688.5113	690.9623	693.4185	698.706	701.1721	706.4694	708.9451	711.4255	716.7366	719.2259	724.5458	727.0436	729.5457	734.878	737.388
18	4095.478	4095.021	4097.449	4097.108	4096.822	4099.415	4099.235	4101.932	4101.853	4101.822	4104.664	4104.726	4107.659	4107.809	4108.002	4111.063	4111.338
19	0.05788	0.091984	0.040013	0.074601	0.109441	0.058052	0.093358	0.042319	0.078081	0.114078	0.063593	0.100031	0.049881	0.08675	0.123842	0.074221	0.111731

	50	51	52	53	54	55	56	57	58	59	60	61	62	63	64	65	66
10																	
11	50	51	52	53	54	55	56	57	58	59	60	61	62	63	64	65	66
12	0.45	0.45	0.45	0.45	0.45	0.45	0.45	0.45	0.45	0.45	0.45	0.45	0.45	0.45	0.45	0.45	0.45
13	NO SOLTN	NO SOLTN	NO SOLTN	NO SOLTN	NO SOLTN	NO SOLTN	NO SOLTN	NO SOLTN	NO SOLTN	NO SOLTN	NO SOLTN	NO SOLTN	NO SOLTN	NO SOLTN	NO SOLTN	NO SOLTN	NO SOLTN
14	21.25	21.375	21.5	21.625	21.75	21.875	22	22.125	22.25	22.375	22.5	22.625	22.75	22.875	23	23.125	23.25
15	238.2353	236.8421	235.4651	234.104	232.7586	231.4286	230.1136	228.8136	227.5281	226.257	225	223.7569	222.5275	221.3115	220.1087	218.9189	217.7419
16	422.8376	420.556	418.3005	416.0704	413.8655	411.6852	409.5292	407.397	405.2883	403.2026	401.1396	399.0989	397.0802	395.083	393.1071	391.1521	389.2177
17	340.5631	340.5631	340.5631	340.5631	340.5631	340.5631	340.5631	340.5631	340.5631	340.5631	340.5631	340.5631	340.5631	340.5631	340.5631	340.5631	340.5631
18	3872.232	3871.092	3869.981	3868.898	3867.842	3866.814	3865.811	3864.835	3863.884	3862.959	3862.058	3861.182	3860.329	3859.501	3858.695	3857.912	3857.152
19	0.403335	0.418672	0.434109	0.449645	0.465278	0.481008	0.496833	0.512753	0.528766	0.544871	0.561068	0.577356	0.593732	0.610197	0.62675	0.643389	0.660114

H.3 TRACTOR CONFIGURATION RESULTS

	Winning Design					
Vh	0.4326		**Hchord**	9.816888		
Ln	25.25 in		**Hspan**	19.63378		
Lh	21 in		**Lfuse**	57.61267 in		
Shor	192.7426 in^2					
Wstab	348.0152 grams		=	0.767242 lbs		
Wfuse	606.0912 grams		=	1.336202 lbs		
Wtotal	3740.916 grams		=	8.247309 lbs		
Xcg	0.113331 in					

Iteration #	0	1	2	3	4	5	6	7	8	9	10	11	12	13	14	15
Vh	0.4326	0.4326	0.4326	0.4326	0.4326	0.4326	0.4326	0.4326	0.4326	0.4326	0.4326	0.4326	0.4326	0.4326	0.4326	0.4326
ln (inches)	19.5	19.5	19.75	19.75	19.75	19.75	19.75	19.75	20	20	20	20	20	20	20.25	20.25
lh (inches)	18	18.25	18.5	18.75	19	19.25	19.5	19.75	20	20.25	20.5	20.75	21	21.25	21.5	21.75
Shor (in^2)	270.375	266.6712	263.0676	259.56	256.1447	252.8182	249.5769	246.4177	243.3375	240.3333	237.4024	234.5422	231.75	229.0235	226.3605	223.7586
Wstab (grams)	475.3246	469.2895	463.4143	457.6926	452.1185	446.6864	441.3906	436.2263	431.1884	426.2723	421.4737	416.7883	412.2122	407.7414	403.3724	399.1017
Wfuse (grams)	522.5201	524.6688	529.6575	531.8333	534.022	536.2231	538.4363	540.6612	545.7236	547.9708	550.2286	552.4966	554.7747	559.8887	562.1859	564.4923
Wtotal (grams)	3784.655	3780.768	3779.882	3776.336	3772.951	3769.719	3766.637	3763.697	3763.722	3761.053	3758.512	3756.095	3753.797	3754.44	3752.368	3750.404
Xcg	0.109886	0.122798	0.051285	0.064989	0.079119	0.093664	0.108615	0.123961	0.054267	0.070303	0.08671	0.103481	0.120606	0.052255	0.070008	0.088097

16	17	18	19	20	21	22	23	24	25	26	27	28	29	30	31	32
0.4326	0.4326	0.4326	0.4326	0.4326	0.4326	0.4326	0.4326	0.4326	0.4326	0.4326	0.4326	0.4326	0.4326	0.4326	0.4326	0.4326
20.25	20.5	20.5	20.5	20.5	20.5	20.75	20.75	20.75	20.75	21	21	21	21	21.25	21.25	21.25
22	22.25	22.5	22.75	23	23.25	23.5	23.75	24	24.25	24.5	24.75	25	25.25	25.5	25.75	26
221.2159	218.7303	216.3	213.9231	211.5978	209.3226	207.0957	204.9158	202.7813	200.6907	198.6429	196.6364	194.67	192.7426	190.8529	189	187.1827
394.9261	390.8422	386.8471	382.9379	379.1119	375.3663	371.6987	368.1066	364.5876	361.1396	357.7604	354.4479	351.2001	348.0152	344.8913	341.8267	338.8196
566.8075	571.9577	574.2899	576.6304	578.9787	581.3348	586.5247	588.8957	591.2738	593.6588	598.8768	601.2752	603.6801	606.0912	611.3347	613.7579	616.1869
3748.544	3749.61	3747.947	3746.378	3744.901	3743.511	3745.033	3743.812	3742.671	3741.608	3743.447	3742.533	3741.69	3740.916	3743.036	3742.395	3741.817
0.106516	0.039144	0.05815	0.077469	0.097096	0.117025	0.050835	0.07131	0.092075	0.113123	0.047813	0.06938	0.091221	0.113331	0.048868	0.071473	0.094338

33	34	35	36	37	38	39	40	41	42	43	44	45	46	47	48	49
0.4326	0.4326	0.4326	0.4326	0.4326	0.4326	0.4326	0.4326	0.4326	0.4326	0.4326	0.4326	0.4326	0.4326	0.4326	0.4326	0.4326
21.25	21.5	21.5	21.5	21.75	21.75	21.75	21.75	22	22	22	22.25	22.25	22.25	22.25	22.5	22.5
26.25	26.5	26.75	27	27.25	27.5	27.75	28	28.25	28.5	28.75	29	29.25	29.5	29.75	30	30.25
185.4	183.6509	181.9346	180.25	178.5963	176.9727	175.3784	173.8125	172.2743	170.7632	169.2783	167.819	166.3846	164.9746	163.5882	162.225	160.8843
335.8685	332.9718	330.1279	327.3355	324.5931	321.8994	319.2531	316.6529	314.0976	311.586	309.1171	306.6897	304.3028	301.9554	299.6464	297.375	295.1402
618.6216	623.8881	626.3338	628.7848	634.0672	636.5285	638.9946	641.4656	646.7676	649.248	651.7328	657.0484	659.542	662.0399	664.5419	669.8742	672.3843
3741.3	3743.67	3743.272	3742.93	3745.47	3745.238	3745.058	3744.929	3747.675	3747.644	3747.66	3750.548	3750.655	3750.805	3750.998	3754.059	3754.334
0.117459	0.053816	0.077412	0.101256	0.038192	0.062498	0.087044	0.111827	0.049546	0.074775	0.100234	0.038509	0.064404	0.090523	0.116863	0.055892	0.082654

50	51	52	53	54	55	56	57	58	59	60	61	62	63	64	65	66
0.46	0.46	0.46	0.46	0.46	0.46	0.46	0.46	0.46	0.46	0.46	0.46	0.46	0.46	0.46	0.46	0.46
31.6875	31.6875	31.75	31.75	31.75	31.8125	31.8125	31.875	31.875	31.9375	31.9375	31.9375	32	32	32.0625	32.0625	32.125
25.125	25.1875	25.25	25.3125	25.375	25.4375	25.5	25.5625	25.625	25.6875	25.75	25.8125	25.875	25.9375	26	26.0625	26.125
205.9701	205.4591	204.9505	204.4444	203.9409	203.4398	202.9412	202.445	201.9512	201.4599	200.9709	200.4843	200	199.5181	199.0385	198.5612	198.0861
352.5587	351.7379	350.9212	350.1083	349.2995	348.4945	347.6934	346.8962	346.1028	345.3132	344.5274	343.7453	342.9669	342.1922	341.4212	340.6538	339.89
703.8825	704.5125	705.8495	706.4801	707.111	708.4488	709.0802	710.4185	711.0506	712.3894	713.022	713.6548	714.9945	715.6278	716.968	717.6019	718.9426
3180.451	3180.26	3180.781	3180.598	3180.42	3180.953	3180.784	3181.325	3181.163	3181.713	3181.559	3181.41	3181.971	3181.83	3182.399	3182.266	3182.843
0.113446	0.120242	0.110739	0.117568	0.124417	0.114952	0.121834	0.112392	0.119308	0.109888	0.116838	0.123806	0.114424	0.121425	0.112065	0.1191	0.109762

67	68	69	70	71	72	73	74	75	76	77	78	79	80	81	82	83
0.46	0.46	0.46	0.46	0.46	0.46	0.46	0.46	0.46	0.46	0.46	0.46	0.46	0.46	0.46	0.46	0.46
32.125	32.125	32.1875	32.1875	32.25	32.25	32.3125	32.3125	32.3125	32.375	32.375	32.4375	32.4375	32.5	32.5	32.5625	32.5625
26.1875	26.25	26.3125	26.375	26.4375	26.5	26.5625	26.625	26.6875	26.75	26.8125	26.875	26.9375	27	27.0625	27.125	27.1875
197.6134	197.1429	196.6746	196.2085	195.7447	195.283	194.8235	194.3662	193.911	193.4579	193.007	192.5581	192.1114	191.6667	191.224	190.7834	190.3448
339.1298	338.3732	337.6201	336.8705	336.1244	335.3817	334.6425	333.9067	333.1743	332.4452	331.7195	330.9971	330.278	329.5622	328.8497	328.1403	327.4342
719.577	720.2117	721.5532	722.1884	723.5304	724.1661	725.5086	726.1447	726.7812	728.1244	728.7613	730.1051	730.7425	732.0867	732.7246	734.0693	734.7076
3182.717	3182.595	3183.183	3183.069	3183.665	3183.558	3184.161	3184.061	3183.965	3184.58	3184.491	3185.112	3185.031	3185.659	3185.584	3186.22	3186.152
0.116829	0.123915	0.114614	0.121732	0.112454	0.119604	0.110348	0.117531	0.124731	0.115511	0.122744	0.113546	0.120811	0.111634	0.118931	0.109775	0.117104

84	85	86	87	88	89	90	91	92	93	94	95	96	97	98	99	100
0.46	0.46	0.46	0.46	0.46	0.46	0.46	0.46	0.46	0.46	0.46	0.46	0.46	0.46	0.4	0.4	0.4
32.5625	32.625	32.625	32.6875	32.6875	32.75	32.75	32.8125	32.8125	32.875	32.875	32.875	32.9375	32.9375	35	35.25	35.5
27.25	27.3125	27.375	27.4375	27.5	27.5625	27.625	27.6875	27.75	27.8125	27.875	27.9375	28	28.0625	36.5	36.75	37
189.9083	189.4737	189.0411	188.6105	188.1818	187.7551	187.3303	186.9074	186.4865	186.0674	185.6502	185.2349	184.8214	184.4098	123.2877	122.449	121.6216
326.7312	326.0314	325.3348	324.6412	323.9508	323.2635	322.5792	321.8979	321.2197	320.5444	319.8721	319.2028	318.5364	317.873	212.6903	211.3376	210.003
735.3462	736.6916	737.3307	738.6765	739.316	740.6623	741.3023	742.6491	743.2895	744.6367	745.2776	745.9187	747.2666	747.9081	847.5341	853.0529	858.5731
3186.087	3186.733	3186.675	3187.328	3187.277	3187.936	3187.891	3188.557	3188.519	3189.191	3189.16	3189.131	3189.813	3189.791	3184.234	3188.401	3192.586
0.12445	0.115331	0.122708	0.11361	0.121019	0.111942	0.119382	0.110326	0.117798	0.108763	0.116266	0.123785	0.114785	0.122335	0.121059	0.091208	0.061441

H.4 EDF CONFIGURATION RESULTS

	5	6	7	8	9	10	11	12	13	14	15	16	17	18	19	20	21
1													Selected Design				
2	9.915553								L_EDF_Tul	18.81166	inches	Vh	0.48	Hchord	10	in	
3	19.83111		Analyze			Clear			W_EDF_Tu	112.6819	grams	ln (inches	24.75	Hspan	20	in	
4	53.18666	in										lh (inches	27	Lfuse	59.25	in	
5	se cone)											Shor (in^2	200				
6	0.683381	lbs										Wstab (gr	284.7575				
7	1.325585	lbs										Wfuse (gr	665.5261				
8	8.79647	lbs										Wtotal (gr	4034.696				
9												Xcg	0.096596				
10												Wtotal (lb	8.894981				
11	3	4	5	6	7	8	9	10	11	12	13	14	15	16	17	18	19
12	0.4326	0.4326	0.4326	0.4326	0.4326	0.4326	0.4326	0.4326	0.4326	0.4326	0.4326	0.4326	0.4326	0.4326	0.4326	0.4326	0.4326
13	19.75	19.75	19.75	19.75	20	20	20	20	20	20.25	20.25	20.25	20.25	20.5	20.5	20.5	20.5
14	18.75	19	19.25	19.5	19.75	20	20.25	20.5	20.75	21	21.25	21.5	21.75	22	22.25	22.5	22.75
15	259.56	256.1447	252.8182	249.5769	246.4177	243.3375	240.3333	237.4024	234.5422	231.75	229.0235	226.3605	223.7586	221.2159	218.7303	216.3	213.9231
16	406.599	401.3622	396.2607	391.2893	386.443	381.7172	377.1075	372.6096	368.2195	363.9333	359.7473	355.6582	351.6625	347.7572	343.939	340.2053	336.5531
17	531.8333	534.022	536.2231	538.4363	543.4874	545.7236	547.9708	550.2286	552.4966	557.601	559.8887	562.1859	564.4923	569.6338	571.9577	574.2899	576.6304
18	4017.192	4014.144	4011.244	4008.486	4008.69	4006.201	4003.838	4001.598	3999.476	4000.294	3998.396	3996.604	3994.915	3996.151	3994.657	3993.255	3991.943
19	0.07245	0.089136	0.106379	0.124168	0.043328	0.062099	0.081385	0.101177	0.121464	0.04269	0.063878	0.085538	0.107661	0.03042	0.053392	0.076807	0.100657
20	8.856393	8.849673	8.843279	8.837198	8.83765	8.832161	8.826952	8.822014	8.817335	8.819139	8.814954	8.811004	8.80728	8.810005	8.806711	8.803621	8.800729

	20	21	22	23	24	25	26	27	28	29	30	31	32	33	34	35	36
12	0.4326	0.4326	0.4326	0.4326	0.4326	0.4326	0.4326	0.4326	0.4326	0.4326	0.4326	0.4326	0.4326	0.4326	0.4326	0.4326	0.4326
13	20.5	20.75	20.75	20.75	21	21	21	21	21.25	21.25	21.25	21.25	21.5	21.5	21.5	21.75	21.75
14	23	23.25	23.5	23.75	24	24.25	24.5	24.75	25	25.25	25.5	25.75	26	26.25	26.5	26.75	27
15	211.5978	209.3226	207.0957	204.9158	202.7813	200.6907	198.6429	196.6364	194.67	192.7426	190.8529	189	187.1827	185.4	183.6509	181.9346	180.25
16	332.9798	329.4829	326.06	322.7087	319.4269	316.2122	313.0628	309.9766	306.9518	303.9864	301.0789	298.2275	295.4305	292.6865	289.994	287.3515	284.7575
17	578.9787	584.1611	586.5247	588.8957	594.1	596.485	598.8768	601.2752	606.5063	608.9174	611.3347	613.7579	619.0131	621.4479	623.8881	629.1601	631.6111
18	3990.719	3992.404	3991.345	3990.364	3992.287	3991.457	3990.7	3990.012	3992.218	3991.664	3991.174	3990.745	3993.204	3992.894	3992.642	3995.272	3995.129
19	0.124935	0.049533	0.074606	0.10009	0.025714	0.051966	0.078614	0.105654	0.032629	0.060403	0.088555	0.11708	0.045363	0.074594	0.104186	0.033409	0.063688
20	8.798028	8.801744	8.799409	8.797248	8.801486	8.799657	8.797987	8.79647	8.801334	8.800112	8.799032	8.798087	8.803507	8.802825	8.802269	8.808066	8.807751

	37	38	39	40	41	42	43	44	45	46	47	48	49
12	0.4326	0.4326	0.4326	0.4326	0.4326	0.4326	0.4326	0.4326	0.4326	0.4326	0.4326	0.4326	0.4326
13	21.75	22	22	22	22	22.25	22.25	22.25	22.5	22.5	22.5	22.75	22.75
14	27.25	27.5	27.75	28	28.25	28.5	28.75	29	29.25	29.5	29.75	30	30.25
15	178.5963	176.9727	175.3784	173.8125	172.2743	170.7632	169.2783	167.819	166.3846	164.9746	163.5882	162.225	160.8843
16	282.2109	279.7103	277.2544	274.8421	272.4722	270.1437	267.8553	265.6062	263.3952	261.2215	259.084	256.982	254.9144
17	634.0672	639.3547	641.8209	644.2919	646.7676	652.0742	654.5591	657.0484	662.3683	664.8661	667.3682	672.7005	675.2105
18	3995.038	3997.825	3997.835	3997.894	3998	4000.978	4001.174	4001.415	4004.523	4004.848	4005.212	4008.442	4008.885
19	0.094319	0.024463	0.055763	0.087405	0.119385	0.050749	0.083378	0.116335	0.048584	0.082175	0.116089	0.049207	0.083741
20	8.807551	8.813695	8.813718	8.813848	8.814081	8.820646	8.82108	8.821609	8.828463	8.829178	8.829981	8.837103	8.838078

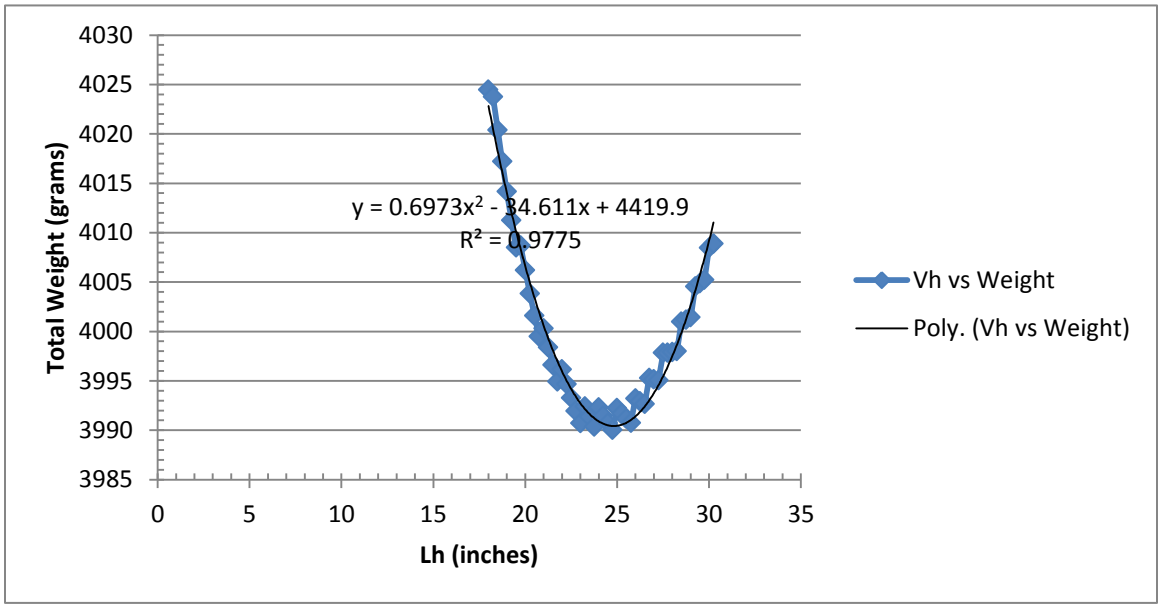

H.5 PROGRAM CODE - CLEAR

```
Sub PusherClear()   ' clears contents on the pusher sheet

Sheet3.Cells.Range("B2:B9") = ClearContents
Sheet3.Cells.Range("B11:EZ19") = ClearContents

End Sub
Sub TractorClear()   ' clears contents on the tractor sheet

Sheet2.Cells.Range("B2:B9") = ClearContents
Sheet2.Cells.Range("B11:EZ19") = ClearContents

End Sub
Sub EDFClear()   ' clears contents on the EDF sheet

Sheet4.Cells.Range("B2:B9") = ClearContents
Sheet4.Cells.Range("B11:EZ19") = ClearContents

End Sub
```

H.6 PROGRAM CODE – PUSHER CONFIG

```
Sub WeightMinPusher()

'length (x) inputs (unit= inches)
Dim Lnose As Double
Lnose = Sheet1.Cells(9, 2)
Dim Ltailcone As Double
Ltailcone = Sheet1.Cells(14, 2)
Dim Lchord As Double            'for the wing
Lchord = Sheet1.Cells(18, 2)    'for the wing
Dim Lmotor As Double
Lmotor = Sheet1.Cells(26, 2)
Dim Lprop As Double
Lprop = Sheet1.Cells(30, 6) * 2
Dim Lbattery As Double
Lbattery = Sheet1.Cells(35, 2)
Dim Lesc As Double
Lesc = Sheet1.Cells(41, 2)
Dim Lservo As Double
Lservo = Sheet1.Cells(47, 2)
Dim Lautopilot As Double
Lautopilot = Sheet1.Cells(54, 2)
Dim Laltimeter As Double
Laltimeter = Sheet1.Cells(60, 2)
Dim Lcamera As Double
Lcamera = Sheet1.Cells(66, 2)
Dim Lc2 As Double
Lc2 = Sheet1.Cells(73, 2)
Dim Lpyro As Double
Lpyro = Sheet1.Cells(79, 2)
Dim Lpara As Double
Lpara = Sheet1.Cells(85, 2)



'XCG inputs (unit = inches)
Dim XCGnose As Double
XCGnose = Sheet1.Cells(8, 6)
Dim XCGtailcone As Double
XCGtailcone = Sheet1.Cells(13, 6)
Dim XCGwing As Double
XCGwing = Sheet1.Cells(18, 6)
Dim XCGmotor As Double
XCGmotor = Sheet1.Cells(25, 6)
Dim XCGprop As Double
XCGprop = Sheet1.Cells(30, 6)
Dim XCGbattery As Double
XCGbattery = Sheet1.Cells(35, 6)
Dim XCGesc As Double
XCGesc = Sheet1.Cells(41, 6)
Dim XCGservo As Double
XCGservo = Sheet1.Cells(47, 6)
Dim XCGautopilot As Double
XCGautopilot = Sheet1.Cells(54, 6)
```

```
Dim XCGaltimeter As Double
XCGaltimeter = Sheet1.Cells(60, 6)
Dim XCGcamera As Double
XCGcamera = Sheet1.Cells(66, 6)
Dim XCGc2 As Double
XCGc2 = Sheet1.Cells(72, 6)
Dim XCGpyro As Double
XCGpyro = Sheet1.Cells(78, 6)
Dim XCGpara As Double
XCGpara = Sheet1.Cells(84, 6)


'Weight inputs (unit=grams)
Dim Wnose As Double
Wnose = Sheet1.Cells(10, 2)
Dim Wtailcone As Double
Wtailcone = Sheet1.Cells(15, 2)
Dim Wwing As Double
Wwing = Sheet1.Cells(22, 2)
Dim Wmotor As Double
Wmotor = Sheet1.Cells(27, 2)
Dim Wprop As Double
Wprop = Sheet1.Cells(32, 2)
Dim Wbattery As Double
Wbattery = Sheet1.Cells(38, 2)
Dim Wesc As Double
Wesc = Sheet1.Cells(44, 2)
Dim Wservo As Double
Wservo = Sheet1.Cells(50, 2)
Dim Wautopilot As Double
Wautopilot = Sheet1.Cells(57, 2)
Dim Waltimeter As Double
Waltimeter = Sheet1.Cells(63, 2)
Dim Wcamera As Double
Wcamera = Sheet1.Cells(69, 2)
Dim Wc2 As Double
Wc2 = Sheet1.Cells(74, 2)
Dim Wpyro As Double
Wpyro = Sheet1.Cells(80, 2)
Dim Wpara As Double
Wpara = Sheet1.Cells(86, 2)

'Quantities (where applicable) and recompute weights
Dim Qservo As Integer
Qservo = Sheet1.Cells(51, 2)
Wservo = Wservo * Qservo
Dim Qc2 As Integer
Qc2 = Sheet1.Cells(75, 2)
Wc2 = Wc2 * Qc2
Dim Qpyro As Integer
Qpyro = Sheet1.Cells(81, 2)
Wpyro = Wpyro * Qpyro

'Main wing characteristics
'Lchord = chord length, previously defined
```

```
'Wwing = weight of the wing, previously defined
'XCGwing = local center of gravity of the wing, previously defined
Dim Wspan As Double
Wspan = Sheet1.Cells(19, 2) 'inches
Dim Swing As Double
Swing = Sheet1.Cells(20, 2) 'inches^2
Dim ARwing As Double
ARwing = (Wspan ^ 2) / Swing
Sheet1.Cells(21, 2) = ARwing

'Fuselage Characteristics
'ln is the distance (inches) from the main wing quarter-chord to the base of the nose cone
Dim minln As Double
minln = Sheet1.Cells(8, 10)
Dim Maxln As Double
Maxln = Sheet1.Cells(9, 10)
Dim minlh As Double
'lh is the distance (inches)from the main wing quarter-chord to the quarter-chord of the horizontal stabilizer
minlh = Sheet1.Cells(10, 10)
Dim maxlh As Double
maxlh = Sheet1.Cells(11, 10)
'pfuse is the density of the fuselage (unit = grams/inch)
Dim pfuse As Double
pfuse = Sheet1.Cells(13, 10)
Dim Dfuse As Double
Dfuse = Sheet1.Cells(14, 10)
Dim Lfusetot As Double
Lfusetot = Sheet1.Cells(12, 10)


'Horizontal knowns
Dim Vh As Double
Vh = Sheet1.Cells(18, 14) 'tail volume ratio
Dim phor As Double
phor = Sheet1.Cells(19, 14) 'denstity of the horizontal


'Horizontal initial estimates
Dim Hchord As Double
Hchord = Sheet1.Cells(18, 10)
Dim Hspan As Double
Hspan = Sheet1.Cells(20, 10)
Dim HS As Double
HS = Sheet1.Cells(21, 10)
Dim HAR As Double
HAR = Sheet1.Cells(22, 10)


'program inputs

Dim fusestep As Double
fusestep = Sheet1.Cells(3, 15)
Dim iter As Integer
iter = Round((maxlh - minlh) / fusestep, 0) + 1
Dim iter2 As Integer
```

```
iter2 = Round((Maxln - minln) / fusestep, 0) + 1
Dim XCGtol As Double
XCGtol = Sheet1.Cells(2, 15)
Dim k As Integer
Dim j As Integer

'Analysis variables
Dim lh As Double    'length from quarter chord of the wing to the quarter chord of the horizontal stabilizer
Dim ln As Double    'length from the quarter chord of the wing to the base of the nose
Dim Wt As Double    'total weight
Dim Wstab As Double  'weight of the horizontal
Dim Wlh As Double   'weight of the tail section
Dim Wln As Double   'weight of the fuselage nose selction
Dim Wfuse As Double 'weight of the fuselage
Dim Hsemi As Double 'horizontal semi-span
Dim CGFtop As Double    'CG function top - numerator
Dim CGFtopR As Double   'CG function top (right side - items from the quarter chord, to the right)
Dim CGFtopL As Double   'CG function top (left side- items from the quater chord to the left)
Dim XCG As Double   'the X cg location
Dim Dnosec As Double 'distance from the tip of the nose to the quarter chord
Dim Dtailc As Double    'distance from the tip of the tail cone to the quarter chord
Dim Lfuse As Double 'total length of the fuselage
Dim XCGln As Double 'XCG location of the length to the nose
Dim XCGlh As Double 'XCG location of the length to the horizontal
'Dim Rlength As Double   'for the remaining length = due to the max fuselage length

'Winning conditions
Dim WtWin As Double

'initial condition
minlh = Round(minlh, 0)
maxlh = Round(maxlh, 0)
minln = Round(minln, 0)
Maxln = Round(Maxln, 0)
WtWin = Exp(100)

'Analysis
For k = 0 To iter

Application.ScreenUpdating = False  'since the program is pretty intense - use this to make it run faster

   j = 0   'to reset the nose loop
   Sheet3.Cells(11, 2 + k) = k

   lh = minlh + fusestep * k   'lh increases from the minimum to maximum

   HS = (Vh * Swing * Lchord) / lh  'calculate the tail area
   Hsemi = ((HAR * HS) ^ (0.5)) / 2    'uses the Horizontal AR to calculate the chord and span of the
horizontal
   Hspan = Hsemi * 2

   'Hsemi = (HS / 2)    'semi span
   'Hchord = Hsemi ^ (0.5)  'estimated chord length - assumes its a square
   Hchord = HS / (Hsemi * 2)
```

```
   Wstab = phor * ((Hchord * Dfuse) + HS) * 1.5 ' horizontal and vertical weight combined - assume the Vert is 1/2 the size of the Hor.
   'Hchord * fuse is for the internal structure of the tails

   Sheet3.Cells(14, 2 + k) = lh    'report lh
   Sheet3.Cells(15, 2 + k) = HS    'report tail area
   Sheet3.Cells(12, 2 + k) = Vh    'report Vh
   Sheet3.Cells(16, 2 + k) = Wstab 'reports the weight of the tail

   Dtailc = lh + 0.75 * Hchord + Ltailcone
   XCGlh = (lh + 0.75 * Hchord) / 2
   Wlh = (lh + 0.75 * Hchord) * pfuse

   'Calculate the nose needed to balance the system
   For j = 0 To iter2
      ln = minln + j * fusestep
      Dnosec = Lnose + ln
      Lfuse = ln + lh + 0.75 * Hchord
      XCGln = ln / 2
      Wln = ln * pfuse

      'Xcg = sum(mi*xi)/sum(mi)   cg function
      'IMPORTANT Xcg is located at the quarter chord, towards the nose is negative X, towards the tail is positive X
      'right side
      CGFtopR = ((XCGtailcone + lh + 0.75 * Hchord) * Wtailcone) + ((Dtailc + XCGmotor) * Wmotor) + ((Dtailc + Lmotor + XCGprop) * Wprop) + (lh * Wservo) + ((lh + 0.25 * Hchord) * Wstab) + (XCGlh * Wlh) + ((XCGwing - 0.25 * Lchord) * Wwing) + (XCGpyro * Wpyro) + ((Lpyro + XCGpara) * Wpara)
      'left side
      CGFtopL = ((ln + XCGnose) * Wnose) + (Wln * XCGln) + (XCGc2 * Wc2) + ((ln - XCGbattery - 2) * Wbattery) + ((ln - 2 - Lbattery - XCGesc - 4) * Wesc) + ((Dnose - XCGcamera) * Wcamera) + ((ln - 2 - XCGautopilot) * Wautopilot) + ((ln - 2 - Lautopilot - XCGaltimeter) * Waltimeter)
      CGFtop = CGFtopR - CGFtopL
      Wt = Wtailcone + Wmotor + Wprop + Wservo + Wstab + Wlh + Wwing + Wpyro + Wnose + Wln + Wc2 + Wbattery + Wesc + Wcamera + Wautopilot + Waltimeter + Wpara
      XCG = CGFtop / Wt
      Sheet3.Cells(13, 2 + k) = ln
      Sheet3.Cells(18, 2 + k) = Wt
      Sheet3.Cells(17, 2 + k) = Wln
      Sheet3.Cells(19, 2 + k) = XCG



      If XCG > 0 And XCG < XCGtol Then
      'system is tail heavy, but within a reasonable range
         Sheet3.Cells(13, 2 + k) = ln
         Sheet3.Cells(18, 2 + k) = Wt
         Sheet3.Cells(17, 2 + k) = Wln + Wlh
         Sheet3.Cells(19, 2 + k) = XCG

            If Wt < WtWin Then 'for finding the minimum weight - winning design
               WtWin = Wt
               Sheet3.Cells(8, 2) = Wt
               Sheet3.Cells(7, 2) = Wln + Wlh
               Sheet3.Cells(6, 2) = Wstab
```

```
            Sheet3.Cells(5, 2) = HS
            Sheet3.Cells(4, 2) = ln
            Sheet3.Cells(3, 2) = lh
            Sheet3.Cells(2, 2) = Vh
            Sheet3.Cells(9, 2) = XCG
            Sheet3.Cells(4, 5) = ln + lh + Hchord * 0.75 + Lnose + Ltailcone
            Sheet3.Cells(2, 5) = Hchord
            Sheet3.Cells(3, 5) = Hspan
        Else
        End If

    j = iter2 + 1
ElseIf XCG < 0 And XCG > (-1 * XCGtol) Then
'system is nose heavy, but within a reasonble range
    Sheet3.Cells(13, 2 + k) = ln
    Sheet3.Cells(18, 2 + k) = Wt
    Sheet3.Cells(17, 2 + k) = Wln + Wlh
    Sheet3.Cells(19, 2 + k) = XCG

        If Wt < WtWin Then 'for finding the minimum weight - winning design
            WtWin = Wt
            Sheet3.Cells(8, 2) = Wt
            Sheet3.Cells(7, 2) = Wln + Wlh
            Sheet3.Cells(6, 2) = Wstab
            Sheet3.Cells(5, 2) = HS
            Sheet3.Cells(4, 2) = ln
            Sheet3.Cells(3, 2) = lh
            Sheet3.Cells(2, 2) = Vh
            Sheet3.Cells(9, 2) = XCG
            Sheet3.Cells(4, 5) = ln + lh + Hchord * 0.75 + Lnose + Ltailcone
            Sheet3.Cells(2, 5) = Hchord
            Sheet3.Cells(3, 5) = Hspan
        Else
        End If

    j = inter2 + 1
ElseIf XCG > 0 And j >= iter2 Then
    Sheet3.Cells(13, 2 + k) = "NO SOLTN - T heavy"
ElseIf XCG < 0 Then
'system is nose heavy, so the nose is long enough, the battery just needs to be moved back
    If j = iter2 Then
    Sheet3.Cells(13, 2 + k) = "NO SOLTN - N heavy"
    Else
    Sheet3.Cells(13, 2 + k) = ln
    Sheet3.Cells(18, 2 + k) = Wt
    Sheet3.Cells(17, 2 + k) = Wln + Wlh
    Sheet3.Cells(19, 2 + k) = XCG
    End If

        If Wt < WtWin Then 'for finding the minimum weight - winning design
            WtWin = Wt
            Sheet3.Cells(8, 2) = Wt
            Sheet3.Cells(7, 2) = Wln + Wlh
            Sheet3.Cells(6, 2) = Wstab
            Sheet3.Cells(5, 2) = HS
```

```
            Sheet3.Cells(4, 2) = ln
            Sheet3.Cells(3, 2) = lh
            Sheet3.Cells(2, 2) = Vh
            Sheet3.Cells(9, 2) = XCG
            Sheet3.Cells(4, 5) = ln + lh + Hchord * 0.75 + Lnose + Ltailcone
            Sheet3.Cells(2, 5) = Hchord
            Sheet3.Cells(3, 5) = Hspan
        Else
        End If

    ElseIf XCG = 0 Then
        MsgBox k
        Sheet3.Cells(13, 2 + k) = ln
        Sheet3.Cells(18, 2 + k) = Wt
        Sheet3.Cells(17, 2 + k) = Wln + Wlh
        Sheet3.Cells(19, 2 + k) = XCG
        Sheet3.Cells(20, 2 + k) = "ERROR!"

    Else
    End If


  Next j

Application.ScreenUpdating = True
Next k
End Sub
```

H.7 PROGRAM CODE – TRACTOR CONFIG

```
Sub WeightMinTractor()

'length (x) inputs (unit= inches)
Dim Lnose As Double
Lnose = Sheet1.Cells(9, 2)
Dim Ltailcone As Double
Ltailcone = Sheet1.Cells(14, 2)
Dim Lchord As Double            'for the wing
Lchord = Sheet1.Cells(18, 2)    'for the wing
Dim Lmotor As Double
Lmotor = Sheet1.Cells(26, 2)
Dim Lprop As Double
Lprop = Sheet1.Cells(30, 6) * 2
Dim Lbattery As Double
Lbattery = Sheet1.Cells(35, 2)
Dim Lesc As Double
Lesc = Sheet1.Cells(41, 2)
Dim Lservo As Double
Lservo = Sheet1.Cells(47, 2)
Dim Lautopilot As Double
Lautopilot = Sheet1.Cells(54, 2)
Dim Laltimeter As Double
Laltimeter = Sheet1.Cells(60, 2)
Dim Lcamera As Double
Lcamera = Sheet1.Cells(66, 2)
Dim Lc2 As Double
Lc2 = Sheet1.Cells(73, 2)
Dim Lpyro As Double
Lpyro = Sheet1.Cells(79, 2)
Dim Lpara As Double
Lpara = Sheet1.Cells(85, 2)



'XCG inputs (unit = inches)
Dim XCGnose As Double
XCGnose = Sheet1.Cells(8, 6)
Dim XCGtailcone As Double
XCGtailcone = Sheet1.Cells(13, 6)
Dim XCGwing As Double
XCGwing = Sheet1.Cells(18, 6)
Dim XCGmotor As Double
XCGmotor = Sheet1.Cells(25, 6)
Dim XCGprop As Double
XCGprop = Sheet1.Cells(30, 6)
Dim XCGbattery As Double
XCGbattery = Sheet1.Cells(35, 6)
Dim XCGesc As Double
XCGesc = Sheet1.Cells(41, 6)
Dim XCGservo As Double
XCGservo = Sheet1.Cells(47, 6)
Dim XCGautopilot As Double
XCGautopilot = Sheet1.Cells(54, 6)
```

```
Dim XCGaltimeter As Double
XCGaltimeter = Sheet1.Cells(60, 6)
Dim XCGcamera As Double
XCGcamera = Sheet1.Cells(66, 6)
Dim XCGc2 As Double
XCGc2 = Sheet1.Cells(72, 6)
Dim XCGpyro As Double
XCGpyro = Sheet1.Cells(78, 6)
Dim XCGpara As Double
XCGpara = Sheet1.Cells(84, 6)


'Weight inputs (unit=grams)
Dim Wnose As Double
Wnose = Sheet1.Cells(10, 2)
Dim Wtailcone As Double
Wtailcone = Sheet1.Cells(15, 2)
Dim Wwing As Double
Wwing = Sheet1.Cells(22, 2)
Dim Wmotor As Double
Wmotor = Sheet1.Cells(27, 2)
Dim Wprop As Double
Wprop = Sheet1.Cells(32, 2)
Dim Wbattery As Double
Wbattery = Sheet1.Cells(38, 2)
Dim Wesc As Double
Wesc = Sheet1.Cells(44, 2)
Dim Wservo As Double
Wservo = Sheet1.Cells(50, 2)
Dim Wautopilot As Double
Wautopilot = Sheet1.Cells(57, 2)
Dim Waltimeter As Double
Waltimeter = Sheet1.Cells(63, 2)
Dim Wcamera As Double
Wcamera = Sheet1.Cells(69, 2)
Dim Wc2 As Double
Wc2 = Sheet1.Cells(74, 2)
Dim Wpyro As Double
Wpyro = Sheet1.Cells(80, 2)
Dim Wpara As Double
Wpara = Sheet1.Cells(86, 2)

'Quantities (where applicable) and recompute weights
Dim Qservo As Integer
Qservo = Sheet1.Cells(51, 2)
Wservo = Wservo * Qservo
Dim Qc2 As Integer
Qc2 = Sheet1.Cells(75, 2)
Wc2 = Wc2 * Qc2
Dim Qpyro As Integer
Qpyro = Sheet1.Cells(81, 2)
Wpyro = Wpyro * Qpyro

'Main wing characteristics
'Lchord = chord length, previously defined
```

```
'Wwing = weight of the wing, previously defined
'XCGwing = local center of gravity of the wing, previously defined
Dim Wspan As Double
Wspan = Sheet1.Cells(19, 2) 'inches
Dim Swing As Double
Swing = Sheet1.Cells(20, 2) 'inches^2
Dim ARwing As Double
ARwing = (Wspan ^ 2) / Swing
Sheet1.Cells(21, 2) = ARwing

'Fuselage Characteristics
'ln is the distance (inches) from the main wing quarter-chord to the base of the nose cone
Dim minln As Double
minln = Sheet1.Cells(8, 10)
Dim Maxln As Double
Maxln = Sheet1.Cells(9, 10)
Dim minlh As Double
'lh is the distance (inches)from the main wing quarter-chord to the quarter-chord of the horizontal stabilizer
minlh = Sheet1.Cells(10, 10)
Dim maxlh As Double
maxlh = Sheet1.Cells(11, 10)
'pfuse is the density of the fuselage (unit = grams/inch)
Dim pfuse As Double
pfuse = Sheet1.Cells(13, 10)
Dim Dfuse As Double
Dfuse = Sheet1.Cells(14, 10)
Dim Lfusetot As Double
Lfusetot = Sheet1.Cells(12, 10)


'Horizontal knowns
Dim Vh As Double
Vh = Sheet1.Cells(18, 14) 'tail volume ratio
Dim phor As Double
phor = Sheet1.Cells(19, 14) 'denstity of the horizontal


'Horizontal initial estimates
Dim Hchord As Double
Hchord = Sheet1.Cells(18, 10)
Dim Hspan As Double
Hspan = Sheet1.Cells(20, 10)
Dim HS As Double
HS = Sheet1.Cells(21, 10)
Dim HAR As Double
HAR = Sheet1.Cells(22, 10)


'program inputs

Dim fusestep As Double
fusestep = Sheet1.Cells(3, 15)
Dim iter As Integer
iter = Round((maxlh - minlh) / fusestep, 0) + 1
Dim iter2 As Integer
```

```
iter2 = Round((Maxln - minln) / fusestep, 0) + 1
Dim XCGtol As Double
XCGtol = Sheet1.Cells(2, 15)
Dim k As Integer
Dim j As Integer

'Analysis variables
Dim lh As Double    'length from quarter chord of the wing to the quarter chord of the horizontal stabilizer
Dim ln As Double    'length from the quarter chord of the wing to the base of the nose
Dim Wt As Double    'total weight
Dim Wstab As Double  'weight of the horizontal
Dim Wlh As Double   'weight of the tail section
Dim Wln As Double   'weight of the fuselage nose selction
Dim Wfuse As Double 'weight of the fuselage
Dim Hsemi As Double 'horizontal semi-span
Dim CGFtop As Double    'CG function top - numerator
Dim CGFtopR As Double   'CG function top (right side - items from the quarter chord, to the right)
Dim CGFtopL As Double   'CG function top (left side- items from the quater chord to the left)
Dim XCG As Double   'the X cg location
Dim Dnosec As Double 'distance from the tip of the nose to the quarter chord
Dim Dtailc As Double    'distance from the tip of the tail cone to the quarter chord
Dim Lfuse As Double 'total length of the fuselage
Dim XCGln As Double 'XCG location of the length to the nose
Dim XCGlh As Double 'XCG location of the length to the horizontal

'Dim Rlength As Double   'for the remaining length = due to the max fuselage length

'Winning conditions
Dim WtWin As Double

'initial condition
minlh = Round(minlh, 0)
maxlh = Round(maxlh, 0)
minln = Round(minln, 0)
Maxln = Round(Maxln, 0)
WtWin = Exp(100)

'Analysis
For k = 0 To iter

Application.ScreenUpdating = False  'since the program is pretty intense - use this to make it run faster

   j = 0   'to reset the nose loop
   Sheet2.Cells(11, 2 + k) = k

   lh = minlh + fusestep * k   'lh increases from the minimum to maximum

   HS = (Vh * Swing * Lchord) / lh  'calculate the tail area
   Hsemi = ((HAR * HS) ^ (0.5)) / 2    'uses the Horizontal AR to calculate the chord and span of the
horizontal
   Hspan = Hsemi * 2

   'Hsemi = (HS / 2)    'semi span
   'Hchord = Hsemi ^ (0.5)  'estimated chord length - assumes its a square
   Hchord = HS / (Hsemi * 2)
```

```
   Wstab = phor * ((Hchord * Dfuse) + HS) * 1.5 ' horizontal and vertical weight combined - assume the Vert is 1/2 the size of the Hor.
   'Hchord * fuse is for the internal structure of the tails

   Sheet2.Cells(14, 2 + k) = lh    'report lh
   Sheet2.Cells(15, 2 + k) = HS    'report tail area
   Sheet2.Cells(12, 2 + k) = Vh    'report Vh
   Sheet2.Cells(16, 2 + k) = Wstab 'reports the weight of the tail

   Dtailc = lh + 0.75 * Hchord + Ltailcone
   XCGlh = (lh + 0.75 * Hchord) / 2
   Wlh = (lh + 0.75 * Hchord) * pfuse

   'Calculate the nose needed to balance the system
   For j = 0 To iter2
      ln = minln + j * fusestep
      Dnosec = Lnose + ln
      Lfuse = ln + lh + 0.75 * Hchord
      XCGln = ln / 2
      Wln = ln * pfuse


      'TRACTOR CONFIGURATION!!!
      'Xcg = sum(mi*xi)/sum(mi)   cg function
      'IMPORTANT Xcg is located at the quarter chord, towards the nose is negative X, towards the tail is positive X
      'right side
      CGFtopR = ((XCGtailcone + lh + 0.75 * Hchord) * Wtailcone) + (lh * Wservo) + ((lh + 0.25 * Hchord) * Wstab) + (XCGlh * Wlh) + ((XCGwing - 0.25 * Lchord) * Wwing) + (XCGpyro * Wpyro) + ((Lpyro + XCGpara) * Wpara)
      'left side
      CGFtopL = (Wln * XCGln) + (XCGc2 * Wc2) + ((ln - XCGbattery - 2) * Wbattery) + ((ln - 2 - Lbattery - XCGesc - 4) * Wesc) + ((ln - XCGcamera - 2) * Wcamera) + ((ln - 2 - XCGautopilot) * Wautopilot) + ((ln - 2 - Lautopilot - XCGaltimeter) * Waltimeter) + ((ln + XCGmotor) * Wmotor) + ((ln + Lmotor + XCGprop) * Wprop) + ((XCGtailcone + ln) * Wtailcone)
      CGFtop = CGFtopR - CGFtopL
      Wt = 2 * Wtailcone + Wmotor + Wprop + Wservo + Wstab + Wlh + Wwing + Wpyro + Wln + Wc2 + Wbattery + Wesc + Wcamera + Wautopilot + Waltimeter + Wpara
      XCG = CGFtop / Wt
      Sheet2.Cells(13, 2 + k) = ln
      Sheet2.Cells(18, 2 + k) = Wt
      Sheet2.Cells(17, 2 + k) = Wln
      Sheet2.Cells(19, 2 + k) = XCG



      If XCG > 0 And XCG < XCGtol Then
      'system is tail heavy, but within a reasonable range
         Sheet2.Cells(13, 2 + k) = ln
         Sheet2.Cells(18, 2 + k) = Wt
         Sheet2.Cells(17, 2 + k) = Wln + Wlh
         Sheet2.Cells(19, 2 + k) = XCG

            If Wt < WtWin Then 'for finding the minimum weight - winning design
               WtWin = Wt
```

```
            Sheet2.Cells(8, 2) = Wt
            Sheet2.Cells(7, 2) = Wln + Wlh
            Sheet2.Cells(6, 2) = Wstab
            Sheet2.Cells(5, 2) = HS
            Sheet2.Cells(4, 2) = ln
            Sheet2.Cells(3, 2) = lh
            Sheet2.Cells(2, 2) = Vh
            Sheet2.Cells(9, 2) = XCG
            Sheet2.Cells(4, 5) = ln + lh + Hchord * 0.75 + 2 * Ltailcone
            Sheet2.Cells(2, 5) = Hchord
            Sheet2.Cells(3, 5) = Hspan
        Else
        End If

    j = iter2 + 1
ElseIf XCG < 0 And XCG > (-1 * XCGtol) Then
'system is nose heavy, but within a reasonble range
    Sheet2.Cells(13, 2 + k) = ln
    Sheet2.Cells(18, 2 + k) = Wt
    Sheet2.Cells(17, 2 + k) = Wln + Wlh
    Sheet2.Cells(19, 2 + k) = XCG

        If Wt < WtWin Then 'for finding the minimum weight - winning design
            WtWin = Wt
            Sheet2.Cells(8, 2) = Wt
            Sheet2.Cells(7, 2) = Wln + Wlh
            Sheet2.Cells(6, 2) = Wstab
            Sheet2.Cells(5, 2) = HS
            Sheet2.Cells(4, 2) = ln
            Sheet2.Cells(3, 2) = lh
            Sheet2.Cells(2, 2) = Vh
            Sheet2.Cells(9, 2) = XCG
            Sheet2.Cells(4, 5) = ln + lh + Hchord * 0.75 + 2 * Ltailcone
            Sheet2.Cells(2, 5) = Hchord
            Sheet2.Cells(3, 5) = Hspan
        Else
        End If

    j = inter2 + 1
ElseIf XCG > 0 And j >= iter2 Then
    Sheet2.Cells(13, 2 + k) = "NO SOLTN - T heavy"
ElseIf XCG < 0 Then
'system is nose heavy, so the nose is long enough, the battery just needs to be moved back
    If j = iter2 Then
    Sheet2.Cells(13, 2 + k) = "NO SOLTN - N heavy"
    Else
    Sheet2.Cells(13, 2 + k) = ln
    Sheet2.Cells(18, 2 + k) = Wt
    Sheet2.Cells(17, 2 + k) = Wln + Wlh
    Sheet2.Cells(19, 2 + k) = XCG
    End If

        If Wt < WtWin Then 'for finding the minimum weight - winning design
            WtWin = Wt
            Sheet2.Cells(8, 2) = Wt
```

```
            Sheet2.Cells(7, 2) = Wln + Wlh
            Sheet2.Cells(6, 2) = Wstab
            Sheet2.Cells(5, 2) = HS
            Sheet2.Cells(4, 2) = ln
            Sheet2.Cells(3, 2) = lh
            Sheet2.Cells(2, 2) = Vh
            Sheet2.Cells(9, 2) = XCG
            Sheet2.Cells(4, 5) = ln + lh + Hchord * 0.75 + 2 * Ltailcone
            Sheet2.Cells(2, 5) = Hchord
            Sheet2.Cells(3, 5) = Hspan
        Else
        End If

    ElseIf XCG = 0 Then
        MsgBox k
        Sheet2.Cells(13, 2 + k) = ln
        Sheet2.Cells(18, 2 + k) = Wt
        Sheet2.Cells(17, 2 + k) = Wln + Wlh
        Sheet2.Cells(19, 2 + k) = XCG
        Sheet2.Cells(20, 2 + k) = "ERROR!"

    Else
    End If


  Next j

Application.ScreenUpdating = True

Next k

End Sub
```

H.8 PROGRAM CODE – EDF CONFIG

```
Sub WeightMinEDF()

'Note - motor, ESC, and battery is different from the motor, ESC and battery for pusher/tractor. Also, there is no prop info

'length (x) inputs (unit= inches)
Dim Lnose As Double
Lnose = Sheet1.Cells(9, 2)
Dim Ltailcone As Double
Ltailcone = Sheet1.Cells(14, 2)
Dim Lchord As Double            'for the wing
Lchord = Sheet1.Cells(18, 2)    'for the wing
Dim Lmotor As Double
Lmotor = Sheet1.Cells(26, 10)
'Dim Lprop As Double
'Lprop = Sheet1.Cells(30, 6) * 2
Dim Lbattery As Double
Lbattery = Sheet1.Cells(35, 10)
Dim Lesc As Double
Lesc = Sheet1.Cells(41, 10)
Dim Lservo As Double
Lservo = Sheet1.Cells(47, 2)
Dim Lautopilot As Double
Lautopilot = Sheet1.Cells(54, 2)
Dim Laltimeter As Double
Laltimeter = Sheet1.Cells(60, 2)
Dim Lcamera As Double
Lcamera = Sheet1.Cells(66, 2)
Dim Lc2 As Double
Lc2 = Sheet1.Cells(73, 2)
Dim Lpyro As Double
Lpyro = Sheet1.Cells(79, 2)
Dim Lpara As Double
Lpara = Sheet1.Cells(85, 2)



'XCG inputs (unit = inches)
Dim XCGnose As Double
XCGnose = Sheet1.Cells(8, 6)
Dim XCGtailcone As Double
XCGtailcone = Sheet1.Cells(13, 6)
Dim XCGwing As Double
XCGwing = Sheet1.Cells(18, 6)
Dim XCGmotor As Double
XCGmotor = Sheet1.Cells(25, 14)
'Dim XCGprop As Double
'XCGprop = Sheet1.Cells(30, 6)
Dim XCGbattery As Double
XCGbattery = Sheet1.Cells(35, 14)
Dim XCGesc As Double
XCGesc = Sheet1.Cells(41, 14)
Dim XCGservo As Double
```

```
XCGservo = Sheet1.Cells(47, 6)
Dim XCGautopilot As Double
XCGautopilot = Sheet1.Cells(54, 6)
Dim XCGaltimeter As Double
XCGaltimeter = Sheet1.Cells(60, 6)
Dim XCGcamera As Double
XCGcamera = Sheet1.Cells(66, 6)
Dim XCGc2 As Double
XCGc2 = Sheet1.Cells(72, 6)
Dim XCGpyro As Double
XCGpyro = Sheet1.Cells(78, 6)
Dim XCGpara As Double
XCGpara = Sheet1.Cells(84, 6)


'Weight inputs (unit=grams)
Dim Wnose As Double
Wnose = Sheet1.Cells(10, 2)
Dim Wtailcone As Double
Wtailcone = Sheet1.Cells(15, 2)
Dim Wwing As Double
Wwing = Sheet1.Cells(22, 2)
Dim Wmotor As Double
Wmotor = Sheet1.Cells(27, 10)
'Dim Wprop As Double
'Wprop = Sheet1.Cells(32, 2)
Dim Wbattery As Double
Wbattery = Sheet1.Cells(38, 10)
Dim Wesc As Double
Wesc = Sheet1.Cells(44, 10)
Dim Wservo As Double
Wservo = Sheet1.Cells(50, 2)
Dim Wautopilot As Double
Wautopilot = Sheet1.Cells(57, 2)
Dim Waltimeter As Double
Waltimeter = Sheet1.Cells(63, 2)
Dim Wcamera As Double
Wcamera = Sheet1.Cells(69, 2)
Dim Wc2 As Double
Wc2 = Sheet1.Cells(74, 2)
Dim Wpyro As Double
Wpyro = Sheet1.Cells(80, 2)
Dim Wpara As Double
Wpara = Sheet1.Cells(86, 2)

'Quantities (where applicable) and recompute weights
Dim Qservo As Integer
Qservo = Sheet1.Cells(51, 2)
Wservo = Wservo * Qservo
Dim Qc2 As Integer
Qc2 = Sheet1.Cells(75, 2)
Wc2 = Wc2 * Qc2
Dim Qpyro As Integer
Qpyro = Sheet1.Cells(81, 2)
Wpyro = Wpyro * Qpyro
```

```
'Main wing characteristics
'Lchord = chord length, previously defined
'Wwing = weight of the wing, previously defined
'XCGwing = local center of gravity of the wing, previously defined
Dim Wspan As Double
Wspan = Sheet1.Cells(19, 2) 'inches
Dim Swing As Double
Swing = Sheet1.Cells(20, 2) 'inches^2
Dim ARwing As Double
ARwing = (Wspan ^ 2) / Swing
Sheet1.Cells(21, 2) = ARwing

'Fuselage Characteristics
'ln is the distance (inches) from the main wing quarter-chord to the base of the nose cone
Dim minln As Double
minln = Sheet1.Cells(8, 10)
Dim Maxln As Double
Maxln = Sheet1.Cells(9, 10)
Dim minlh As Double
'lh is the distance (inches)from the main wing quarter-chord to the quarter-chord of the horizontal stabilizer
minlh = Sheet1.Cells(10, 10)
Dim maxlh As Double
maxlh = Sheet1.Cells(11, 10)
'pfuse is the density of the fuselage (unit = grams/inch)
Dim pfuse As Double
pfuse = Sheet1.Cells(13, 10)
Dim Dfuse As Double
Dfuse = Sheet1.Cells(14, 10)
Dim Lfusetot As Double
Lfusetot = Sheet1.Cells(12, 10)
Dim pEDFTube As Double
pEDFTube = Sheet1.Cells(49, 10)



'Horizontal knowns
Dim Vh As Double
Vh = Sheet1.Cells(18, 14) 'tail volume ratio
Dim phor As Double
phor = Sheet1.Cells(19, 14) 'denstity of the horizontal


'Horizontal initial estimates
Dim Hchord As Double
Hchord = Sheet1.Cells(18, 10)
Dim Hspan As Double
Hspan = Sheet1.Cells(20, 10)
Dim HS As Double
HS = Sheet1.Cells(21, 10)
Dim HAR As Double
HAR = Sheet1.Cells(22, 10)


'program inputs
```

```
Dim fusestep As Double
fusestep = Sheet1.Cells(3, 15)
Dim iter As Integer
iter = Round((maxlh - minlh) / fusestep, 0) + 1
Dim iter2 As Integer
iter2 = Round((Maxln - minln) / fusestep, 0) + 1
Dim XCGtol As Double
XCGtol = Sheet1.Cells(2, 15)
Dim k As Integer
Dim j As Integer

'Analysis variables
Dim lh As Double    'length from quarter chord of the wing to the quarter chord of the horizontal stabilizer
Dim ln As Double    'length from the quarter chord of the wing to the base of the nose
Dim Wt As Double    'total weight
Dim Wstab As Double  'weight of the horizontal
Dim Wlh As Double   'weight of the tail section
Dim Wln As Double   'weight of the fuselage nose selction
Dim Wfuse As Double 'weight of the fuselage
Dim Hsemi As Double 'horizontal semi-span
Dim CGFtop As Double    'CG function top - numerator
Dim CGFtopR As Double   'CG function top (right side - items from the quarter chord, to the right)
Dim CGFtopL As Double   'CG function top (left side- items from the quater chord to the left)
Dim XCG As Double   'the X cg location
Dim Dnosec As Double 'distance from the tip of the nose to the quarter chord
Dim Dtailc As Double    'distance from the tip of the tail cone to the quarter chord
Dim Lfuse As Double 'total length of the fuselage
Dim XCGln As Double 'XCG location of the length to the nose
Dim XCGlh As Double 'XCG location of the length to the horizontal
'Dim Rlength As Double   'for the remaining length = due to the max fuselage length
Dim LEDFTube As Double  'the length of the edf tube
Dim XCGedfTube As Double    'the xcg location of the edf tube
Dim WedfTube As Double      'the weight of the edf tube

'EDF stuff
Dim Dmotor As Double    'for the Diameter of the EDF
Dmotor = Sheet1.Cells(25, 10)

'Winning conditions
Dim WtWin As Double

'initial condition
minlh = Round(minlh, 0)
maxlh = Round(maxlh, 0)
minln = Round(minln, 0)
Maxln = Round(Maxln, 0)
WtWin = Exp(100)

'Analysis
For k = 0 To iter

Application.ScreenUpdating = False  'since the program is pretty intense - use this to make it run faster
```

```
    j = 0   'to reset the nose loop
    Sheet4.Cells(11, 2 + k) = k

    lh = minlh + fusestep * k   'lh increases from the minimum to maximum

    HS = (Vh * Swing * Lchord) / lh  'calculate the tail area
    Hsemi = ((HAR * HS) ^ (0.5)) / 2    'uses the Horizontal AR to calculate the chord and span of the
horizontal
    Hspan = Hsemi * 2

    'Hsemi = (HS / 2)    'semi span
    'Hchord = Hsemi ^ (0.5)  'estimated chord length - assumes its a square
    Hchord = HS / (Hsemi * 2)
    Wstab = phor * ((Hchord * Dfuse * (1 - Dmotor / Dfuse)) + HS) * 1.5 ' horizontal and vertical weight
combined - assume the Vert is 1/2 the size of the Hor.
    'Hchord * fuse is for the internal structure of the tails
    LEDFTube = (lh + (0.75 * Hchord)) - ((0.75 * Lchord) + 4)
    XCGedfTube = (lh + 0.75 * Hchord) - (LEDFTube / 2)
    WedfTube = LEDFTube * pEDFTube


    Sheet4.Cells(14, 2 + k) = lh    'report lh
    Sheet4.Cells(15, 2 + k) = HS    'report tail area
    Sheet4.Cells(12, 2 + k) = Vh    'report Vh
    Sheet4.Cells(16, 2 + k) = Wstab 'reports the weight of the tail

    Dtailc = lh + 0.75 * Hchord + Ltailcone
    XCGlh = (lh + 0.75 * Hchord) / 2
    Wlh = (lh + 0.75 * Hchord) * pfuse

    'Calculate the nose needed to balance the system
    For j = 0 To iter2
        ln = minln + j * fusestep
        Dnosec = Lnose + ln
        Lfuse = ln + lh + 0.75 * Hchord
        XCGln = ln / 2
        Wln = ln * pfuse


        'EDF CONFIGURATION!!!
        'Xcg = sum(mi*xi)/sum(mi)   cg function
        'IMPORTANT Xcg is located at the quarter chord, towards the nose is negative X, towards the tail is
positive X
        'right side
        CGFtopR = (lh * Wservo) + ((lh + 0.25 * Hchord) * Wstab) + (XCGlh * Wlh) + ((XCGwing - 0.25 *
Lchord) * Wwing) + (XCGpyro * Wpyro) + ((0.75 * Hchord + XCGmotor + 4) * Wmotor) + ((WedfTube)
* XCGedfTube)
        'left side
        CGFtopL = ((ln + XCGnose) * Wnose) + (Wln * XCGln) + (XCGc2 * Wc2) + ((ln + Lnose - Lpara -
XCGbattery - 2) * Wbattery) + ((ln + Lnose - Lpara - 2 - Lbattery - XCGesc - 4) * Wesc) + ((ln + Lnose -
Lpara - XCGcamera - 2) * Wcamera) + ((ln + Lnose - Lpara - 2 - XCGautopilot) * Wautopilot) + ((ln +
Lnose - Lpara - 2 - Lautopilot - XCGaltimeter) * Waltimeter) + ((ln + Lnose - XCGpara) * Wpara)
        CGFtop = CGFtopR - CGFtopL
        Wt = Wnose + Wtailcone + Wmotor + Wservo + Wstab + Wlh + Wwing + Wpyro + Wln + Wc2 +
Wbattery + Wesc + Wcamera + Wautopilot + Waltimeter + Wpara
```

```
XCG = CGFtop / Wt
Sheet4.Cells(13, 2 + k) = ln
Sheet4.Cells(18, 2 + k) = Wt
Sheet4.Cells(17, 2 + k) = Wln
Sheet4.Cells(19, 2 + k) = XCG



If XCG > 0 And XCG < XCGtol Then
'system is tail heavy, but within a reasonable range
   Sheet4.Cells(13, 2 + k) = ln
   Sheet4.Cells(18, 2 + k) = Wt
   Sheet4.Cells(17, 2 + k) = Wln + Wlh
   Sheet4.Cells(19, 2 + k) = XCG

      If Wt < WtWin Then 'for finding the minimum weight - winning design
         WtWin = Wt
         Sheet4.Cells(8, 2) = Wt
         Sheet4.Cells(7, 2) = Wln + Wlh
         Sheet4.Cells(6, 2) = Wstab
         Sheet4.Cells(5, 2) = HS
         Sheet4.Cells(4, 2) = ln
         Sheet4.Cells(3, 2) = lh
         Sheet4.Cells(2, 2) = Vh
         Sheet4.Cells(9, 2) = XCG
         Sheet4.Cells(4, 5) = ln + lh + Hchord * 0.75
         Sheet4.Cells(2, 5) = Hchord
         Sheet4.Cells(3, 5) = Hspan
         Sheet4.Cells(2, 14) = LEDFTube
         Sheet4.Cells(3, 14) = WedfTube
      Else
      End If

   j = iter2 + 1
ElseIf XCG < 0 And XCG > (-1 * XCGtol) Then
'system is nose heavy, but within a reasonble range
   Sheet4.Cells(13, 2 + k) = ln
   Sheet4.Cells(18, 2 + k) = Wt
   Sheet4.Cells(17, 2 + k) = Wln + Wlh
   Sheet4.Cells(19, 2 + k) = XCG

      If Wt < WtWin Then 'for finding the minimum weight - winning design
         WtWin = Wt
         Sheet4.Cells(8, 2) = Wt
         Sheet4.Cells(7, 2) = Wln + Wlh
         Sheet4.Cells(6, 2) = Wstab
         Sheet4.Cells(5, 2) = HS
         Sheet4.Cells(4, 2) = ln
         Sheet4.Cells(3, 2) = lh
         Sheet4.Cells(2, 2) = Vh
         Sheet4.Cells(9, 2) = XCG
         Sheet4.Cells(4, 5) = ln + lh + Hchord * 0.75
         Sheet4.Cells(2, 5) = Hchord
         Sheet4.Cells(3, 5) = Hspan
         Sheet4.Cells(2, 14) = LEDFTube
```

```
            Sheet4.Cells(3, 14) = WedfTube
        Else
        End If

    j = inter2 + 1
ElseIf XCG > 0 And j >= iter2 Then
    Sheet4.Cells(13, 2 + k) = "NO SOLTN - T heavy"
ElseIf XCG < 0 Then
'system is nose heavy, so the nose is long enough, the battery just needs to be moved back
    If j = iter2 Then
    Sheet4.Cells(13, 2 + k) = "NO SOLTN - N heavy"
    Else
    Sheet4.Cells(13, 2 + k) = ln
    Sheet4.Cells(18, 2 + k) = Wt
    Sheet4.Cells(17, 2 + k) = Wln + Wlh
    Sheet4.Cells(19, 2 + k) = XCG
    End If

        If Wt < WtWin Then 'for finding the minimum weight - winning design
            WtWin = Wt
            Sheet4.Cells(8, 2) = Wt
            Sheet4.Cells(7, 2) = Wln + Wlh
            Sheet4.Cells(6, 2) = Wstab
            Sheet4.Cells(5, 2) = HS
            Sheet4.Cells(4, 2) = ln
            Sheet4.Cells(3, 2) = lh
            Sheet4.Cells(2, 2) = Vh
            Sheet4.Cells(9, 2) = XCG
            Sheet4.Cells(4, 5) = ln + lh + Hchord * 0.75
            Sheet4.Cells(2, 5) = Hchord
            Sheet4.Cells(3, 5) = Hspan
            Sheet4.Cells(2, 14) = LEDFTube
            Sheet4.Cells(3, 14) = WedfTube
        Else
        End If

ElseIf XCG = 0 Then
    MsgBox k
    Sheet4.Cells(13, 2 + k) = ln
    Sheet4.Cells(18, 2 + k) = Wt
    Sheet4.Cells(17, 2 + k) = Wln + Wlh
    Sheet4.Cells(19, 2 + k) = XCG
    Sheet4.Cells(20, 2 + k) = "ERROR!"

Else
End If


  Next j

Application.ScreenUpdating = True
Next k
End Sub
```

Flight Conditions	
Density (slugs/ft^3):	0.0023769
Abs. Viscosity (slugs/(ft-s):	3.7373E-07
Speed of Sound (ft/s):	1117
Velocity (ft/s):	136.1710914
S_{ref} (sq. ft):	12

Calculate Drag

Input:
Output:
Drag Output:

Fuselage Drag Buildup	
Length (ft):	4.166666667
Max Diameter (ft):	0.333333333
S_{wet} (sq. ft):	4.991915962
Interference Factor, Q:	1.2
Reynolds Number:	3.60E+06
Skin Friction Coeff, C_f:	0.003551339
f:	12.5
Form Factor, FF:	1.06197
D/q (ft^2):	0.022591906
Cdo:	0.001882659

Horizontal Tail Drag Buildup	
Cdo:	0.02
S_{ht} (sq. ft):	1.388888889
Interference factor Q	1.2
D/q (ft^2):	0.033333333
Cdo:	0.002777778

Complete Aircraft (- Wing)	
D/q (ft^2):	0.072591906
Cdo:	0.006049326

Complete Aircraft (w/ Wing	
D/q (ft^2):	0.116256723
Cdo (total):	0.00968806

C_{Do} Breakdown	
Fuselage:	0.0019
Wing:	0.00843
Horizontal Tail:	0.003
Vertical Tail:	0.0014
Total	0.0097

Vertical Tail Buildup	
Cdo:	0.02
S_{vt} (sq. ft):	0.694444444
Interference factor, Q	1.2
D/q (ft^2):	0.016666667
Cdo:	0.001388889

Reynolds number for Horizontal/Vertical
Re: 721699.9
Chord 0.833333333 ft

Wing Drag Buildup	
MAC (ft):	1.0625
S_{wet} (sq. ft):	13.08952347
Position of Max. Thickness (x/c):	0.308627451
Thickness Ratio (t/c):	0.199843137
Interference Factor, Q:	1.2
Reynolds Number:	918468.2404
Skin Friction Coeff, C_f:	0.00453627
Form Factor, FF:	1.419777692
D/q (ft^2):	0.101163609
Cdo:	0.008430301

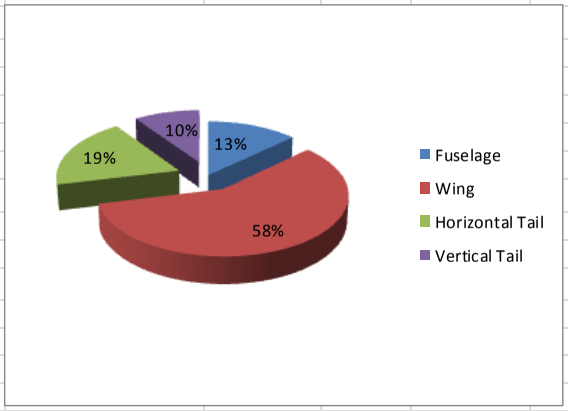

I.2 PROGRAM CODE – DRAG ANALYSIS

```
Sub Drag()

Dim V As Double, Cdo As Double

V = Sheet5.Cells(7, 2).Value

Dim DoQtotal As Double
'flight variables
Dim rho As Double, mu As Double, ao As Double, Ma As Double
'fuselage variables
Dim length As Double, diameter As Double, SWETf As Double, Qf As Double
Dim REf As Double, CFfuse As Double, f As Double, FFfuse As Double, DoQf As Double, CdoFuse As
Double
'wing variables
Dim Sref As Double, MACw As Double, SWETw As Double, XoCw As Double, ToCw As Double, Qw
As Double
Dim REw As Double, CFwing As Double, FFwing As Double, DoQw As Double, CdoWing As Double
'horizontal tail variables
Dim CdoHT As Double, Sht As Double, Qht As Double, DoQht As Double
'vertical tail variables
Dim CdoVT As Double, Svt As Double, Qvt As Double, DoQvt As Double

'reads in flight variables
rho = Sheet5.Cells(4, 2).Value
mu = Sheet5.Cells(5, 2).Value
ao = Sheet5.Cells(6, 2).Value
Ma = V / ao
Sref = Sheet5.Cells(8, 2).Value

'reads in fuselage variables
length = Sheet5.Cells(11, 2).Value
diameter = Sheet5.Cells(12, 2).Value
SWETf = Sheet5.Cells(13, 2).Value
Qf = Sheet5.Cells(14, 2).Value

'Calculates fuselage drag outputs
REf = (rho * V * length) / mu

If REf > 500000 Then
   CFfuse = 0.455 / (((Log(REf) / Log(10)) ^ 2.58) * ((1 + 0.144 * Ma ^ 2) ^ 0.65))
Else
   CFfuse = 1.328 / (REf ^ (1 / 2))
End If

f = length / diameter
FFfuse = 1 + (60 / (f ^ 3)) + (f / 400)

'calculates D/q and Cdo for fuselage
DoQf = CFfuse * FFfuse * Qf * SWETf
CdoFuse = DoQf / Sref

'outputs fuselage data into spreadsheet
Sheet5.Cells(16, 2).Value = REf
```

```
Sheet5.Cells(17, 2).Value = CFfuse
Sheet5.Cells(18, 2).Value = f
Sheet5.Cells(19, 2).Value = FFfuse
Sheet5.Cells(21, 2).Value = DoQf
Sheet5.Cells(22, 2).Value = CdoFuse

'reads in wing variables
MACw = Sheet5.Cells(25, 2).Value
SWETw = Sheet5.Cells(26, 2).Value
XoCw = Sheet5.Cells(27, 2).Value
ToCw = Sheet5.Cells(28, 2).Value
Qw = Sheet5.Cells(29, 2).Value

'Calculates wing drag outputs
REw = (rho * V * MACw) / mu

If REw > 500000 Then
   CFwing = 0.455 / (((Log(REw) / Log(10)) ^ 2.58) * ((1 + 0.144 * Ma ^ 2) ^ 0.65))
Else
   CFwing = 1.328 / (REw ^ (1 / 2))
End If

FFwing = (1 + (0.6 / XoCw) * (ToCw) + 100 * (ToCw) ^ 4) * 1.34 * Ma ^ 0.18

'calculates D/q and Cdo for wing
DoQw = CFwing * FFwing * Qw * SWETw
CdoWing = DoQw / Sref

'outputs wing data into spreadsheet
Sheet5.Cells(31, 2).Value = REw
Sheet5.Cells(32, 2).Value = CFwing
Sheet5.Cells(33, 2).Value = FFwing
Sheet5.Cells(35, 2).Value = DoQw
Sheet5.Cells(36, 2).Value = CdoWing

'reads in horizontal tail variables
CdoHT = Sheet5.Cells(11, 6).Value
Sht = Sheet5.Cells(12, 6).Value
Qht = Sheet5.Cells(13, 6).Value

'calculates D/q for horizontal tail
DoQht = CdoHT * Sht * Qht

'outputs horizontal tail data into spreadsheet
Sheet5.Cells(15, 6).Value = DoQht

'reads in vertical tail variables
CdoVT = Sheet5.Cells(19, 6).Value
Svt = Sheet5.Cells(20, 6).Value
Qvt = Sheet5.Cells(21, 6).Value

'Calculates vertical tail drag outputs

'calculates D/q and Cdo for vertical tail
DoQvt = CdoVT * Svt * Qvt
```

```
'outputs horizontal tail data into spreadsheet
Sheet5.Cells(23, 6).Value = DoQvt

'outputs aircraft total drag minus the wing
DoQtotal = DoQf + DoQht + DoQvt
Sheet5.Cells(11, 9).Value = DoQtotal
Cdo = DoQtotal / Sref
Sheet5.Cells(12, 9).Value = Cdo

End Sub
```

J. AIRCRAFT ANALYSIS

J.1: WING AIRFOIL DATA CORRECTED FOR 3D EFFECTS

a0=	0.0744	per degree		References:			
e=	0.95	spanwise effectivness (typical 0.95		Anderson Ch 2			
alpha(cl=0)=	-2.975490196	deg					
AR=	5.76						
Clαw	0.059616805	/deg	=	3.415791	/radian		
a=	0.059616805	per degree		High AR, straight wing, incompressible			
				Anderson Eq 2.15			

Alfa	CL	CDp	CL/CD
-8	-0.29954522	0.03225413	-9.28703589
-7	-0.23992842	0.02989013	-8.02701267
-6	-0.18031161	0.02834453	-6.36142634
-5	-0.12069481	0.02761243	-4.37103239
-4	-0.061078	0.02742328	-2.22723216
-3	-0.0014612	0.02719533	-0.05372968
-2	0.058155609	0.02704793	2.150094977
-1	0.117772414	0.02711233	4.343869865
0	0.177389219	0.02525833	7.022999947
1	0.237006024	0.02470513	9.593394844
3	0.356239634	0.02738933	13.00651356
4	0.415856439	0.02912563	14.27802601
5	0.475473244	0.02982403	15.94262463
6	0.535090049	0.02978293	17.96633606
7	0.594706854	0.03041603	19.5524183
8	0.654323659	0.03208173	20.39552575
9	0.713940464	0.03299983	21.6346739
10	0.773557269	0.03375253	22.91850038
12	0.892790879	0.03780259	23.61719091
13	0.952407684	0.04082149	23.33103933

J.2: TAIL AIRFOIL DATA

e=	0.95	spanwise effectivness (typical 0.95)				Anderson Ch 2	
alpha(cl=0)=	0	deg					
AR=	2						
Clαw	0.10829	/deg	=	6.20456	/radian		
a=	0.10829	per degree		High AR, straight wing, incompressible			
				Anderson Eq 2.15			

NACA 0006 - Re = 500000				
Alfa	Cl	Cd	Cl/Cd	Cm
-5	-0.541	0.0146	-37.08	-0.003
-3	-0.341	0.0083	-41.06	0.0017
-2	-0.244	0.0059	-41.27	0.0034
-1	-0.147	0.0047	-31.36	0.008
0	0	0.0048	0	0
1	0.1475	0.0047	31.383	-0.008
2	0.2437	0.0059	41.305	-0.003
3	0.341	0.0083	41.084	-0.002
4	0.4391	0.0121	36.289	0.0014
5	0.5415	0.0146	37.089	0.0033

J.3: PROPULSION ANALYSIS DATA

GTOW	8.894981	lb							Vmin Drag	44.62469961	ft/s
GTOW*	10	lb	*Adjusted - assume final weight will be higher						CLmin Drag	0.676065005	
Swing	6.25	ft^2							Vmin Power	33.90743923	ft/s
AR	5.76								CLmin Power	0.390326313	
W/S	1.6	lb/ft^2									
T/W	0.35274	lb/lb							Note:		
									Vmax loiter = Vmin Power (for prop)		
Steady, Level Flight Conditions					Flight Conditions				R/C max	17.68334063	
CD0	0.025258				Density:	0.002377 slugs/ft^3					
K	0.055262										
CL	0.177389	alpha = 0									
CLmax	0.952408	alpha= 13									
L/Dmax	23.61719										
										Climb speed at 45	
V (ft/s)	q (psi)	Reqd CL	Dp (lb)	Di (lb)	Dtot (lb)		Max Thrust (lb)	Excess Power	R/C (rate of climb)	deg angle climb	
5	0.029711	53.85166	0.00469	29.75957	29.76426		3.527396192	-131.1843383	-13.11843383	-18.55226704	
10	0.118845	13.46291	0.018761	7.439893	7.458655		3.527396192	-39.31258595	-3.931258595	-5.559639222	
15	0.267401	5.983517	0.042213	3.306619	3.348832		3.527396192	2.678456097	0.26784561	0.378790894	
20	0.47538	3.365728	0.075046	1.859973	1.935019		3.527396192	31.84754411	3.184754411	4.503922881	
25	0.742781	2.154066	0.117259	1.190383	1.307642		3.527396192	55.49386089	5.549386089	7.848017069	
30	1.069605	1.495879	0.168853	0.826655	0.995508		3.527396192	75.95666031	7.595666031	10.74189392	
35	1.455851	1.099013	0.229827	0.607338	0.837166		3.527396192	94.1580737	9.41580737	13.31596248	
40	1.90152	0.841432	0.300183	0.464993	0.765176		3.527396192	110.4888114	11.04888114	15.62547756	
45	2.406611	0.664835	0.379919	0.367402	0.747321		3.527396192	125.1033968	12.51033968	17.69229205	
50	2.971125	0.538517	0.469035	0.297596	0.766631		3.527396192	138.0382596	13.80382596	19.52155788	
55	3.595061	0.445055	0.567533	0.245947	0.81348		3.527396192	149.2654148	14.92654148	21.1093174	
60	4.27842	0.37397	0.675411	0.206664	0.882074		3.527396192	158.7193023	15.87193023	22.44629899	
65	5.021201	0.318649	0.79267	0.176092	0.968762		3.527396192	166.3112388	16.63112388	23.51996094	
70	5.823405	0.274753	0.919309	0.151835	1.071144		3.527396192	171.9376759	17.19376759	24.31565932	
75	6.685031	0.239341	1.055329	0.132265	1.187594		3.527396192	175.4851555	17.54851555	24.81734869	
80	7.60608	0.210358	1.20073	0.116248	1.316979		3.527396192	176.8334063	17.68334063	25.00802014	
85	8.586551	0.186338	1.355512	0.102974	1.458486		3.527396192	175.8573476	17.58573476	24.86998461	
90	9.626445	0.166209	1.519674	0.091851	1.611525		3.527396192	172.4284257	17.24284257	24.38506181	
95	10.72576	0.149174	1.693217	0.082436	1.775654		3.527396192	166.4155273	16.64155273	23.53470956	
100	11.8845	0.134629	1.876141	0.074399	1.95054		3.527396192	157.6856197	15.76856197	22.30011419	
105	13.10266	0.122113	2.068446	0.067482	2.135928		3.527396192	146.1042078	14.61042078	20.66225521	
110	14.38025	0.111264	2.270131	0.061487	2.331617		3.527396192	131.5356664	13.15356664	18.60195233	
115	15.71725	0.101799	2.481197	0.056256	2.537453		3.527396192	113.8434859	11.38434859	16.09990017	
120	17.11368	0.093492	2.701643	0.051666	2.753309		3.527396192	92.89045644	9.289045644	13.13669433	
125	18.56953	0.086163	2.93147	0.047615	2.979086		3.527396192	68.53880819	6.853880819	9.692851209	
130	20.08481	0.079662	3.170678	0.044023	3.214701		3.527396192	40.6503188	4.06503188	5.748823217	
135	21.6595	0.073871	3.419267	0.040822	3.46009		3.527396192	9.086397327	0.908639733	1.285010633	
140	23.29362	0.068688	3.677236	0.037959	3.715195		3.527396192	-26.29185	-2.629185	-3.718229085	
145	24.98716	0.064033	3.944587	0.035386	3.979973		3.527396192	-65.62356752	-6.562356752	-9.280573921	
150	26.74013	0.059835	4.221317	0.033066	4.254384		3.527396192	-109.0481084	-10.90481084	-15.42173139	
155	28.55251	0.056037	4.507429	0.030967	4.538396		3.527396192	-156.7050011	-15.67050011	-22.16143378	
160	30.42432	0.05259	4.802921	0.029062	4.831983		3.527396192	-208.7339215	-20.87339215	-29.51943427	
165	32.35555	0.049451	5.107794	0.027327	5.135121		3.527396192	-265.2746713	-26.52746713	-37.51550379	
170	34.34621	0.046584	5.422048	0.025744	5.447791		3.527396192	-326.4671588	-32.64671588	-46.16942837	
175	36.39628	0.043961	5.745682	0.024294	5.769976		3.527396192	-392.4513843	-39.24513843	-55.50100702	
180	38.50578	0.041552	6.078697	0.022963	6.10166		3.527396192	-463.3674267	-46.33674267	-65.53004992	
185	40.6747	0.039336	6.421093	0.021738	6.442831		3.527396192	-539.3554334	-53.93554334	-76.27637689	
190	42.90305	0.037293	6.772869	0.020609	6.793478		3.527396192	-620.5556111	-62.05556111	-87.75981614	
195	45.19081	0.035405	7.134026	0.019566	7.153592		3.527396192	-707.108218	-70.7108218	-100.0002032	
200	47.538	0.033657	7.504564	0.0186	7.523164		3.527396192	-799.1535576	-79.91535576	-113.01738	

Vmax	136.1711	ft/s		92.84393	mph		
Vstall	39.43251	ft/s	@ Clmax	26.8858	mph		
Vmin	91.36971	ft/s	@ Level Flight	62.29753	mph		
Max Climb Angle							
16.161	deg	Steeper than stall angle!					
V@ Max Climb Angle							
35.562	ft/s	Below stall speed!					
Min Glide Angle							
2.4246	deg						
Min Take off Distance (est) - Anderson eq 6.95							
91.102	feet						

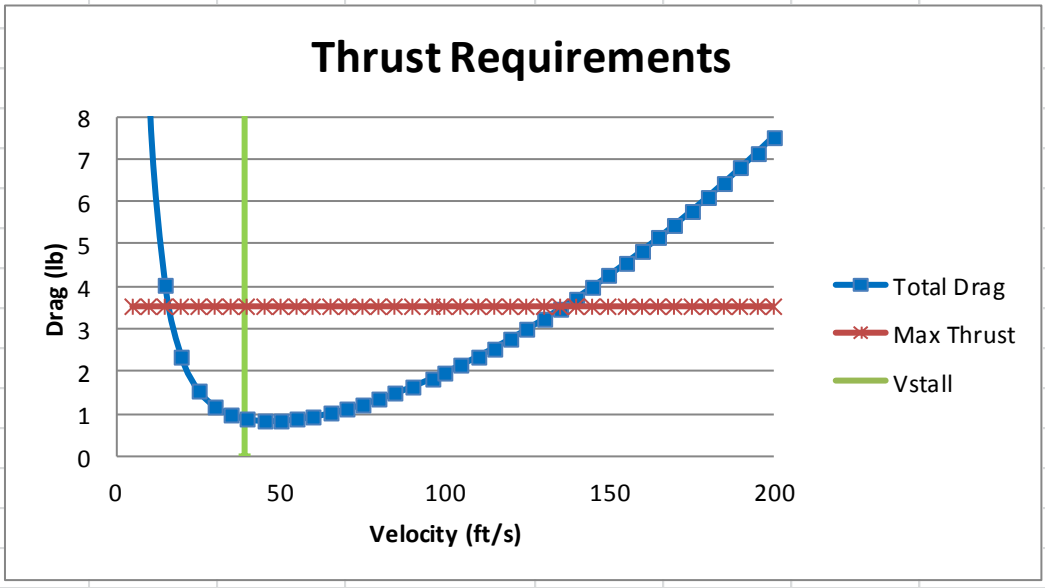

J.4: AIRCRAFT STABILITY AND CONTROL SURFACES

Main Wing					**Horizontal Tail**					**Reference Geometry / Fuselage Data**				**Vertical Tail**	
Chord (c)	12.5 in				Chord (c)	10 in				lh	27			Chord (c)	10 in
Span (b)	72 in				Span (b)	20 in				Vh	0.48			Span (b)	10 in
Area (S)	900 in				Area (S)	200 in				Vv	0.041667			Area (S)	100 in
AR=	5.76				AR=	2								AR=	1
iw	0 deg				it	0 deg								lv	27
e=	0.95	spanwise effectivness (typical 0.95)			e=	0.95	spanwise effectivness (typical 0.95)								
alpha(cl=0)=	-2.97549	deg			alpha(cl=0)=	0	deg								
Cmacw	-0.0548				Cmact	0									
Clαw	0.059617	/deg	=	3.415791 /radian	Clαt	0.10829	/deg	=	6.20456 /radian						
CLαw	2.873398	per radian			CLαt	3.121813	per radian								
CL0w	0.149222				CL0w	0									
CL(α=0)	0.177389														
Xcg/c	0.25														
Xac/c	0.25														
Xnp/c	0.574618	57.46%													
Static Margin	0.324618	32.46%													
ε0	0.016493	rad	0.944957	deg											
dε/dα	0.377528														
n	1				n	1				n	1				
Cm0w	-0.0548				Cm0t	0.024714				Cm0f	0				
Cmαw	0	per radian			Cmαt	-0.93276	per radian			Cmαf	0				

Full Aircraft		
Cm0	-0.03009	
Cmα	-0.93276	per radian

Full Aircraft	
α	Cm
-10	0.13271
-5	0.051312
0	-0.03009
5	-0.11148
10	-0.19288

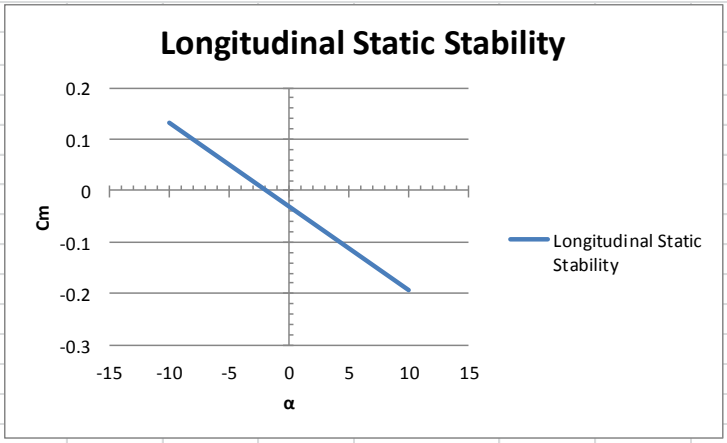

X- intercept

x_1	0.13271	y_1	-10	
x_2	0	y_2	-1.84809	Answer
x3	-0.19288	y3	10	

Flap Sizing

Forward Most CG Position Cm		
Cm0	-0.2	
Cmα	-0.01628	per deg
Landing Angle	10	deg
ΔCmcg	-0.3628	
Max (+) Deflection	20	deg
Max (-) Deflection	-25	deg
Cmδe	-0.01451	per deg

Flap Effectiveness	
τ	0.554878

Use Figure 2.21 in Stability Book - Nelson	
Se/St	0.35
Se/2	35 in^2
Se	70 in^2

Trim Flying Condition		
αtrim	0	deg
δtrim	-2.07322	deg

Full Aircraft		
Cm0	-0.03009	
Cmα	-0.93276	per radian

δ =	-10	deg
Full Aircraft w/ flaps		
α	Cm	
-10	0.277829	
-5	0.196431	
0	0.115032	
5	0.033634	
10	-0.04776	

δ =	-5	deg
Full Aircraft w/ flaps		
α	Cm	
-10	0.20527	
-5	0.123871	
0	0.042473	
5	-0.03893	
10	-0.12032	

δ =	-2.07322	deg
Full Aircraft w/ flaps		
α	Cm	
-10	0.162797	
-5	0.081398	
0	0	
5	-0.0814	
10	-0.1628	

δ =	0	deg
Full Aircraft w/ flaps		
α	Cm	
-10	0.13271	
-5	0.051312	
0	-0.03009	
5	-0.11148	
10	-0.19288	

δ =	5	deg
Full Aircraft w/ flaps		
α	Cm	
-10	0.060151	
-5	-0.02125	
0	-0.10265	
5	-0.18404	
10	-0.26544	

δ =	10	deg
Full Aircraft w/ flaps		
α	Cm	
-10	-0.01241	
-5	-0.09381	
0	-0.1752	
5	-0.2566	
10	-0.338	

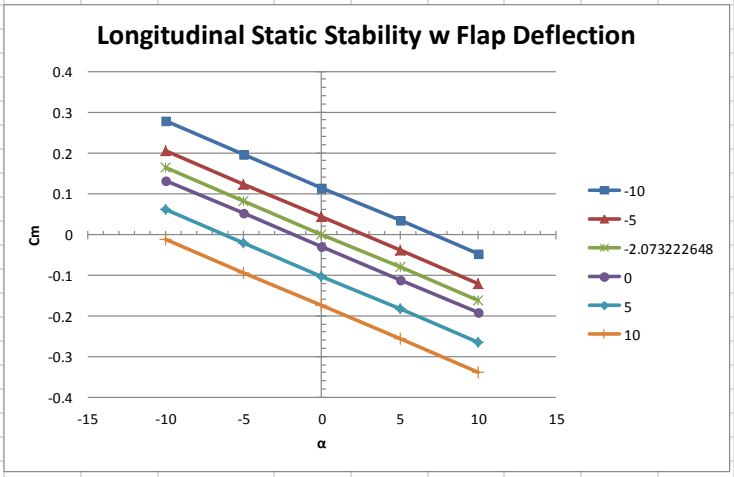

J.5: CONTROL SURFACE SERVO SIZING

Use Xfoil to obtain Hinge Moment

Data From Xfoil		
Hinge moment / Span =	0.010089	x 1/2 rho V^2 c^2
x-Force /span =	0.011288	x 1/2 rho V^2 c^2
y-Force /span =	-0.09558	x 1/2 rho V^2 c^2

density (ρ) =	0.002377	slugs/ft^3		
Max Velocity =	136.3378	ft/s	=	92.9576 mph

Horizontal Stabilizer

Stabilizer Chord (c) =	10 in	=	25.4 cm	
Stabilizer Span (b) =	20 in	=	50.8 cm	
# of Servos =	2			
Safety Factor =	1.25			
Moment/Span =	0.154774 lbf	=	0.070204 kg	
Hinge Moment =	1.547744 lbf*in	=	1.783194 kg*cm	= 24.76391 oz*in
W/ SF =	1.93468		2.228993	30.95489
Servo Torque =	1.8 kg/cm			

vo Arm Length		Servo Force		Serv
0.3 in	0.762 cm	1.3716 kg	48.38177 oz	
0.425 in	1.0795 cm	1.9431 kg	68.54084 oz	
0.55 in	1.397 cm	2.5146 kg	88.6999 oz	
0.65 in	1.651 cm	2.9718 kg	104.8272 oz	

Rudder

Stabilizer Chord (c) =	10 in	=	25.4 cm	
Stabilizer Span (b) =	10 in	=	25.4 cm	
# of Servos =	2			
Safety Factor =	1.25			
Moment/Span =	0.154774 lbf	=	0.070204 kg	
Hinge Moment =	0.773872 lbf*in	=	0.891597 kg*cm	= 12.38195 oz*in
	0.96734		1.114496	15.47744
Servo Torque =	1.8 kg/cm			

vo Arm Length		Servo Force		
0.3 in	0.762 cm	1.3716 kg	48.38177 oz	
0.425 in	1.0795 cm	1.9431 kg	68.54084 oz	
0.55 in	1.397 cm	2.5146 kg	88.6999 oz	
0.65 in	1.651 cm	2.9718 kg	104.8272 oz	

K. AIRCRAFT FLIGHT TEST – FIRST LAUNCH RESULTS

Simulation results

Engine selection

[J350W-None]

Comments

Added wind effects

Simulation control parameters

- Flight resolution: 800.000000 samples/second
- Descent resolution: 1.000000 samples/second
- Method: Explicit Euler

Launch conditions

- Altitude: 1280.00000 Ft.
- Relative humidity: 50.000 %
- Temperature: 95.000 Deg. F
- Pressure: 2.49279 Ft.

Wind speed model: Breezy (15-25 MPH)

  - Low wind speed: 15.0000 MPH
  - High wind speed: 25.0000 MPH

Wind turbulence: Very turbulent (0.09)

  - Frequency: 0.090000 rad/second

- Wind starts at altitude: 0.00000 Ft.
- Launch guide angle: 0.000 Degrees from vertical
- Latitude: 1.571 Degrees

Launch guide data:

- Launch guide length: 108.0000 In.
- Velocity at launch guide departure: 72.8419 ft/s
- The launch guide was cleared at : 0.238 Seconds
- User specified minimum velocity for stable flight: 43.9993 ft/s
- Minimum velocity for stable flight reached at: 38.5701 In.

Max data values:

- Maximum acceleration:Vertical (y): 11.089 geeHorizontal (x): 0.104 geeMagnitude: 11.089 gee
- Maximum velocity:Vertical (y): 318.1627 ft/sHorizontal (x): 36.6667 ft/sMagnitude: 327.7036 ft/s
- Maximum range from launch site: 1493.60811 Ft.
- Maximum altitude: 1659.78391 Ft.

Recovery system data

- P: Parachute Deployed at : 10.453 Seconds
- Velocity at deployment: 64.9885 ft/s
- Altitude at deployment: 1659.78390 Ft.
- Range at deployment: -578.84000 Ft.

Time data

- Time to burnout: 1.901 Sec.
- Time to apogee: 10.453 Sec.
- Optimal ejection delay: 8.551 Sec.

Landing data

- Successful landing
- Time to landing: 81.335 Sec.
- Range at landing: 1493.60811
- Velocity at landing: Vertical: -23.3232 ft/s , Horizontal: 22.8269 ft/s , Magnitude: 32.6349 ft/s

Altimeter Data

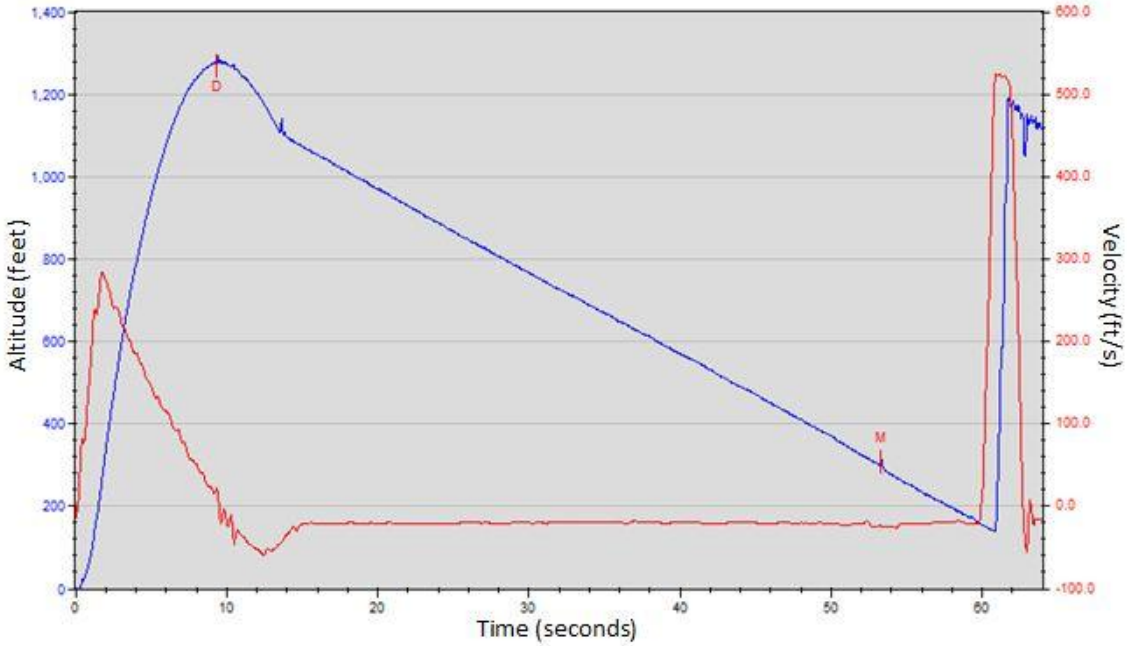

L. AIRCRAFT FLIGHT TEST – FULL SYSTEM RESULTS

Combined Altimeters and Ardupilot Mega Data

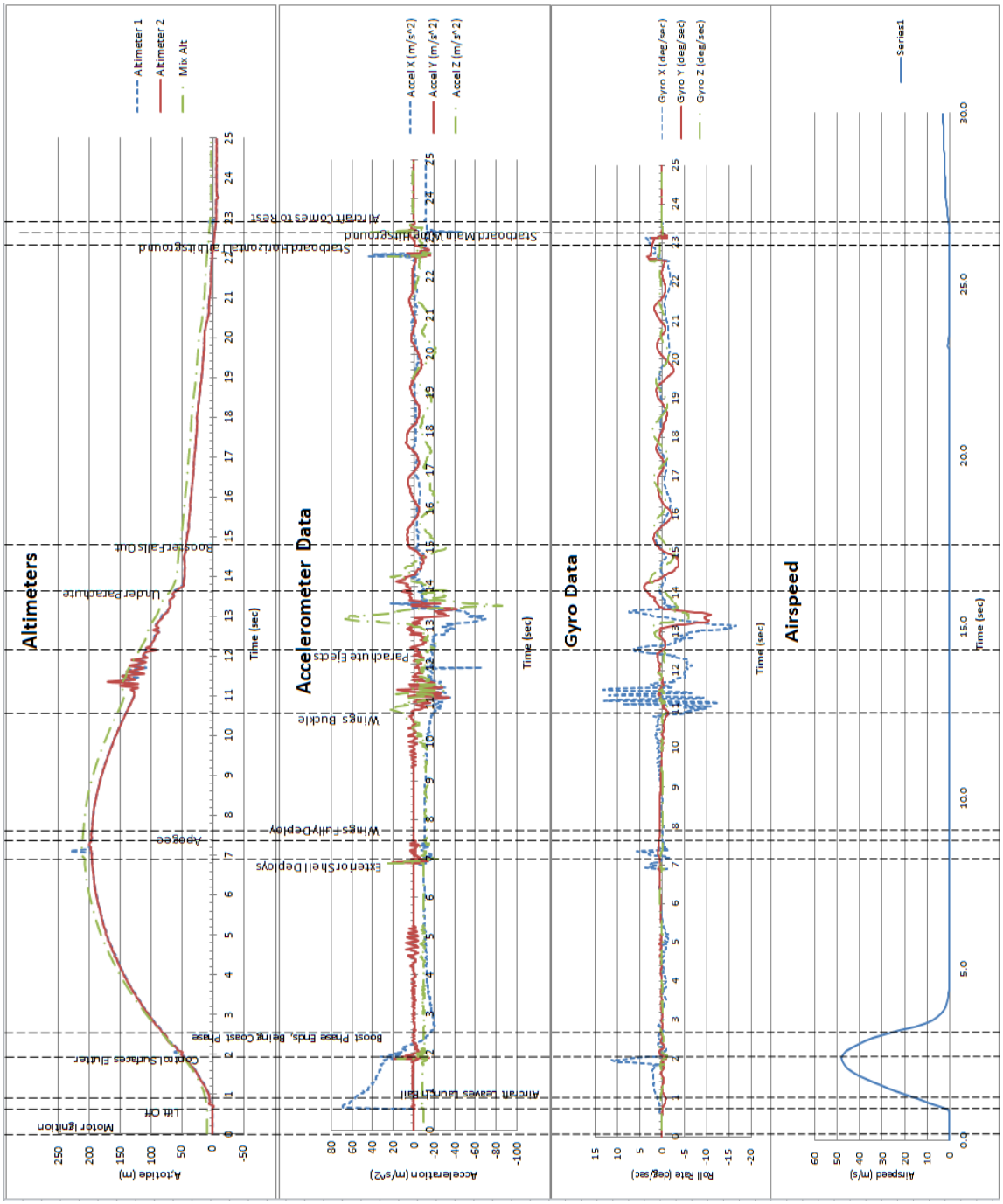

CHAPTER IX

REFERENCES

[1] William Graham, Tim Smith David Cadogan, "Inflatable and Rigidizable Wings for Unmanned Aerial Vehicles," *AIAA*.

[2] Weng (Ben) Kheong Loh, "Deployment of Inflatable Wings," Stillwater, OK, 2006.

[3] David Cadogan et al., "Recent Development and Test of Inflatable Wings," AIAA, AIAA SDM 2006, 2006.

[4] (2012, October) Fiddlers Green. [Online]. http://www.fiddlersgreen.net/models/aircraft/Cruise-Missile.html

[5] "Tomahawk Cruise Missile RGM/UGM-109, Rev 15," Technical Manual SW820-AP-MMI-010, 2009.

[6] Jamey D Jacob, Andrew Simpson, and Suzanne Smith, "Design and Flight Testing of Infltable Wings with Wing Warping," University of Kentucky, Lexington, KY, 05WAC-61, 2005.

[7] Tony Frackowiak, Joe Mello, Brook Norton James E. Murray, "Ground and Flight Evaluation of a Small-Scale Inflatable-Winged Aircraft," *NASA*, 2002.

[8] (2012, October) Integrated Publishing. [Online]. http://armyaviation.tpub.com/AL0926/AL09260037.htm

[9] Erich M. McCoy, Mark Krasinski, Satyajit Limaye, Frank Uhelsky, William Graham Timothy R. Smith, "Ballute and Parachute Decelerators for FASM/Quicklook UAV".

[10] NASA Space Vehicle Design Criteria (Chemical Propulsion), "Liquid Rocket Presure Regulator, Relief Valves, Check Valves, Burst Disks, and Explosive Valves," NASA, SP-8080, 1973.

[11] "Liquid Rocket Pressure Regulators, Relief Valves, Check Valves, Burst Disks, and Explosive Valves," NASA, NASA SP-8080, 1973.

[12] (2012, October) National Association of Rocketry. [Online]. http://www.nar.org

[13] Nancy Atkinson. (2011, October) io9. [Online]. http://io9.com/5848127/amazing-amatuer-rocket-launch-reaches-121000-feet

[14] (2012, October) High Powered Rocketry: Dual Deployment. [Online]. http://westrocketry.com/articles/DualDeploy/DualDeployment.html

[15] (2003) Rouse Tech. [Online]. http://www.rouse-tech.com/index.htm

[16] "Rouse Tech CD3 Manual," User Manual 2009.

[17] Glen Brown, Roy Haggard, and Brook Norton, "Inflatable Structures for Deployable Wings," Vertigo Inc., Lake Elsinore, CA, AIAA-2001-2068, 2001.

[18] Richard Innes, "Computation Fluid Dynamic Study of Flow Over an Inflatable Aerofoil," Loughborough University, 2006.

[19] Mars Airplane Team, "Design and Flight Testing of a Mars Aircraft Prototype Using Inflatable Wings," Oklahoma State Univerisity, Stillwater, 2007.

[20] Raymond P. LeBeau, Suzanne W. Smith Daniel A. Reasor, "Flight Testing and Simulation of a Mars Aircraft Design Using Inflatable Wings," Stillwater,.

[21] (2012, November) Co2 In Refrigeration Applications. [Online]. http://www.achrnews.com/articles/print/co2-in-refrigeration-applications

[22] Jack N Nielsen, *Missile Aerodynamics*.: McGraw-Hill Book Company, 1960.

[23] (2012, November) Scotglas. [Online]. http://www.scotglas.com/

[24] (2012, November) Caslte Creations. [Online]. http://www.ecalc.ch/motorcalc_e.htm?castle

[25] Jordan Hiller. (2012, November) Model Rocket Parachute Descent Rate Calculator. [Online]. http://www.onlinetesting.net/cgi-bin/descent3.3.cgi

[26] Carroll Smith, *Engineer to Win*.: MBI Publishing Company, 1984.

[27] Robert C. Nelson, *Flight Stability and Automatic Control 2nd Ed.*: McGraw Hill, 1998.

[28] Jeff Wise. (2006, June) Popular Mechanics. [Online]. http://www.popularmechanics.com/technology/aviation/news/2932316

[29] Marty Curry. (2009, August) NASA. [Online]. http://www.nasa.gov/centers/dryden/history/pastprojects/AD1/index.html

[30] David A. Neal et al., "Design and Wind-Tunnel Analysis of a Fully Adaptive Aircraft Configuration," *AIAA*, 2004.

[31] John D. Anderson, *Aircraft Performance and Design*.: McGraw-Hill, 1999.

[32] Daniel P. Raymer, *Aircraft Design: A Conceptual Approach*, 4th ed.: American Institute of Aeronautics and Astronautics, 2006.

VITA

Cory Wayne Sudduth

Candidate for the Degree of

Master of Science

Thesis: DESIGN OF A HYBRID ROCKET / INFLATABLE WING UAV

Major Field: Mechanical and Aerospace Engineering

Biographical:

Education:

Completed the requirements for the Master of Science in Mechanical and Aerospace Engineering at Oklahoma State University, Stillwater, Oklahoma in December, 2012.

Completed the requirements for the Bachelor of Science in Mechanical and Aerospace Engineering at Oklahoma State University, Stillwater, Oklahoma in May, 2011.

Experience:

Professional Memberships: